

2

AD-A228 722

FILE COPY

GL-TR-90-0049  
ENVIRONMENTAL RESEARCH PAPERS, NO. 1056

A Seismic/Acoustic Study of Low Altitude  
Air Blasts at Ft Devens, Massachusetts

JANET C. JOHNSTON



9 March 1990



Approved for public release; distribution unlimited.



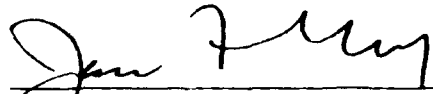
DTIC  
ELECTE  
NOV 07 1990  
S E D



EARTH SCIENCES DIVISION PROJECT 2000  
**GEOPHYSICS LABORATORY**  
HANSCOM AFB, MA 01731-5000

90 11 7 021

This technical report has been reviewed and is approved for publication.

  
JAMES LEWKOWICZ  
Earth Sciences Division

FOR THE COMMANDER

  
DONALD H. ECKHARDT  
Division Director

This report has been reviewed by the ESD Public Affairs (PA) and is releasable to the National Technical Information Service (NTIS).

Qualified requestors may obtain additional copies from the Defense Technical Information Center. All others should apply to the National Technical Information Center.

If your address has changed, or if you wish to be removed from the mailing list, or if the addressee is no longer employed by your organization, please notify GL/IMA, Hanscom AFB, MA 01731-5000. This will assist us in maintaining a current mailing list.

Do not return copies of this report unless contractual obligations or notices on a specific document requires that it be returned.

# REPORT DOCUMENTATION PAGE

Form Approved  
OMB No. 0704-0188

1a. REPORT SECURITY CLASSIFICATION Unclassified			1b. RESTRICTIVE MARKINGS		
2a. SECURITY CLASSIFICATION AUTHORITY			3. DISTRIBUTION / AVAILABILITY OF REPORT Approved for public release; Distribution unlimited		
2b. DECLASSIFICATION / DOWNGRADING SCHEDULE			5. MONITORING ORGANIZATION REPORT NUMBER(S)		
4. PERFORMING ORGANIZATION REPORT NUMBER(S) GL-TR-90-0049 ERP, No. 1056			7a. NAME OF MONITORING ORGANIZATION		
6a. NAME OF PERFORMING ORGANIZATION Geophysics Laboratory	6b. OFFICE SYMBOL (If applicable) LWH	7b. ADDRESS (City, State, and ZIP Code)			
3c. ADDRESS (City, State, and ZIP Code) Hanscom AFB Massachusetts 01731-5000		9. PROCUREMENT INSTRUMENT IDENTIFICATION NUMBER			
8a. NAME OF FUNDING / SPONSORING ORGANIZATION	8b. OFFICE SYMBOL (If applicable)	10. SOURCE OF FUNDING NUMBERS			
3c. ADDRESS (City, State, and ZIP Code)		PROGRAM ELEMENT NO. 61102F	PROJECT NO. 2309	TASK NO. G2	WORK UNIT ACCESSION NO. 05
11. TITLE (Include Security Classification) A Seismic/Acoustic Study of Low Altitude Air Blasts at Ft. Devens, Massachusetts					
12. PERSONAL AUTHOR(S) Johnston, J.C.					
13a. TYPE OF REPORT Scientific, Final	13b. TIME COVERED FROM _____ TO _____	14. DATE OF REPORT (Year, Month, Day) 1990 March 9		15. PAGE COUNT 90	
6. SUPPLEMENTARY NOTATION					
7. COSATI CODES			18. SUBJECT TERMS (Continue on reverse if necessary and identify by block number)		
FIELD	GROUP	SUB-GROUP	Seismic/Acoustic Aerial Blasts, Air Blasts, (60) Seismic Detection; Aerial Explosions		
9. ABSTRACT (Continue on reverse if necessary and identify by block number)					
<p>On 5 May 1986, 3 packages of TNT were detonated 100 ft in the air above the Turner Drop Zone at Ft. Devens, Massachusetts. The aerial explosions were recorded by seismic and acoustic sensors over 2 linear arrays that covered the distance range from 0 to 1000 meters. One array was installed over flat topography, while the other was installed across a hill with 80 ft of relief. The goal of the experiment was to examine the response of the ground and the air to a unit impulse. Although recording of the higher frequencies generated by the blasts was limited by the sampling rate capability of the equipment (100 and 200 samples/sec) it was clear that the hill produced a sheltering effect. Considerable transverse motion appeared in the records. Reduced time plots revealed a propagation speed of 0.35 km/sec corresponding primarily to an airwave induced seismic signal, although some seismic precursors are evident. The ratio of peak seismic velocity to pressure ranged from <math>10^{-4}</math> cm/sec/Pa for the line that transversed the hill to <math>10^{-5}</math> cm/sec/Pa for the flat array. The experiment should be repeated in the same area during different seasonal coverings (snow and ice) and extended to areas with more complex topography and different vegetation.</p>					
10. DISTRIBUTION/AVAILABILITY OF ABSTRACT <input type="checkbox"/> UNCLASSIFIED/UNLIMITED <input type="checkbox"/> SAME AS RPT. <input type="checkbox"/> DTIC USERS			21. ABSTRACT SECURITY CLASSIFICATION Unclassified		
12a. NAME OF RESPONSIBLE INDIVIDUAL Janet C. Johnston			22b. TELEPHONE (Include Area Code) (617) 377-3767	22c. OFFICE SYMBOL GL/LWH	

UNCLASSIFIED

SECURITY CLASSIFICATION OF THIS PAGE

In future experiments the position of the air blasts should be varied to facilitate discrimination of paths to the receivers. The results could be extrapolated to an extended, continuous source such as a low flying aircraft or cruise missile.

UNCLASSIFIED

SECURITY CLASSIFICATION OF THIS PAGE

## Preface

The author thanks the many people whose cooperation made this experiment possible. These include Ken Dallas, who coordinated balloon support, Bob Reinke and Al Leverett from the Weapons Laboratory, all Solid Earth Geophysics Branch personnel who helped install the equipment and students and other last minute assistants; Katharine Kadinsky-Cade, Joe Sabeni, Janet Oliveira-Jones and Dave Shorter. Also, locations were surveyed by Ted Writanen (formerly of the Geodesy and Gravity Branch) and Lee Stevens of GL did a fine job of photography as well as digging holes.

A special thanks goes to SMSgt Roger Sands (Geodesy and Gravity Branch) without whose assistance the experiment would not have been possible.

The author benefited from many helpful discussions of seismo-acoustic interaction with James C. Battis of the Solid Earth Geophysics Branch (GL).

Thank you also to John Cipar (Solid Earth Geophysics Branch, GL) and James C. Battis for reviewing this manuscript.



Accession For	
NTIS GRA&I	<input checked="" type="checkbox"/>
DTIC TAB	<input type="checkbox"/>
Unannounced	<input type="checkbox"/>
Justification	
By	
Distribution/	
Availability Codes	
Dist	Avail and/or Special
A-1	

## Contents

1. INTRODUCTION	1
2. GENERAL GEOLOGIC SETTING AND TOPOGRAPHIC INFORMATION	2
3. SEISMO-ACOUSTIC ARRAY	2
4. ANALYSIS AND INTERPRETATION	6
5. DISCUSSION	57
REFERENCES	59
APPENDIX A: EQUIPMENT PARAMETERS	61
APPENDIX B: X- AND Y-LINE PROPERTIES	63
APPENDIX C: AMPLITUDE SPECTRA FOR SELECTED SEISMOGRAMS	73

## Illustrations

1. Structural Dislocations in Eastern Massachusetts (Modified from Castle et al, 1976)	3
2. Site Map with Topographic Contours	4
3. X- and Y-Line	5
4. Seismograms - X-Line	7-23
5. Seismograms - Y-Line	24-30
6. Maximum Amplitude vs Distance - X-Line	32
7. Maximum Amplitude vs Distance - Y-Line	33
8. Particle Motion Plots	35-40
9. Ideal Blast Wave (Modified from Baker, 1973)	41
10. Possible Acoustic Wave Reflective Sources	42
11. X-Line Record Section	43-45
12. Y-Line Record Section	46-48
13. Air Wave Geometry	49
14. Pressure Sensor Data - X-Line	50-52
15. Pressure Sensor Data - Y-Line	53-55

## Tables

1. Station Location Data	6
2. Ratio of Peak Vertical Seismic Motion to Peak Pressure	56
A-1. Clock Correction Data	61
A-2. Pressure Sensor Calibration Data	62
A-3. Recorder, Seismometer & Pressure Sensor List	62
B-1. Seismometer Constants (X-Line Properties)	65-66
B-2. DCS-302 Recorder Constants (X-Line Properties)	67-68
B-3. Seismometer Constants (Y-Line Properties)	70
B-4. DCS-302 Recorder Constants (Y-Line Properties)	71

## **A Seismic/Acoustic Study of Low Altitude Air Blasts at Ft Devens, Massachusetts**

### **1. INTRODUCTION**

On 5 May 1986, three packages of dynamite, two 5-pound bundles and one 10-pound bundle, were detonated in the Turner Drop Zone area on Fort Devens Army Base in eastern Massachusetts. The packages were suspended approximately 100 feet in the air by balloon. The ground motions and airwaves resulting from the three separate shots were recorded by a digital array consisting of 10 seismic and 9 acoustic stations. A crew of 25 scientists, engineers, and technicians from the Earth Sciences Division, Aerospace Instrumentation Division (balloon support) of the Geophysics Laboratory, and the Civil Engineering Research Division of the Weapons Laboratory assembled and installed the equipment in one day at the Turner Drop Zone.

The goal of this experiment was to examine the response of the ground to what may be considered essentially a unit impulse. The results may be then extrapolated to an extended, continuous source such as a low flying aircraft or a cruise missile. The experiment was designed to be repeated in the same area during different seasonal coverings (snow and ice) and extended to areas of more complex topography, terrain and differing vegetation.

---

(Received for publication 20 February 1990)

## 2. GENERAL GEOLOGIC SETTING AND TOPOGRAPHIC INFORMATION

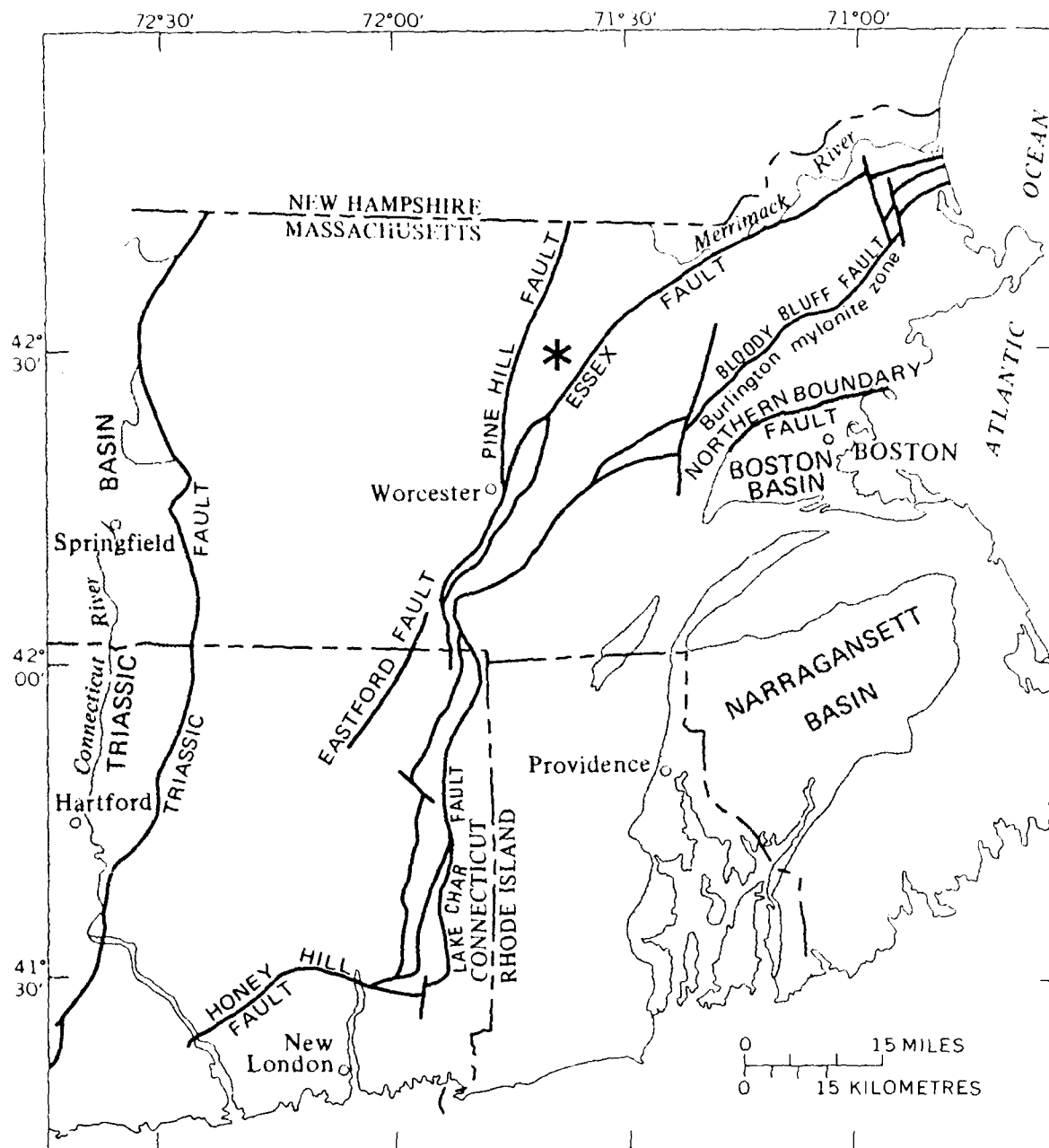
Fort Devens lies between the Essex Fault and the Pine Hill Fault in northeastern Massachusetts (Figure 1). The Essex Fault is a regionally developed, east-northeast trending dislocation that separates the Merrimac Group on the north and west from a possibly Precambrian and generally much more highly metamorphosed terrain on the south and east.<sup>1</sup> The Pine Hill Fault generally marks the boundary between the Merrimac Group and Worcester Phyllite. The Merrimac Group consists of layered schists and gneisses of probable Ordovician-Silurian age.<sup>2</sup> Also, the Ayer granite (Ordovician) has been mapped in the quadrangle.<sup>1</sup> As with all of central and eastern Massachusetts, the structural characteristics result from a long and complex tectonic history. The drop zone is a relatively flat open field with a hill of 80-ft relief in its northeast corner. Both the field and the hill lack significant vegetation. There were a few trees and a covering of grass. The soil was rocky and some large boulders were apparent on the north side of the hill. The edge of a wooded zone ran north-south about 75 meters from ground zero. In the immediate area of the experiment, (see topographic map, Figures 2 & 3)<sup>3</sup>, it was possible to lay out a relatively flat east-west profile (X-line) in contrast to a north-south profile (Y-line) that stretched over a hill with a relief of 80-ft (25 m). These profiles and station locations, as well as the shot position in the air, were folded onto two dimensions in Figure 3.

## 3. SEISMO-ACOUSTIC ARRAY

The three-component seismic ground motions and air pressures from the blasts were recorded digitally on an array consisting of two approximately radial profiles (Figure 3). One profile ran approximately north of the shots (Y-line), the other approximately west (X-line) of the shots. The shot point is referred to as "ground zero" for the remainder of this report. The X-line consisted of six 3-component seismic and pressure stations, and the Y-line consisted of four 3-component seismic stations and three pressure stations (at station locations: Y1, Y2, Y3).

Timing was accomplished by setting all the recorder clocks to a master clock before the first shot. Recorder clock offsets were measured with respect to a single recorder after the experiment (Appendix A, Table A-1). Geospace HS-10 seismometers with a natural period at 1 Hz and Sprengnether S-6000 seismometers with a natural period of 2 Hz were connected to the Terra Technology DCS-302 seismic recorders. The seismometers were buried in shallow holes to minimize wind noise. Pressure was recorded by Model MLR pressure transducers ( $\pm 0.5$  PSI full scale and  $\pm 1.5$  PSI full scale). For some of the stations, in-ground calibration tests were run as teardown time permitted. Recorder/seismometer pairs were calibrated in the laboratory, as were all the pressure

- 
1. Castle, R.O., Dixon, M.R., Grew, E.S., Griscom, A., and Zietz, I. (1976) *Structural Dislocations in Eastern Massachusetts*, Geological Survey Bulletin 1410, U.S. Government Printing Office, Washington, DC.
  2. Van Diver, B.B. (1987) *Roadside Geology of Vermont and New Hampshire*, Mountain Press Publishing Company, Missoula, pp.1-29.
  3. United States Army Forces Command, 584th Engineer Company (Cartographic), 30th Engineer Battalion (Topographic) (Army), Fort Belvoir, VA 22060, (Feb, 1986) Fort Devens Special Map, edition 2-DMATC, Series V8145.



**\* Location of  
Fort Devens, Turner Drop Zone**

Figure 1. Structural Dislocations in Eastern Massachusetts (Modified from Castle et al, 1976)

# FT DEVENS TURNER DROP ZONE

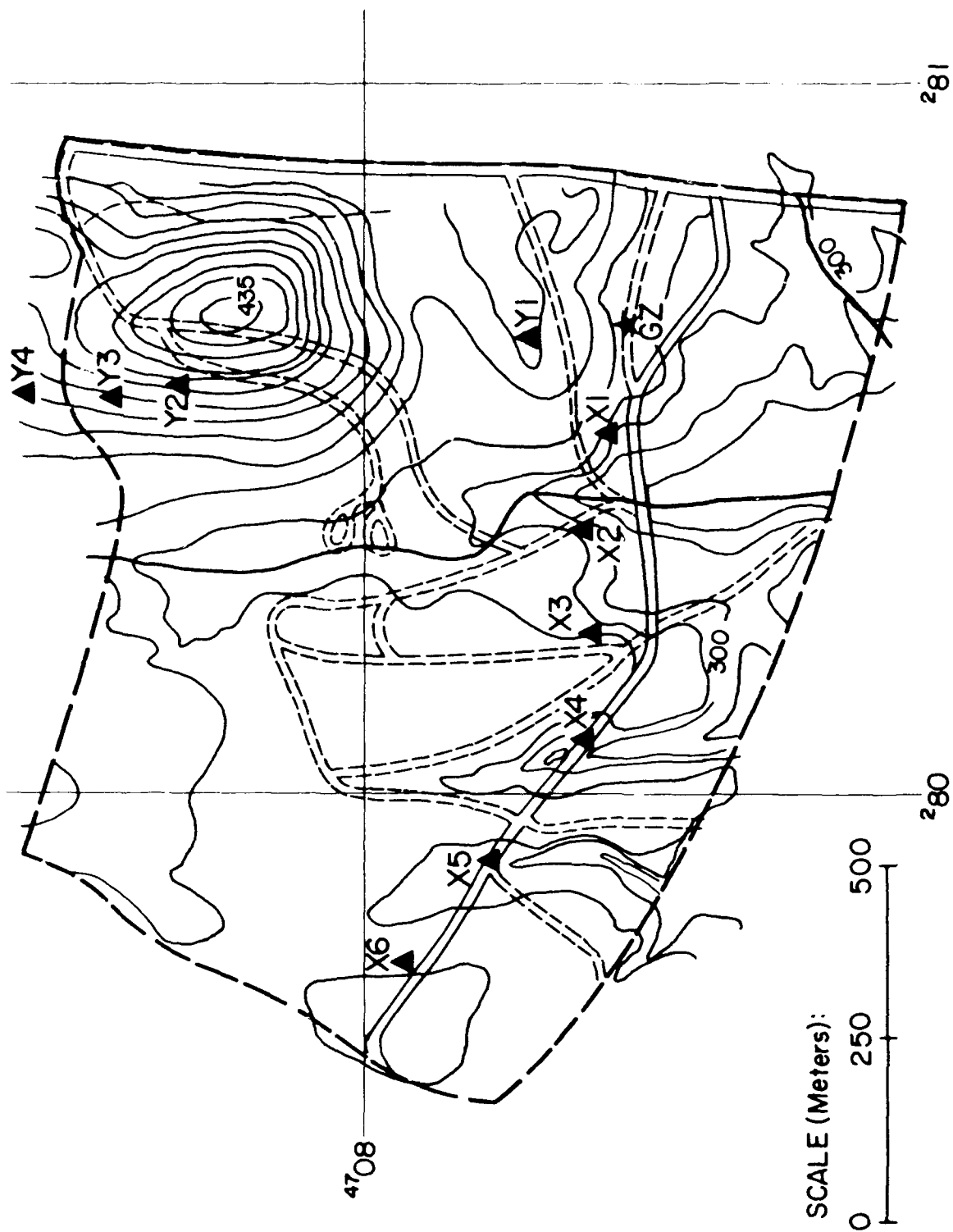


Figure 2. Site Map with Topographic Contours

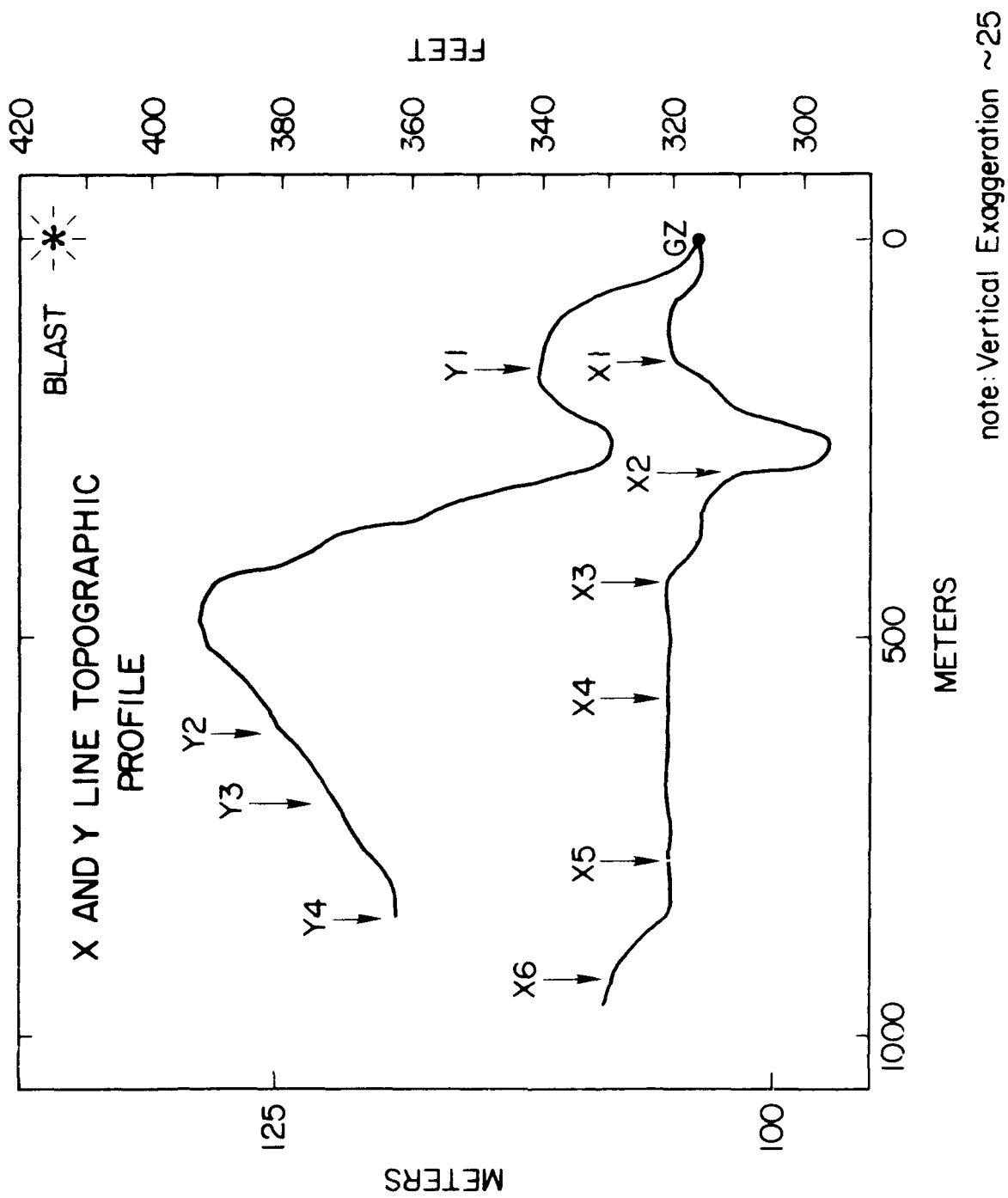


Figure 3. X- and Y-Line

transducers (Appendix A, Table A-2). The Terra Technology DCS-302 recorders used cassette tapes to record the signals. For the majority of the stations the recorders were triggered remotely using cables. Some stations were set on trigger manually a few seconds before shot times.

The shots were recorded at either 200 samples per second or 100 samples per second. Table A-3, in Appendix A contains information on sampling rates for each station and Appendix B contains additional information on the instruments for the X- and Y-lines. The response of the recorder's amplifier is flat from DC to the anti-aliasing filter cut-off frequency of 30 Hz or 70 Hz. Above that cut-off frequency, the response rolls off at 6 dB per octave using a 6-pole Butterworth filter. The recorders that were attached to seismometers were set at automatic gain ranging; the recorders attached to the pressure sensors were set to fixed gain.

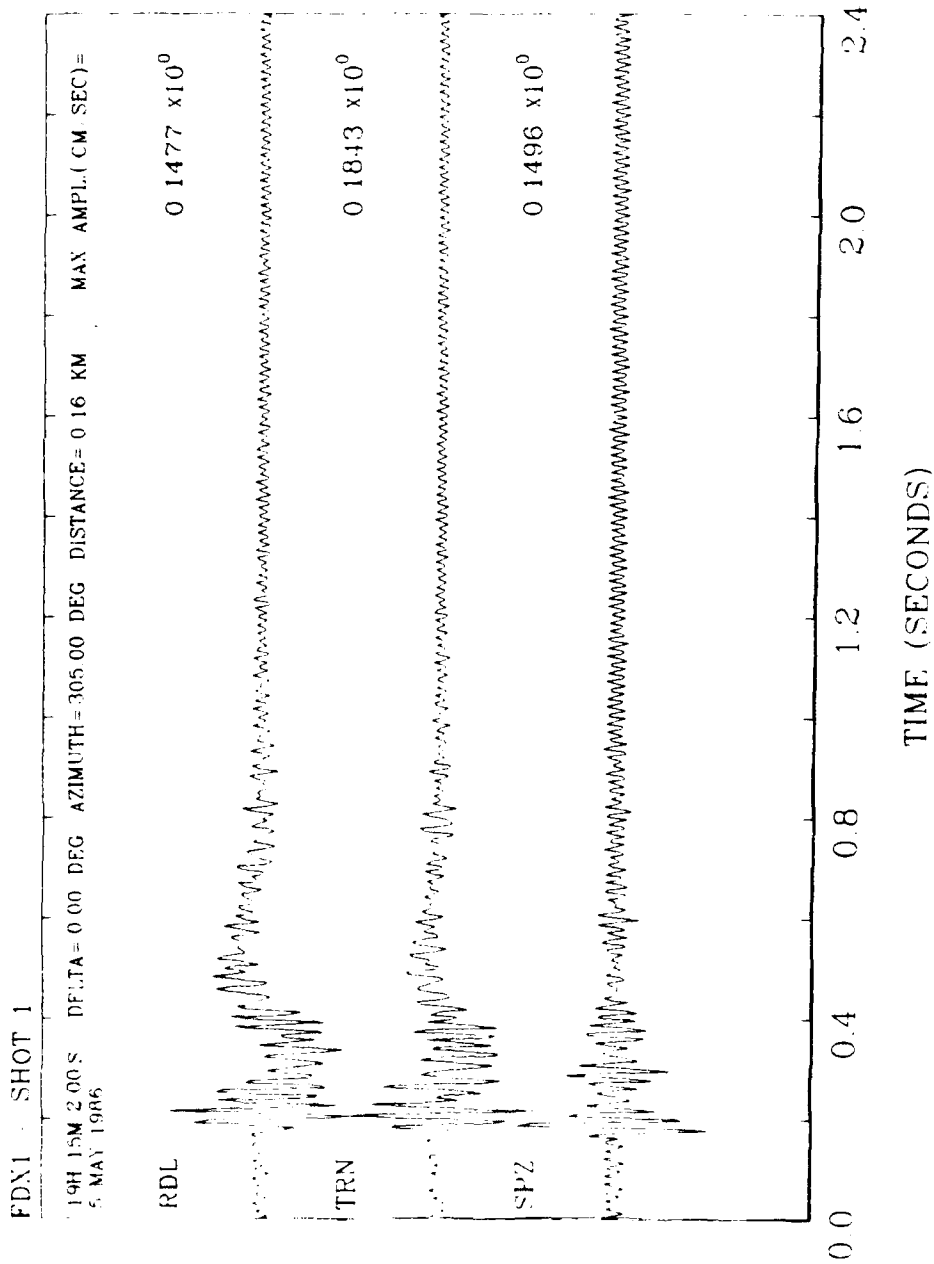
#### 4. ANALYSIS AND INTERPRETATION

Table 1 lists distances to ground zero and azimuths for each station. The seismogram recordings

Table 1. Station Location Data

Map Symbol	Station	Distance to G.Z. (Meters)	Map Elev. (Meters)	Bearing from G.Z. (Magnetic)	Back Azimuth
Y1	FDY1	147.218	105.156	00°	180°
Y2	FDY2	643.433	123.444	00°	180°
Y3	FDY3	744.626	117.348	00°	180°
Y4	FDY4	850.697	114.300	15°	192°
G.Z.	Porta Corder	0	97.536		
X1	FDX1	160.325	94.488	305°	125°
X2	FDX2	309.677	91.44	305°	125°
X3	FDX3	445.008	96.012	280°	100°
X4	FDX4	593.750	94.488	295°	115°
X5	FDX5	742.493	97.536	300°	120°
X6	FDX 6	891.235	97.536	305°	125°

were rotated into radial and transverse components. Figures 4 and 5 display all the seismic waveforms from the X- and Y-line respectively in order of station location. Amplitude spectra were computed for vertical components and can be found in Appendix C. In Figures 4 and 5, the numbers positioned on the right sides of the plots give the maximum amplitude of the signal in cm/sec. The high frequency background on station FDX1 and FDY2 for all shots resulted from a malfunction internal to the recorder. The very long period motion at station FDX1 radial component is probably a ground roll phenomenon. FDX1 was one of the closest stations to the shots at 160 m. However, this

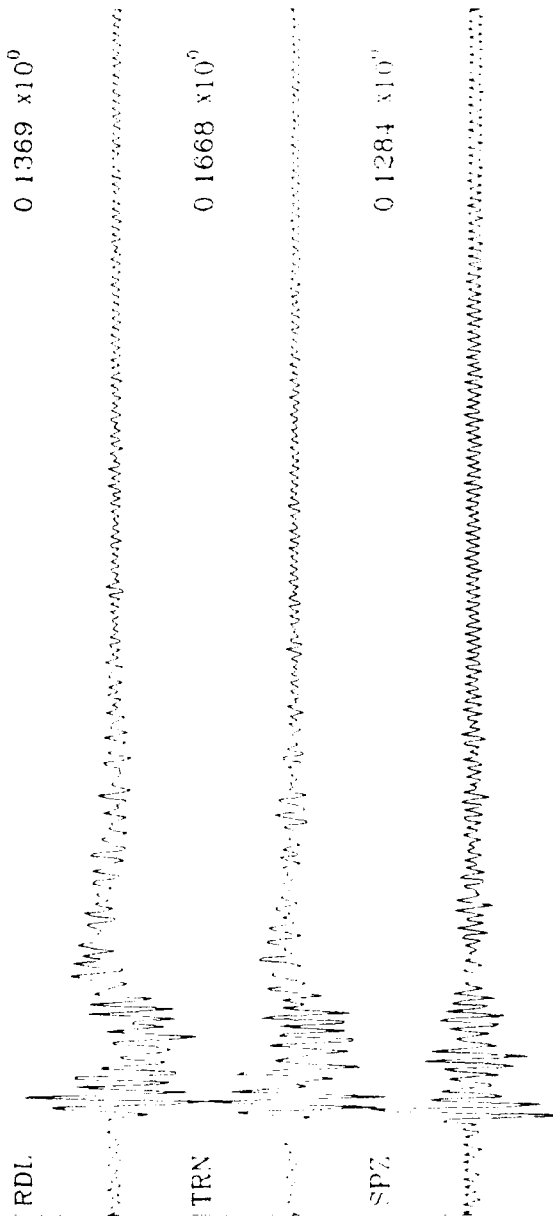


11-JUL-88 13-59-12

Figure 4. Seismograms - X-Line

# FDX1 - SHOT 2

19H 39M 49.00S DELTA = 0.00 DEG AZIMUTH = 305.00 DEG DISTANCE = 0.16 KM MAX AMPL. (CM SEC) =  
5 MAY 1986



0.0 0.4 0.8 1.2 1.6 2.0 2.4  
TIME (SECONDS)

11-JUL-88 14-00-27

Figure 4. Seismograms - X-Line (Cont'd)

# FDX1 - SHOT 3

20H 3M 39.00 S DELTA = 0.00 DEG AZIMUTH = 305.00 DEG DISTANCE = 0.16 KM MAX AMPL (CM/SEC) =

5 MAY 1986

RDL

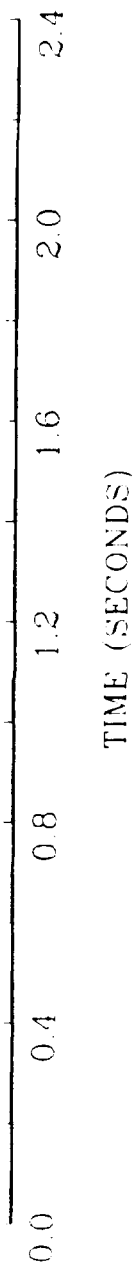
0.2007 x 10<sup>0</sup>

TRN

0.2386 x 10<sup>0</sup>

SPZ

0.1873 x 10<sup>0</sup>

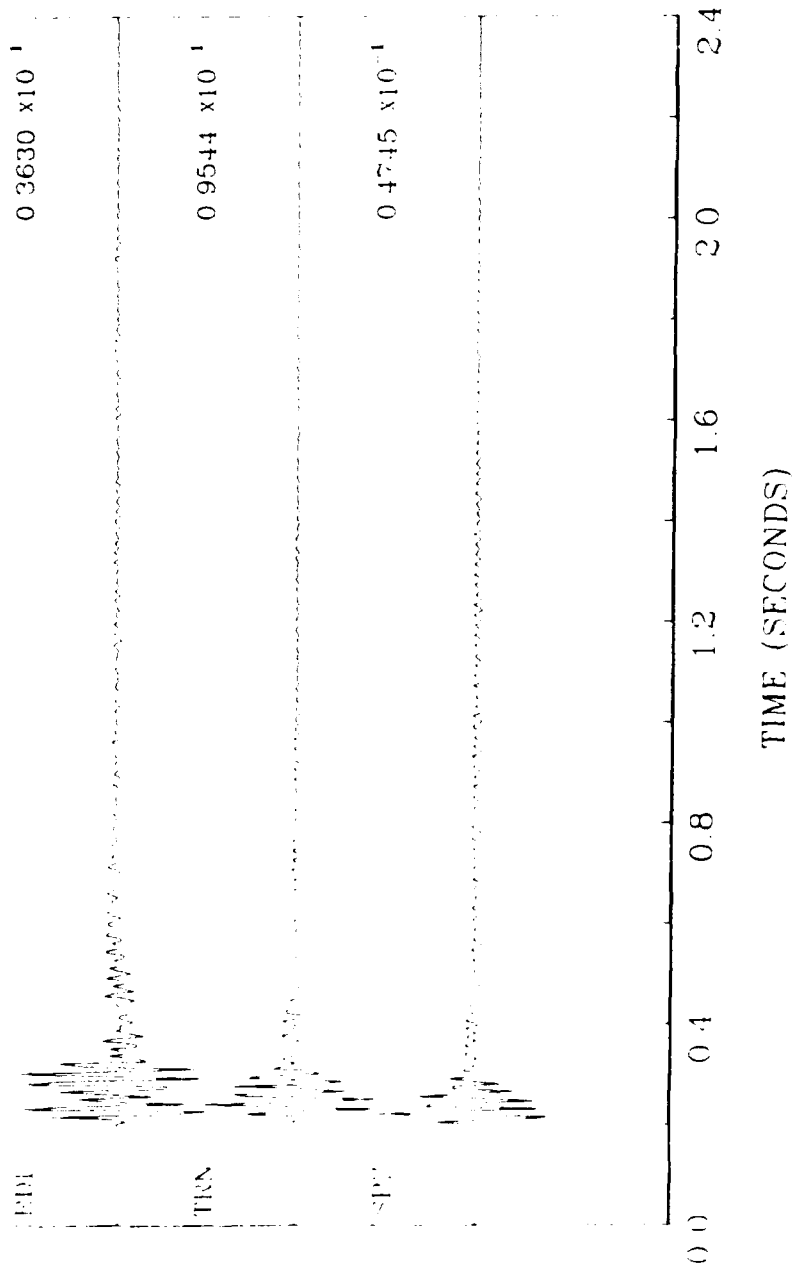


11 JUL-88 14 01 19

Figure 4. Seismograms - X-Line (Cont'd)

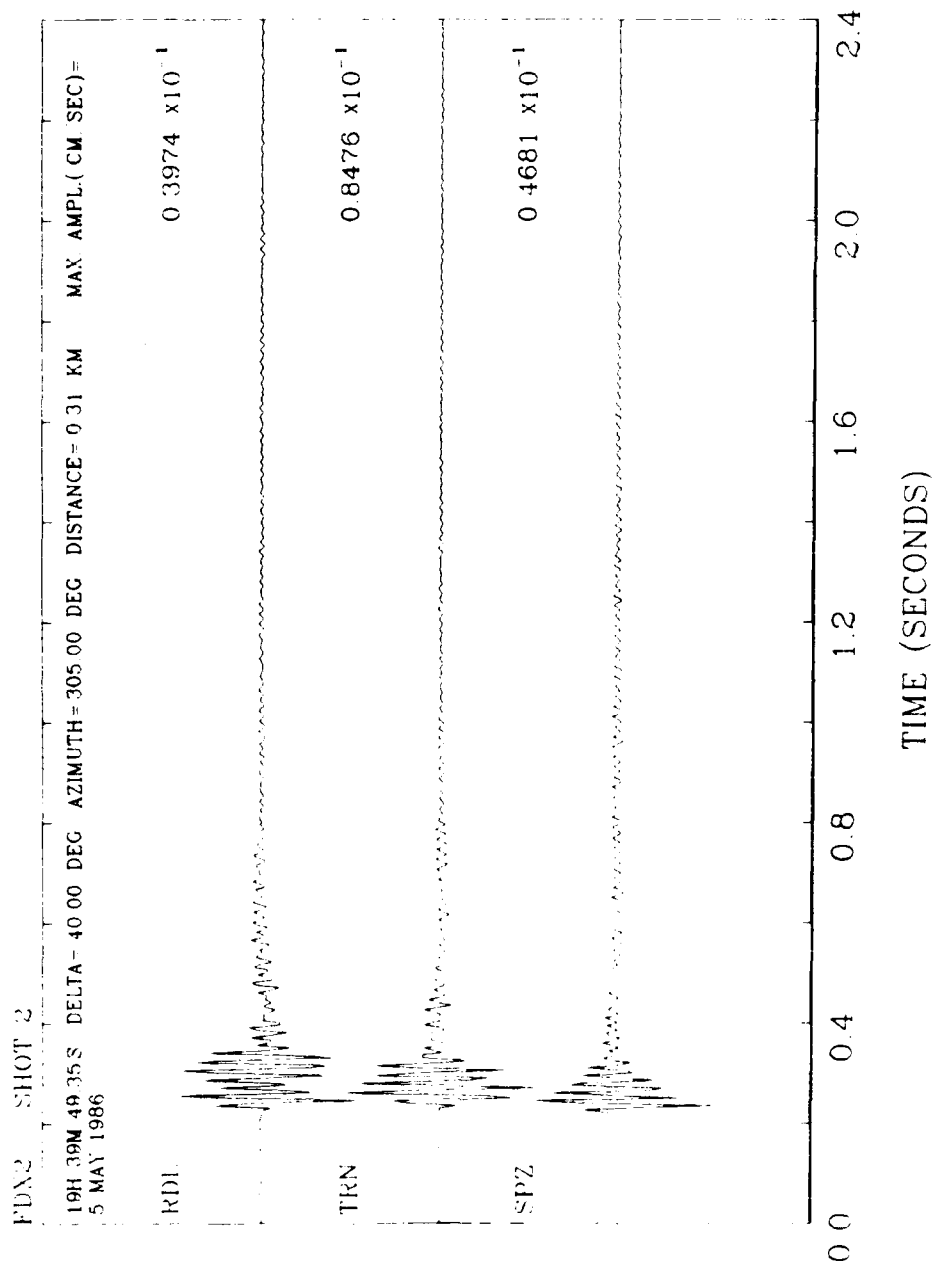
# FDX2 SHOT 1

19H 15M 23.5 S EFLTA= 40 00 DEG AZIMUTH= 305 00 DEG DISTANCE= 0.31 KM MAX AMPL (CM SEC)=  
 17 MAY 1986



11-JUL-88 14-02-11

Figure 4. Seismograms - X-Line (Cont'd)



11-JUL-88 14-03-26

Figure 4. Seismograms - X-Line (Cont'd)

FDX2 - SHOT 3

20H 3M 38 35 S DELTA=40 00 DEG AZIMUTH=305 00 DEG DISTANCE=0.31 KM MAX. AMPL.(CM. SEC)=  
5 MAY 1986

0.3717  $\times 10^{-1}$

0.1059  $\times 10^0$

0.5246  $\times 10^{-1}$

RDL

TRN

SPZ

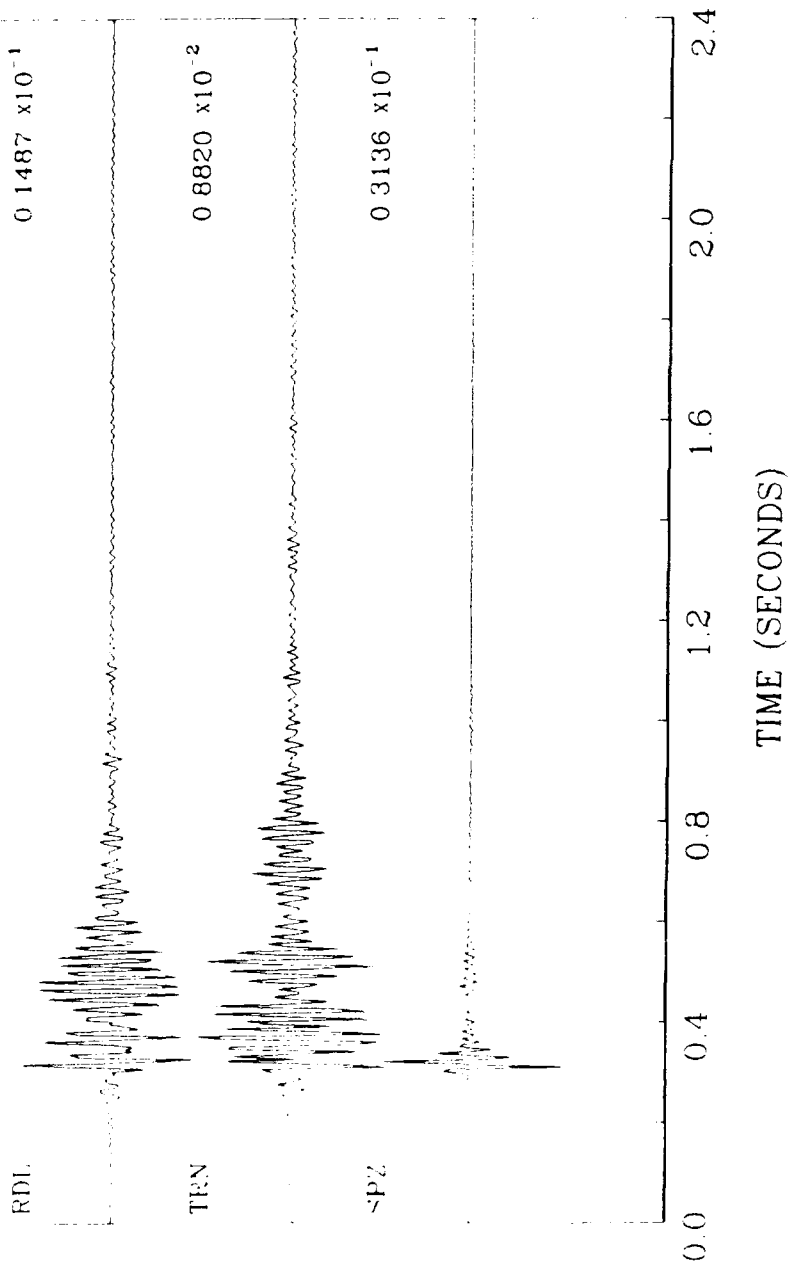
0.0 0.4 0.8 1.2 1.6 2.0 2.4  
TIME (SECONDS)

11-JUL-88 14-04-29

Figure 4. Seismograms - X-Line (Cont'd)

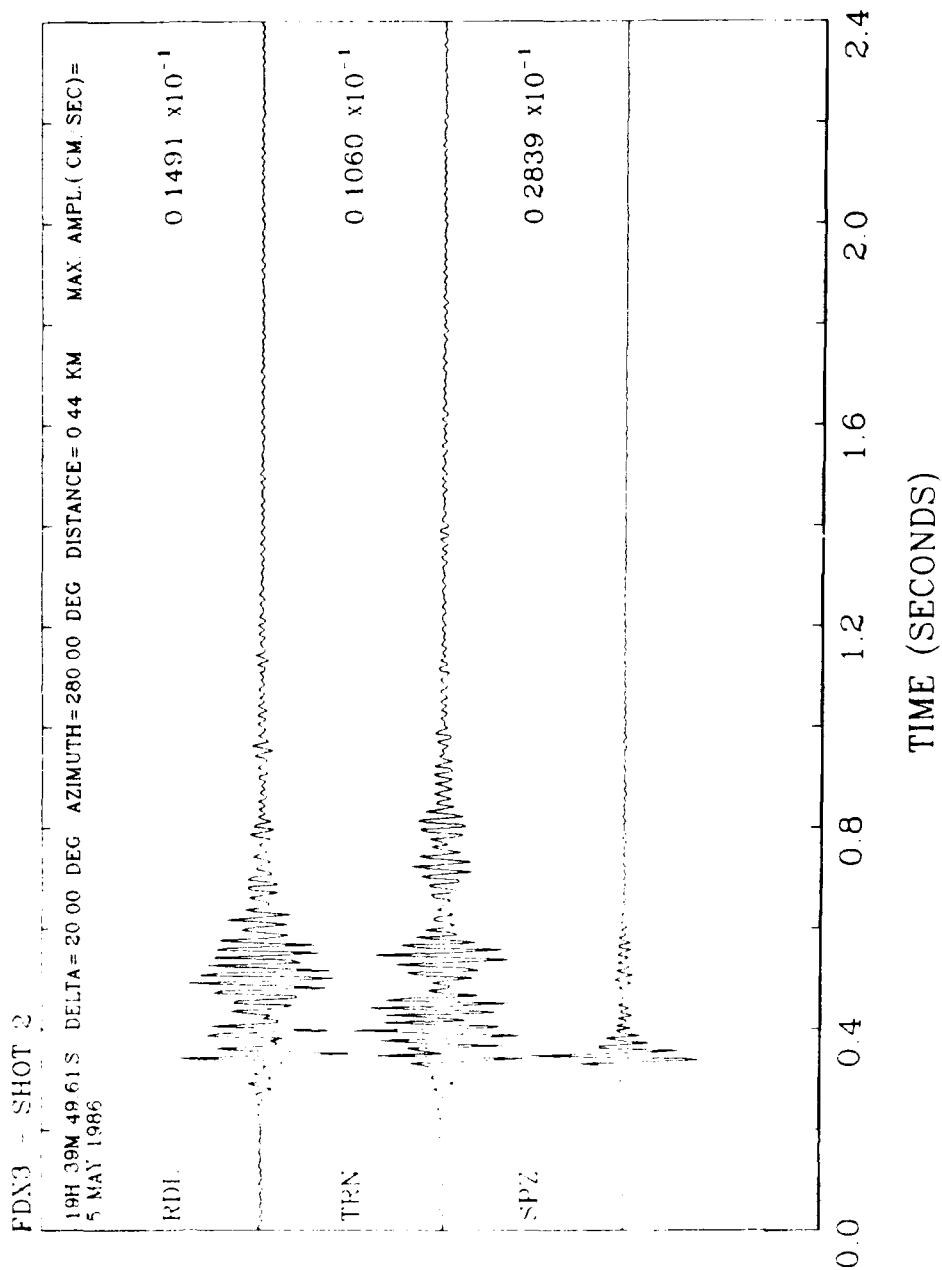
FDX3 SHCT 1

19H 15M 2.61S DELTA=20.00 DEG AZIMUTH=280.00 DEG DISTANCE=0.44 KM MAX AMPL. (CM SEC)=  
5 MAY 1986



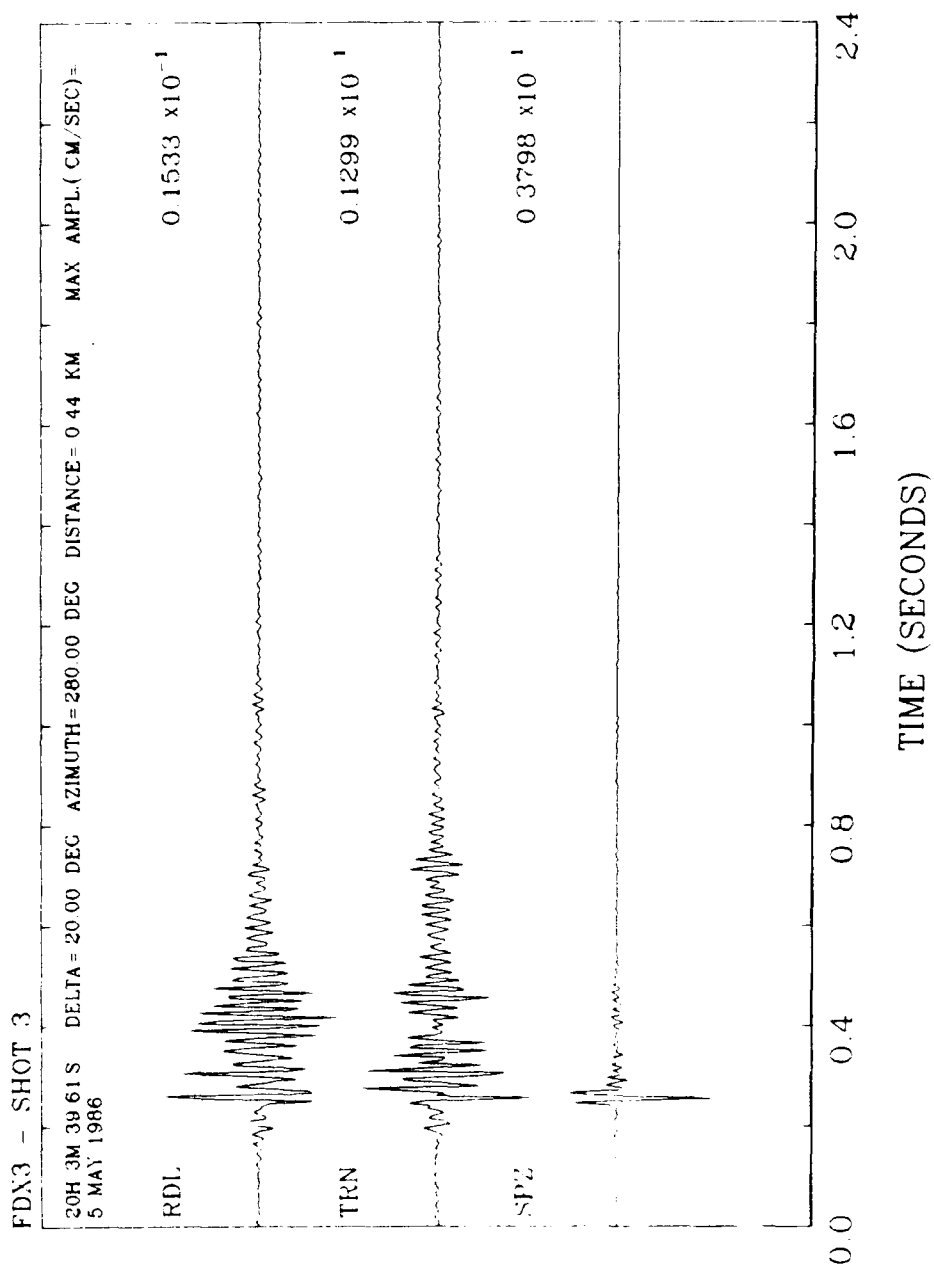
11-JUL-88 14-06-05

Figure 4. Seismograms - X-Line (Cont'd)



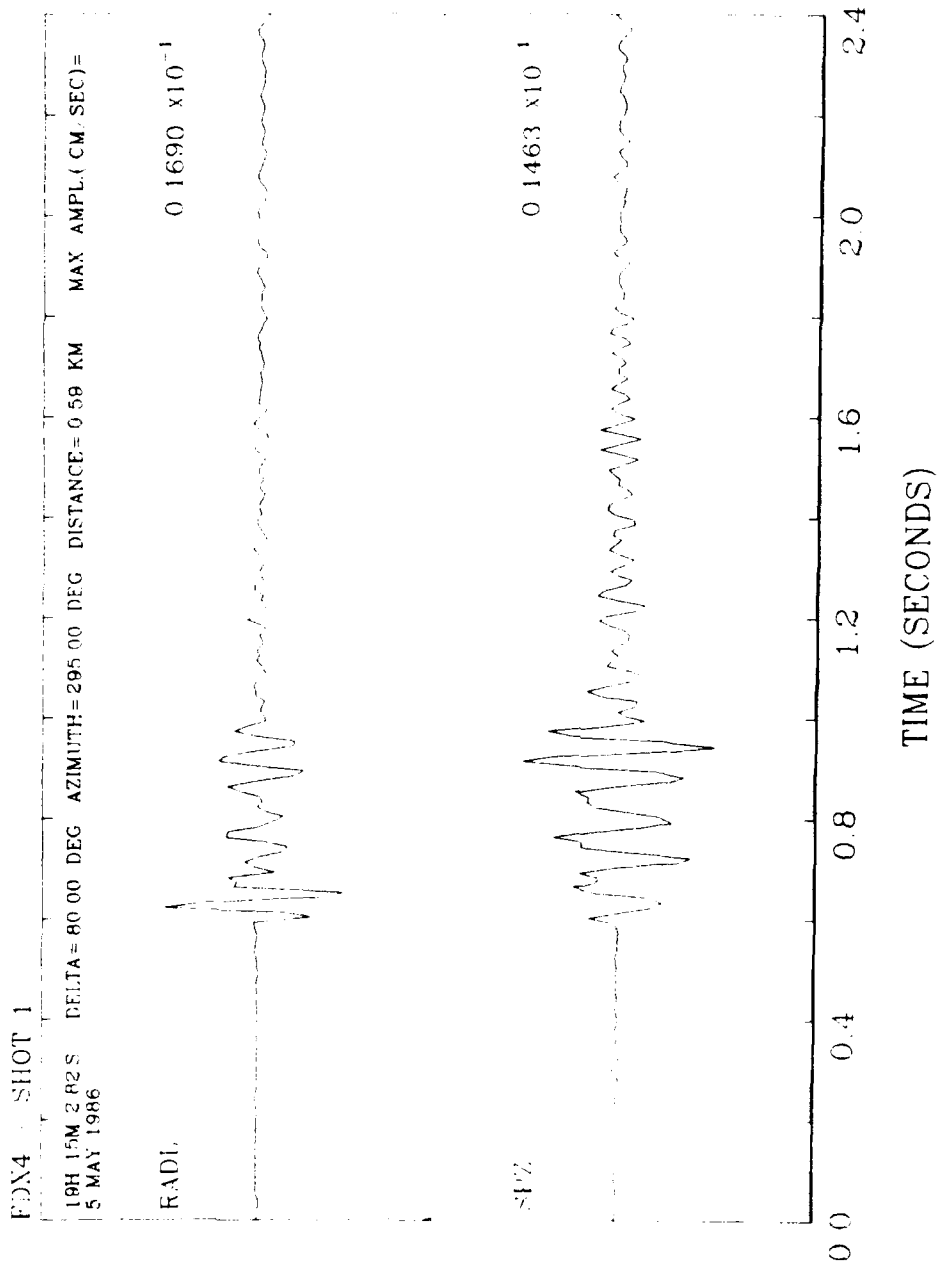
11-JUL-88 14-07-13

Figure 4. Seismograms - X-Line (Cont'd)



11-JUL-88 14-08-22

Figure 4. Seismograms - X-Line (Cont'd)



11-JUL-88 14-09-34

Figure 4. Seismograms - X-Line (Cont'd)

# FDX4 - SHOT 2

19H 39M 49.82S DELTA = 80 00 DEG AZIMUTH = 295 00 DEG DISTANCE = 0 58 KM MAX AMPL. (CM/SEC) =  
5 MAY 1986

RADL

0.1414  $\times 10^{-1}$

SPZ

0.1276  $\times 10^{-1}$

0.0 0.4 0.8 1.2 1.6 2.0 2.4  
TIME (SECCNDS)

11-JUL-88 14-10-45

Figure 4. Seismograms - X-Line (Cont'd)

# FDX4 - SHOT 3

20H 3M 39 82 S DELTA= 80 00 DEG AZIMUTH= 295 00 DEG DISTANCE= 9 59 KM MAX AMPL. ( CM SEC ) =  
5 MAY 1986

RADL

0 2416  $\times 10^{-1}$

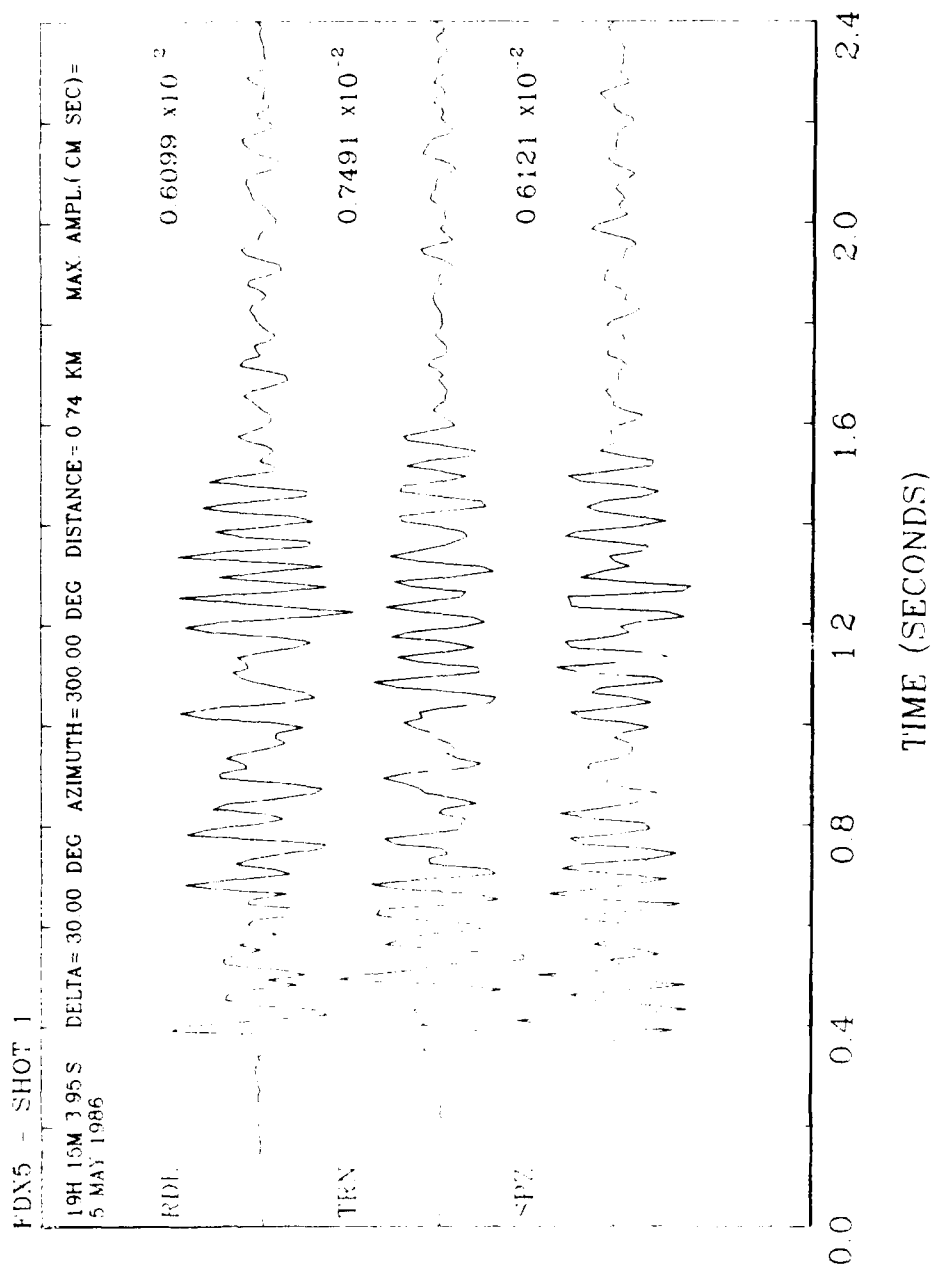
SPZ

0 2400  $\times 10^{-1}$

0.0 0.4 0.8 1.2 1.6 2.0 2.4  
TIME (SECONDS)

11-JUL-88 14-11-50

Figure 4. Seismograms - X-Line (Cont'd)



11-JUL-88 14-13-23

Figure 4. Seismograms - X-Line (Cont'd)

FDN5 - SHOT 2

19H 39M 50.95.S DELTA= 30.00 DEG AZIMUTH=300.00 DEG DISTANCE= 0.74 KM MAX. AMPL. (CM SEC)=  
5 MAY 1986

RDL

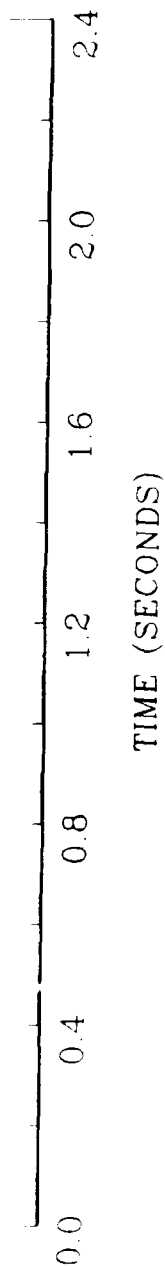
0.6001  $\times 10^{-2}$

TRN

0.7680  $\times 10^{-2}$

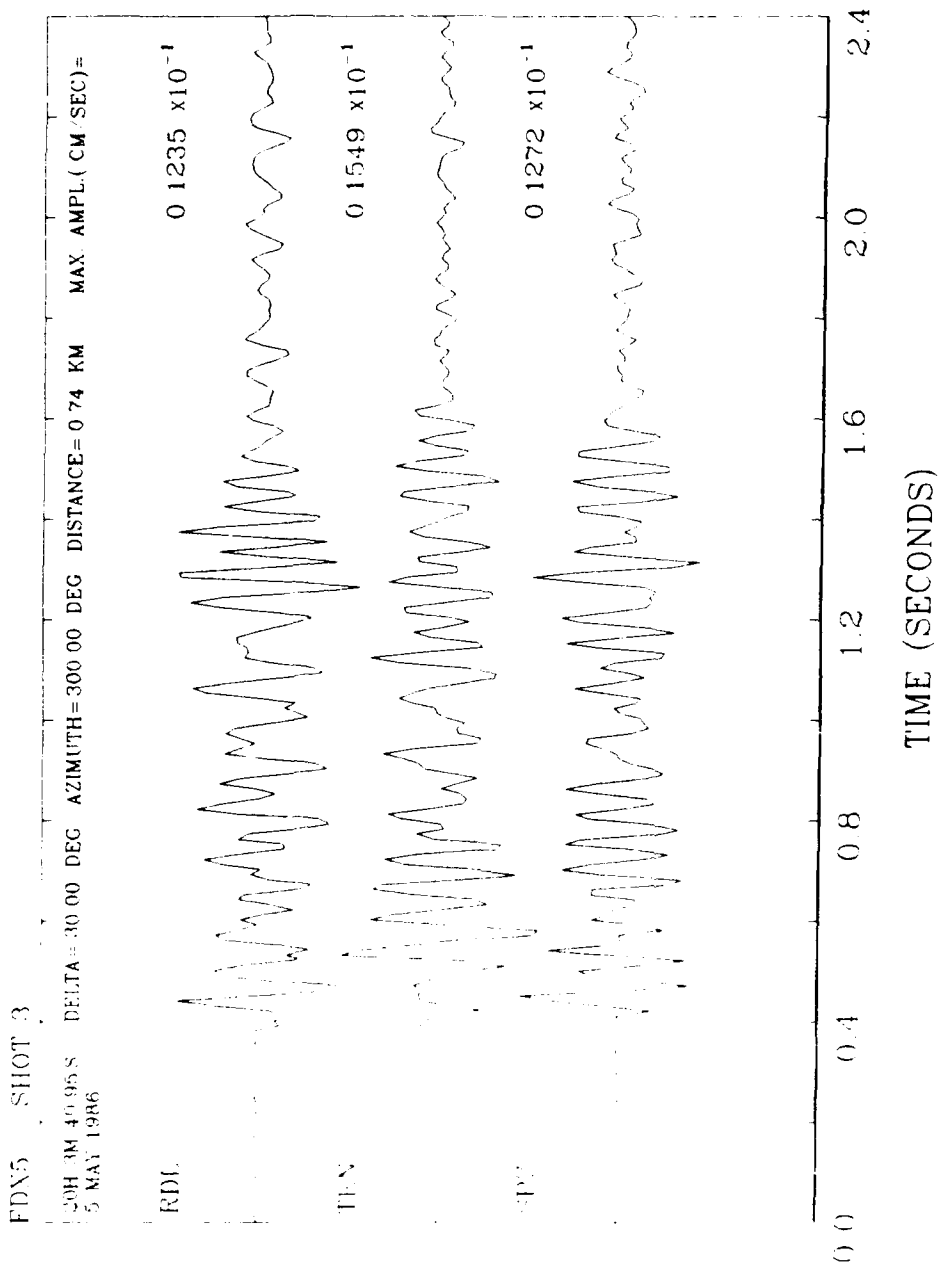
SPZ

0.5916  $\times 10^{-2}$



11-JUL-88 14-15-19

Figure 4. Seismograms - X-Line (Cont'd)



11-JUL-88 14-16-21

Figure 4. Seismograms - X-Line (Cont'd)

FDX6 SHOT 1

19H 15M 3.77S  
5 MAY 1986

DELTA = 0.00 DEG AZIMUTH = 305.00 DEG DISTANCE = 0.89 KM MAX. AMPL. (CM SEC) =

RDI

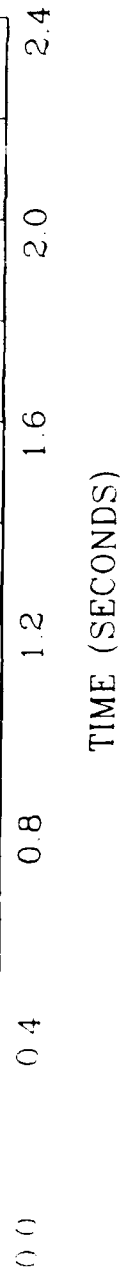
0.6711  $\times 10^{-2}$

TEN

0.3701  $\times 10^{-2}$

SPZ

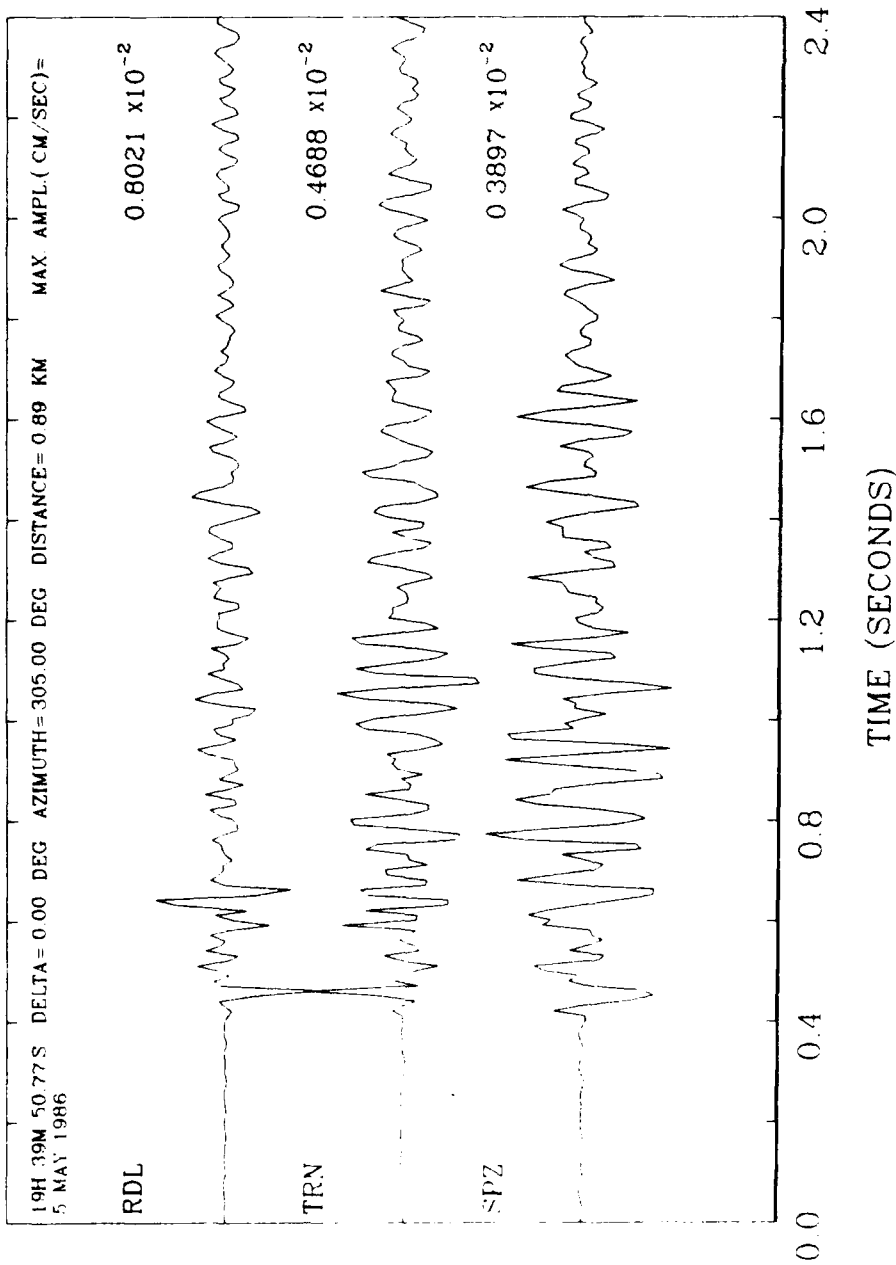
0.3811  $\times 10^{-2}$



11 JUL-88 16-46-54

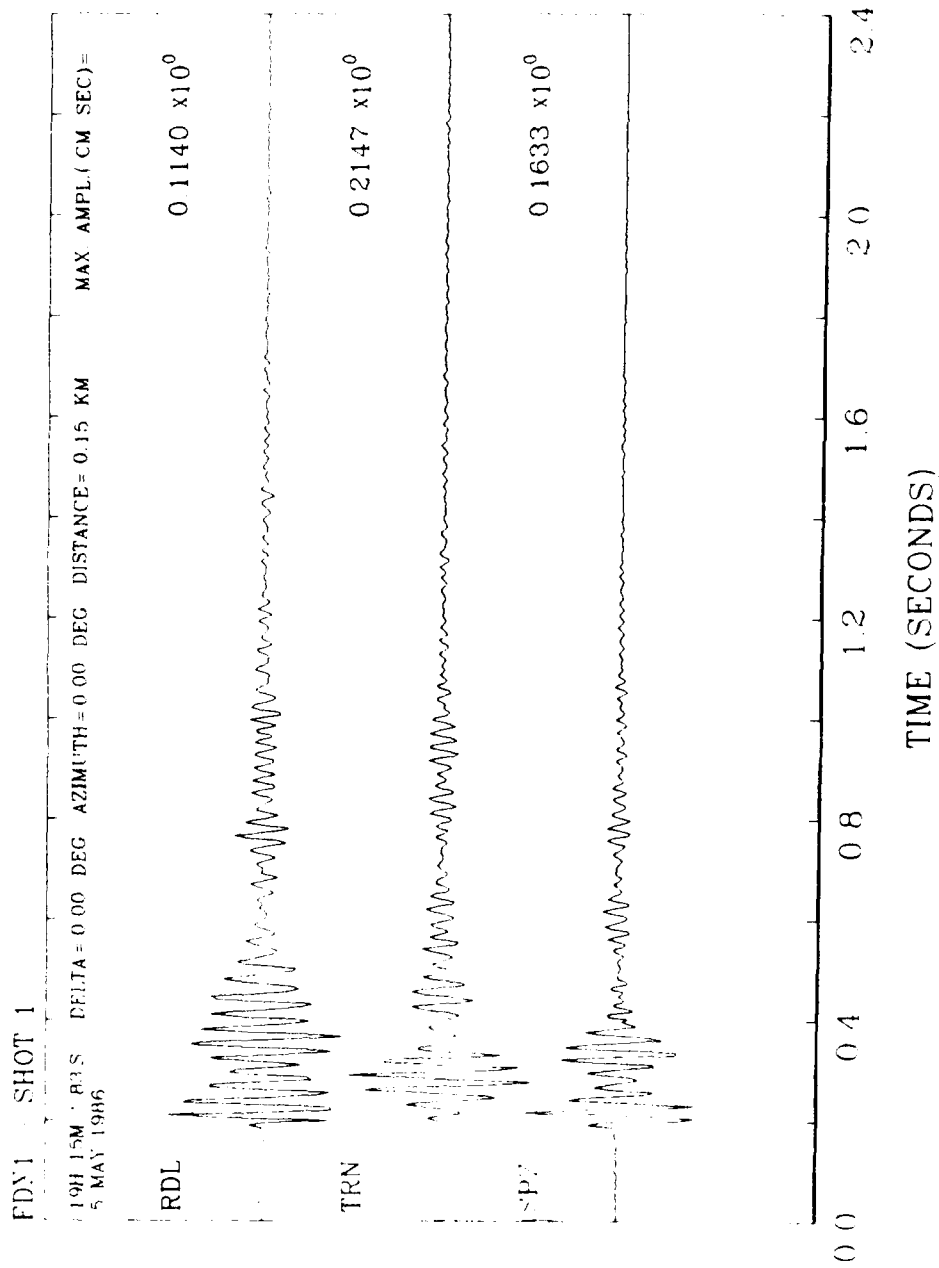
Figure 4. Seismograms - X-Line (Cont'd)

# FDX6 - SHOT 2



11 - JUL - 88 14 - 18 - 12

Figure 4. Seismograms - X-Line (Cont'd)

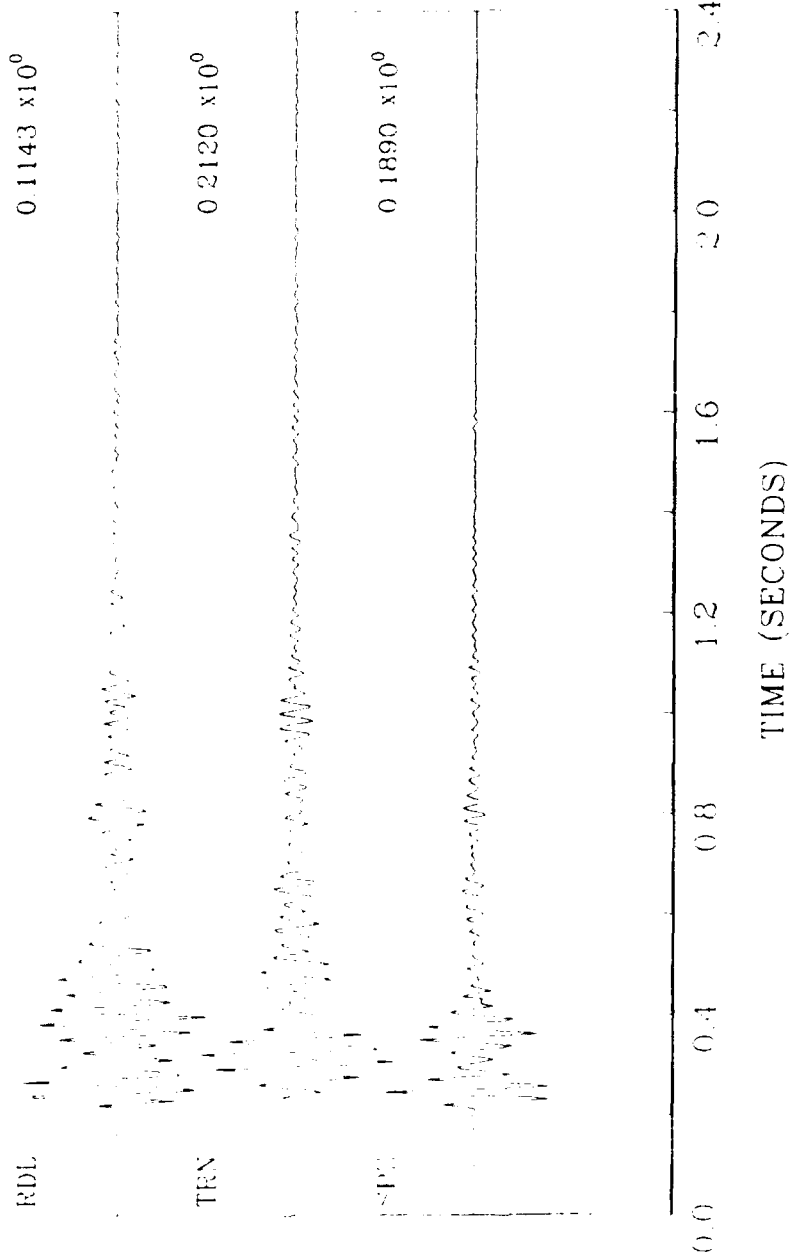


7 JUL 88 15 10 55

Figure 5. Seismograms - Y-Line

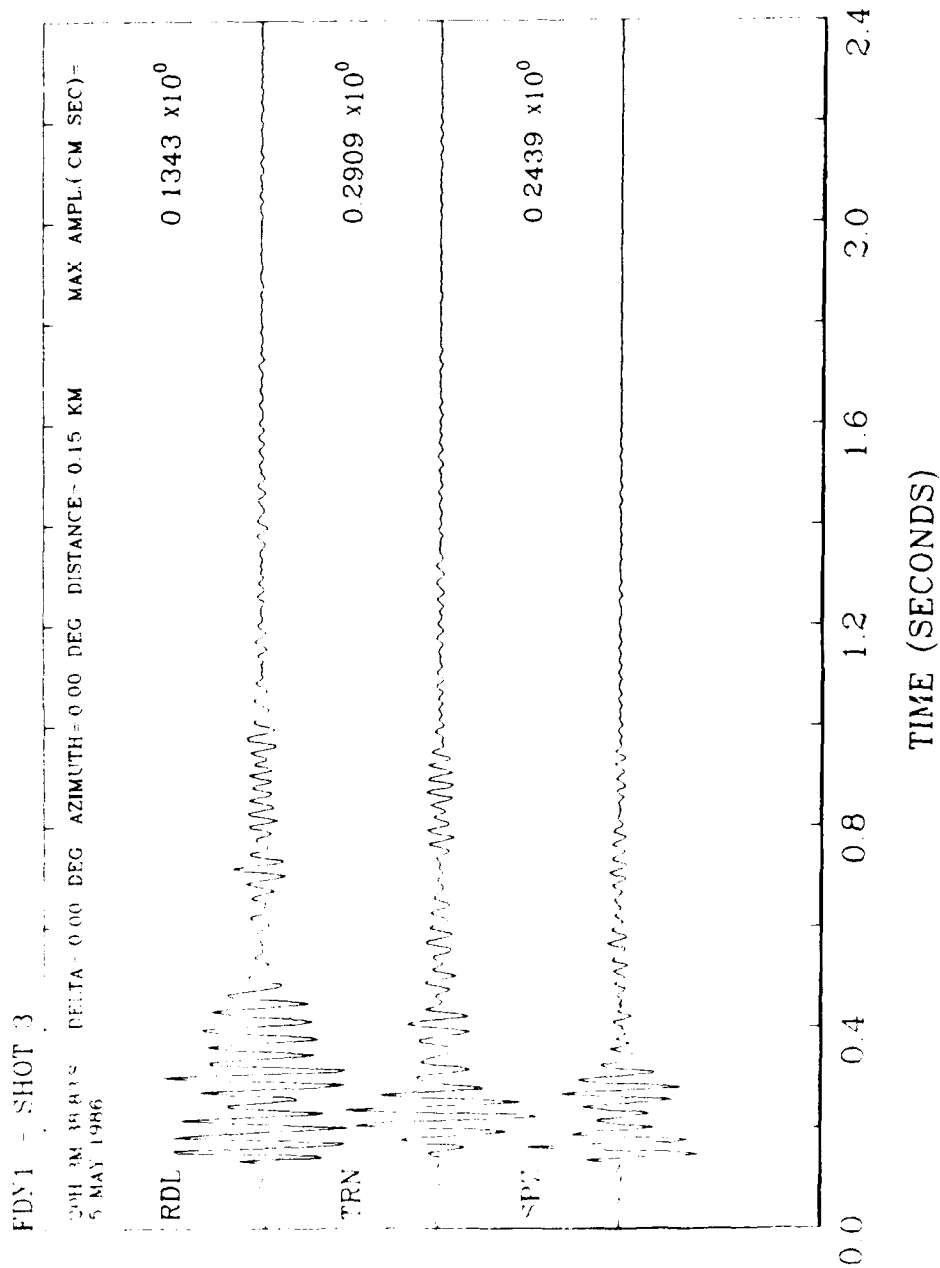
# FDY1 - SHOT 2

194 CM 48 BC DELTA 0.00 DEG AZIMUTH 0.00 DEG DISTANCE 0.15 KM MAX AMPL (CM SEC) -  
 5 MAY 1986



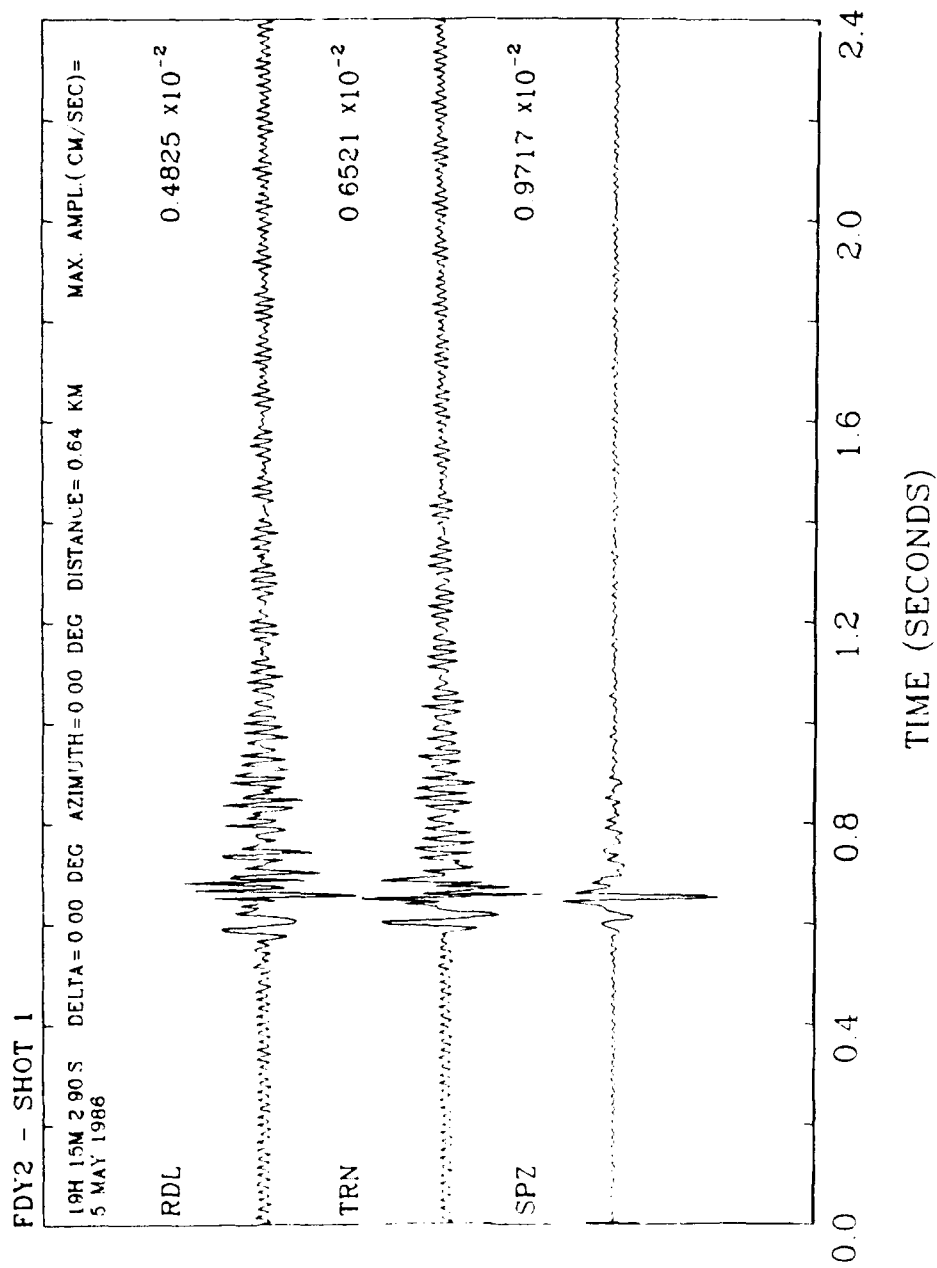
7 JUL 88 15 20 21

Figure 5. Seismograms - Y-Line (Cont'd)



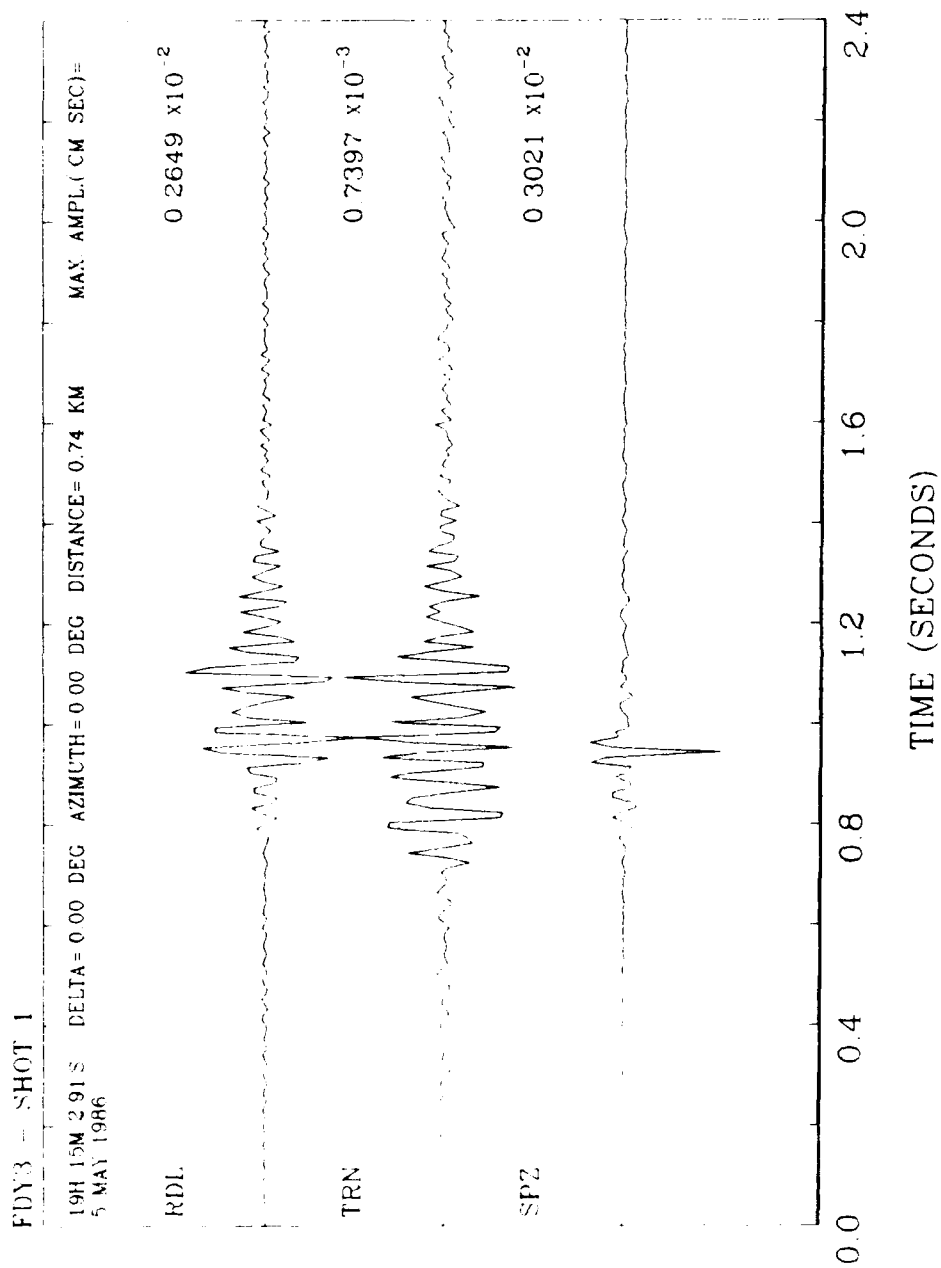
7-JUL-88 15-18-54

Figure 5. Seismograms - Y-Line (Cont'd)



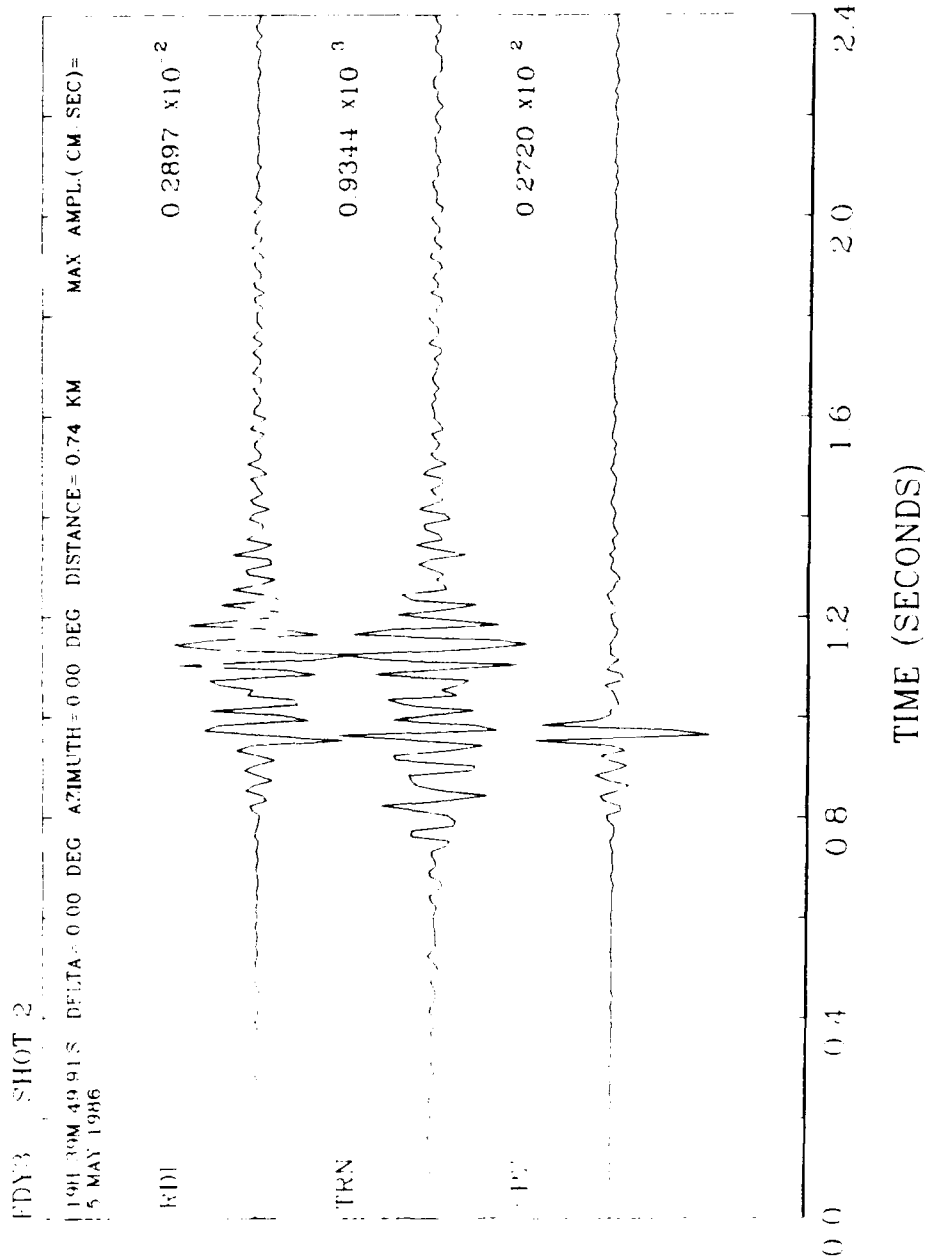
7-JUL-88 16-36-12

Figure 5. Seismograms - Y-Line (Cont'd)



7-JUL-88 16-38-57

Figure 5. Seismograms - Y-Line (Cont'd)



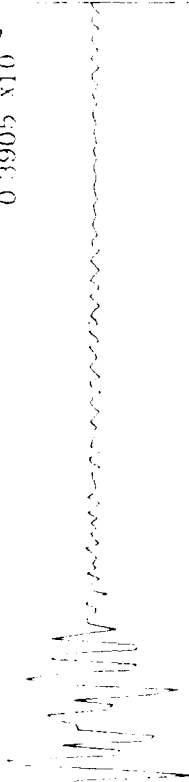
7 JUL 88 16:40:00

Figure 5. Seismograms - Y-Line (Cont'd)

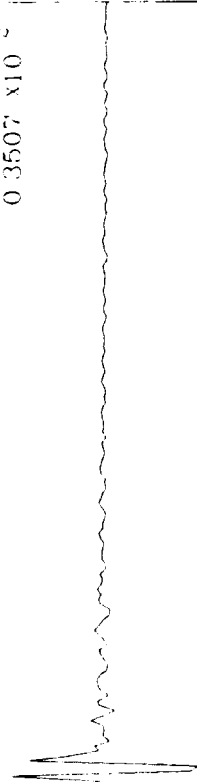
# FDY3 - SHOT 3

20H W 3491N E-LIA- 0.00 DEG AZIMUTH- 0.00 DEG DISTANCE- 0.74 KM MAX AMPL. (CM SEC) =  
 7 MAY 1986

RDI 0.3905 x10<sup>2</sup>



SP1 0.3507 x10<sup>2</sup>



0.0 0.4 0.8 1.2 1.6 2.0 2.4  
 TIME (SECONDS)

7-JUL-88 16-41-04

Figure 5. Seismograms - Y-Line (Cont'd)

effect is not seen at the closest Y-line station, FDY1. Generally, the radial component was of marginally larger amplitude than the transverse and the vertical. Explosive sources at these distances usually generate considerable radial and vertical motion. Maximum amplitudes for shots 1 and 3 (all 3 components) are plotted on Figures 6 and 7 for the X- and Y-line.

The amplitudes are scattered, but it can be seen that the X- and Y-lines have similar values on the ground zero side (less than 350 m) of the Y-line hill and the values begin to diverge after that. In fact, at the 750 m range the Y-line amplitudes are less than the X-line amplitudes by a factor of approximately 3 on instruments with similar response characteristics. Attenuation with distance should not be measured from this plot since a change in instrumentation occurs in the middle of the lines.

Mederis<sup>4</sup> fit peak amplitudes of velocity to curve of the form

$$V = aL^bW^c \quad (1)$$

where V is the peak ground velocity in inches/per second, L is the distance to a detonation (in feet) and W is the explosive weight in pounds. For the vertical component, the arbitrary constants, a, b, and c are 69.2, -1.37, and 0.59 respectively, with a standard error of 2.10. These values were obtained using in-ground or surface shot data primarily from quarries, but the predictions conform within the error to measurements of the aerial shots used in this report for the flat X-line.

Additionally, ratios of maximum amplitude at the same station for different shots reveal that doubling the amount of explosive increased the observed amplitudes by a factor of 1.1 to 1.5. (The higher factors corresponded to the Y-line stations sheltered by the hill). Nicholls et al<sup>5</sup> found similar results for scaled distance versus overpressure for a range of shot sizes.

Amplitude spectra for vertical components (shot 1) seismograms that appear in Appendix C show variation of peak energy with frequency. This is a reflection of the different instrument responses. The spikes in the spectra at approximately 50 Hz for FDX1, FDX2, and FDY2 are a result of a malfunction in the recorders (this high frequency noise can be observed on the seismograms). Most of the records exhibit peaks in their seismic spectra between 10 and 25 Hz. An exception is FDX3 shot 1 which peaks at 60 Hz. Completely unexplained is the large dip in the FDY3 spectrum at 22 Hz. A less pronounced dip can be observed on the other Y-line stations. It may be the result of destructive interference between a direct acoustic induced wave at the station and air coupled seismic waves that originate on the blast side of the hill and travel on multiple paths. In a seismic/acoustic study at Vandenberg AFB, Battis<sup>6</sup> found that for similar sized explosions at a distance of 300 m, the energy peaked at approximately 18 Hz. Peaks at this frequency are evident in some of the spectra, however many of the characteristics remain unexplained at this time. If the experiment were to be repeated, varying the position of the shot, at least in the vertical direction, would help to unravel the complexities of the spectra and seismic waveforms.

- 
4. Medearis, K. (1979) *Dynamic Characteristics of Ground Motions Due to Blasting*, Bull. Seis. Soc. Am., **69**(No. 2):627-639.
  5. Nicholls, M.R., Johnson, C.F., and Duval, W.I. (1971) *Blasting Vibrations and Their Effects on Structures*, Bulletin 656, US Dept. of the Interior, Bureau of Mines, pp. 65-66.
  6. Battis, J.C. (1985) *Vibro-Acoustic Forecasts for STS Launches at V23, Vandenberg AFB: Results Summary and the Payload Preparation Room*, AFGL-TR-85-0013, ADA162192.

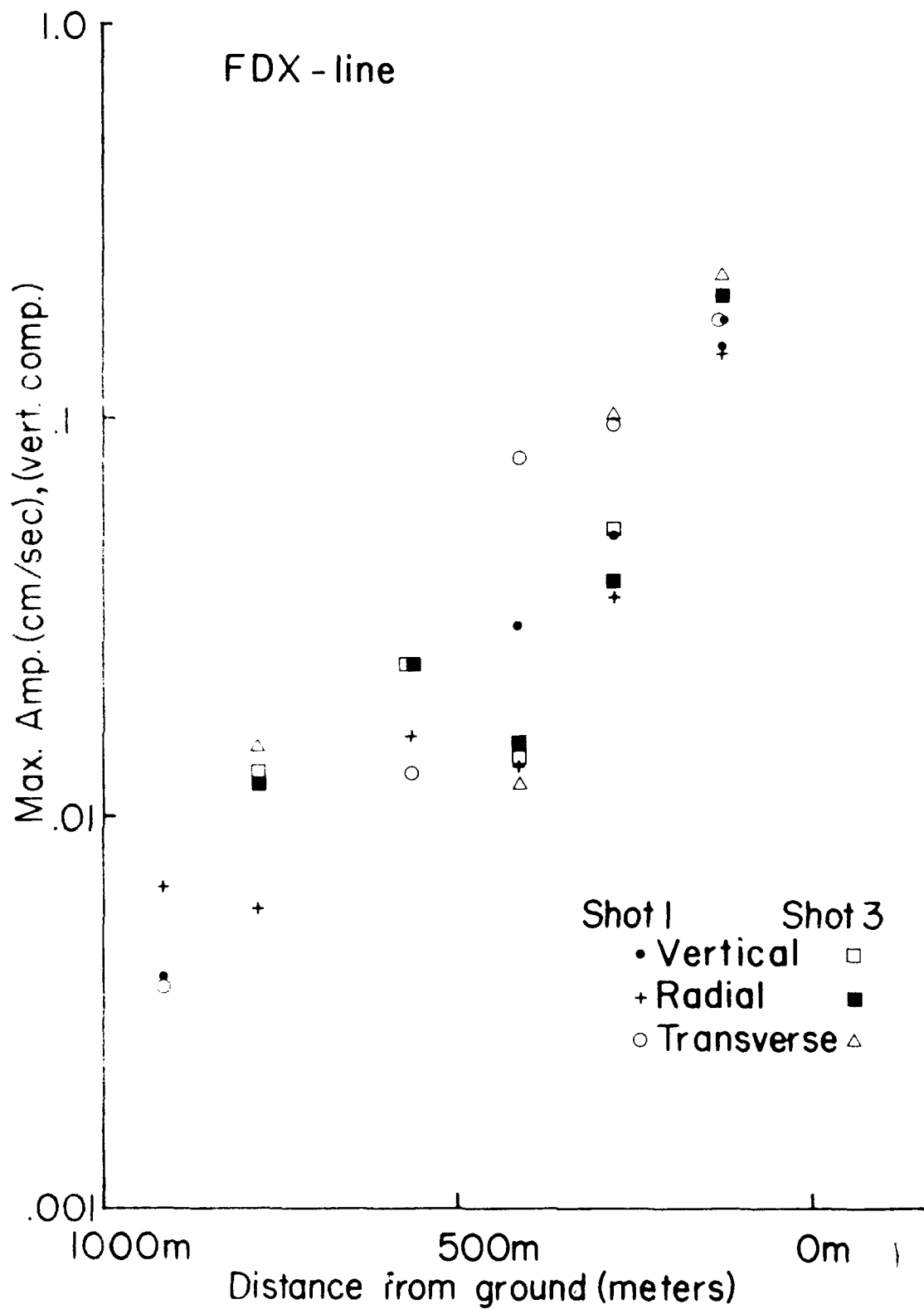


Figure 6 - Maximum Amplitude vs Distance - X-Line

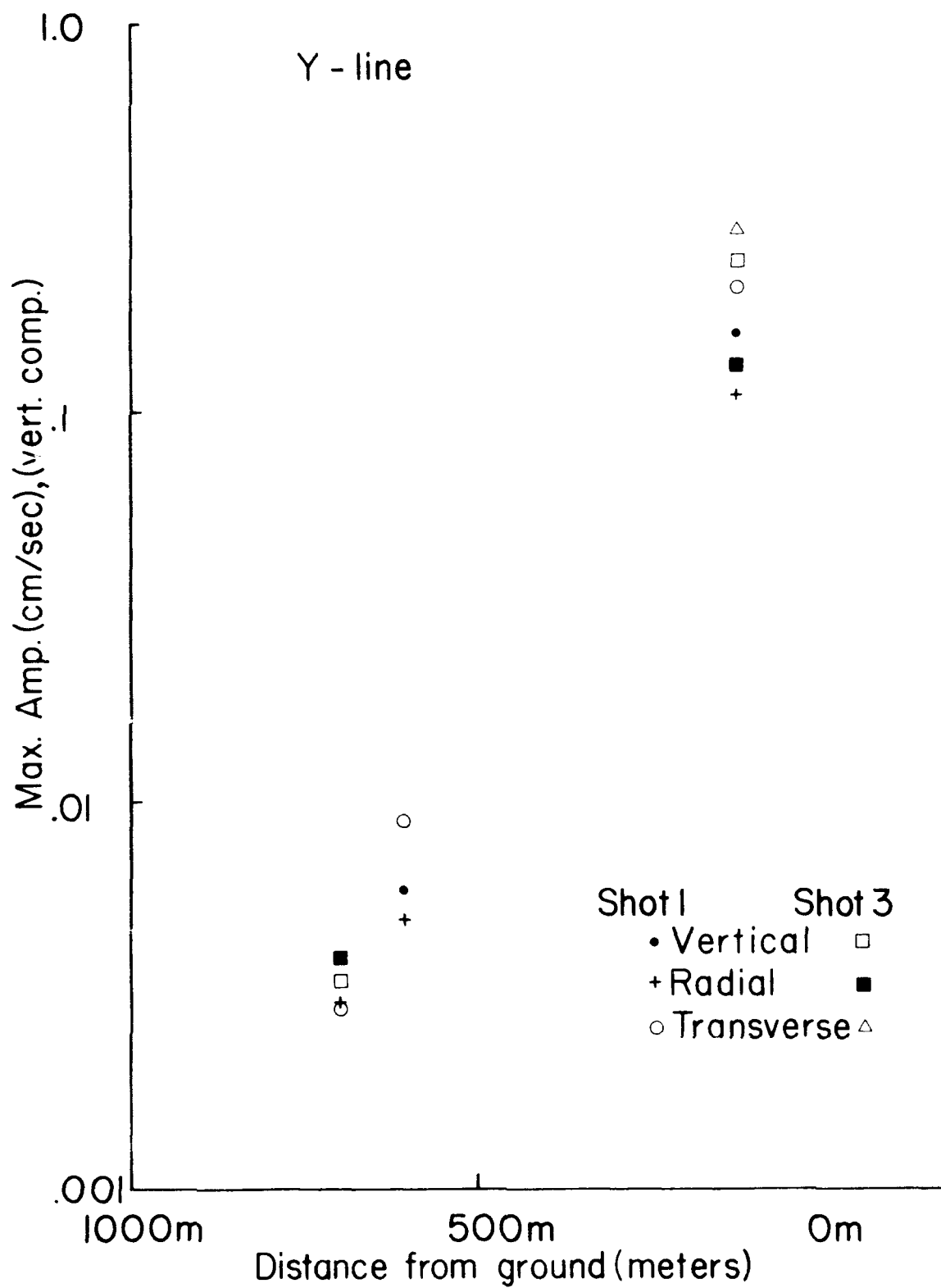


Figure 7. Maximum Amplitude vs Distance - Y-Line

A particle motion plot of FDY3 shot 1 is included in the next figure. Figures 8a, b, c, d, e, and f are particle-motion plots of selected stations. To understand these plots, consider Figure 8a, Station FDX1 (the closest station). The boxed area delineates the part of the waveform analyzed. The bottom 2 plots show that there was little transverse motion generated and that the rays came from the east-west (that is radial) direction. This pattern is repeated in Figure 8b, station FDX 2. As the box moves further into the waveform (Figure 8c), transverse motion begins to appear. In Figures 8d, e, and f, transverse motion is already apparent in the first motion portion of the record. Generally, the main cause of observed transverse motion from explosive sources is scattering of the waveforms by inhomogenieties along the ray path or reflections from a surface or boundary. Pressure waves, which are shown in idealized form in Figure 9, can be reflected off sides of hills, trees, and cloud layers. The shot day was clear, free of reflecting clouds. Figure 10 illustrates how the pressure wave from the explosions might reflect off the side of the Y-line hill and possibly off the trees defining the north-south boundary of the wooded area. However, in this experiment there was no evidence of reflected acoustic energy on the pressure recordings. Figures 11 and 12 are record section plots using the vertical components for the X- and Y-lines, shots 1, 2, and 3. These plots are vertical seismogram components stacked in order of their distance from the source. The horizontal axis is "reduced time", which is computed by taking the observed travel time and subtracting the recording station's distance from the source divided by an estimate of the speed of the wave that is measured across the line.

Several points are apparent from these plots. First, station FDX5 has an obvious timing error. The change in frequency content of the waveforms between FDX3 and FDX4 and between FDY2 and FDY3 can be explained by the different instrumentation. (For close in stations the 200 sample per second recorders were paired with the 2 Hz natural period seismometers because the highest frequency signals were expected closer to the source.) For the X-line, a reduction velocity of 0.39 km/sec is shown. This lines up the waveforms of the first three stations, but FDX4 and FDX5 appear to be arriving late. This would suggest that either a slightly slower reduction velocity should be used or the propagation characteristics change at the farther stations, or the physics of the wave propagation at the farther stations is different. A velocity of 0.39 km/sec is quite slow for propagation of seismic waves in the crust. It seems likely that at least the close in stations were recording the direct air-blast-coupled ground wave. For the Y-line, a reduction velocity of 0.33 km/sec was used for the plot. However, the smaller number of stations and ambiguity in picking the onset of first motion on the 1 Hz (100 samples per second) instruments of FDY3 and FDY4, makes this number uncertain. To understand the physics involved, the geometry of the suspended shot must be considered. For the Y-line this geometry is complicated because of the hill. For the X-line a simple example is illustrated in Figure 13. In general, if the first motion energy is caused by the impact of the acoustic wave at the recording site, then the acoustic velocity is slower than the 0.39 km/sec apparent velocity used for the X-line.

In Figures 14 and 15, the waveforms recorded by the pressure transducers are displayed. Because of equipment limitations, one recorder was used for every 3 stations. The pressure sensors were attached with long cables. This setup had the drawback that if one recorder failed information at three stations would be lost. Because of the anticipated high frequency content of the signals, the higher sampling rate recorders were slated for this operation, but some last minute equipment problems necessitated substituting a 100 sample per sec instrument at the FDY sites. There were substantial equipment failures on these pressure sensor channels. The best data consisted of the

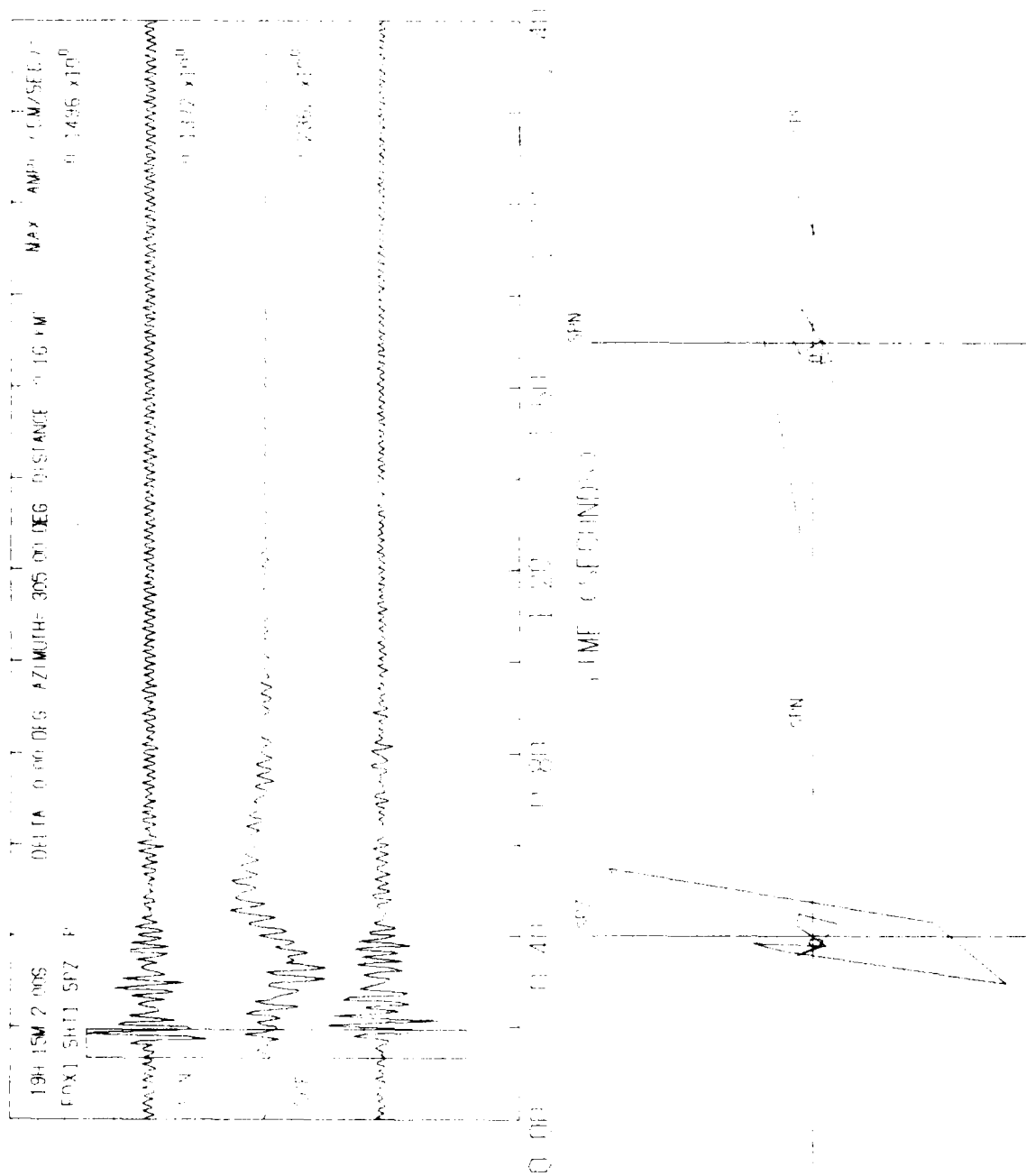


Figure 8. Particle Motion Plots

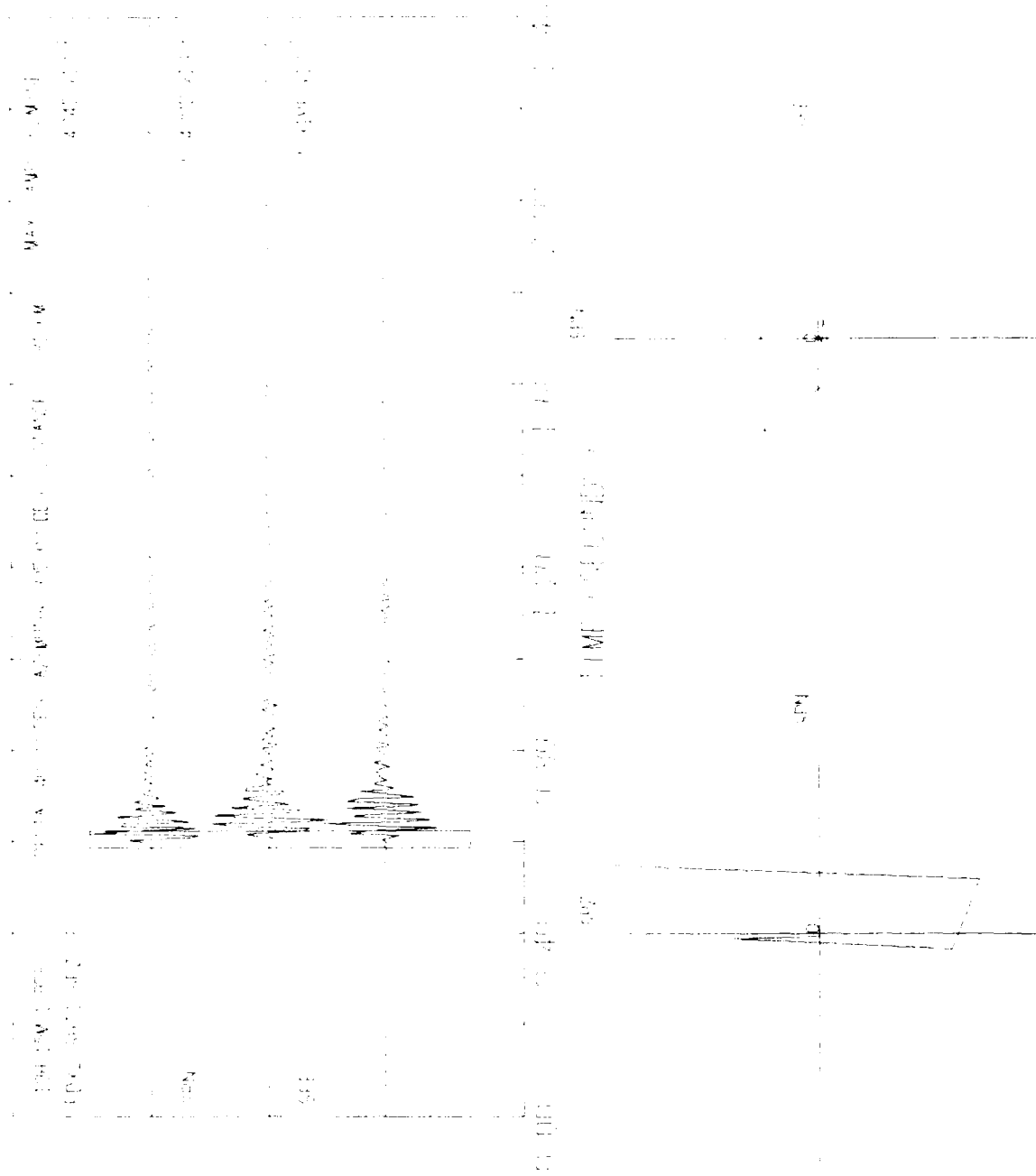


Figure 8. Particle Motion Plots (Cont'd)

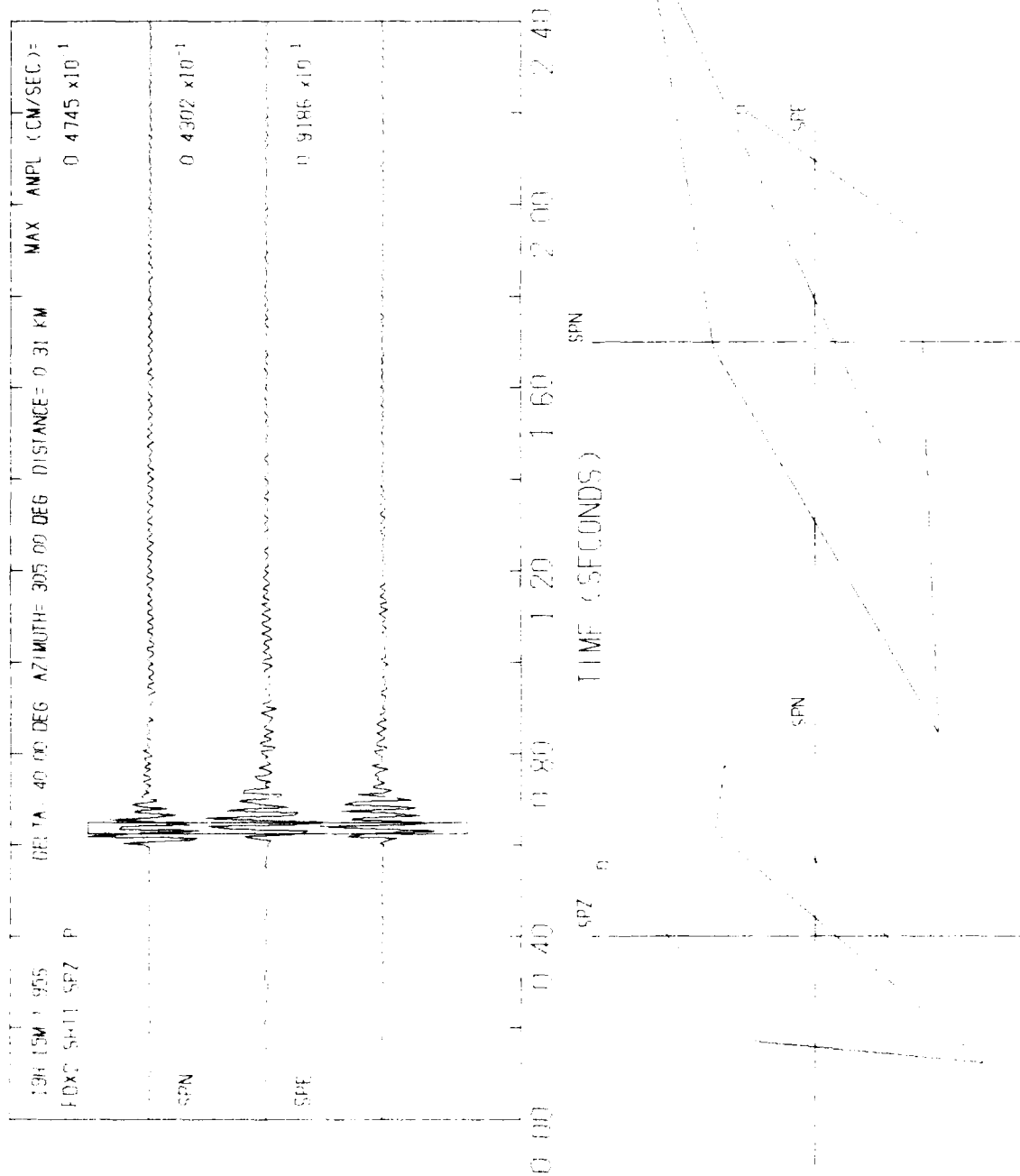


Figure 8. Particle Motion Plots (Cont'd)

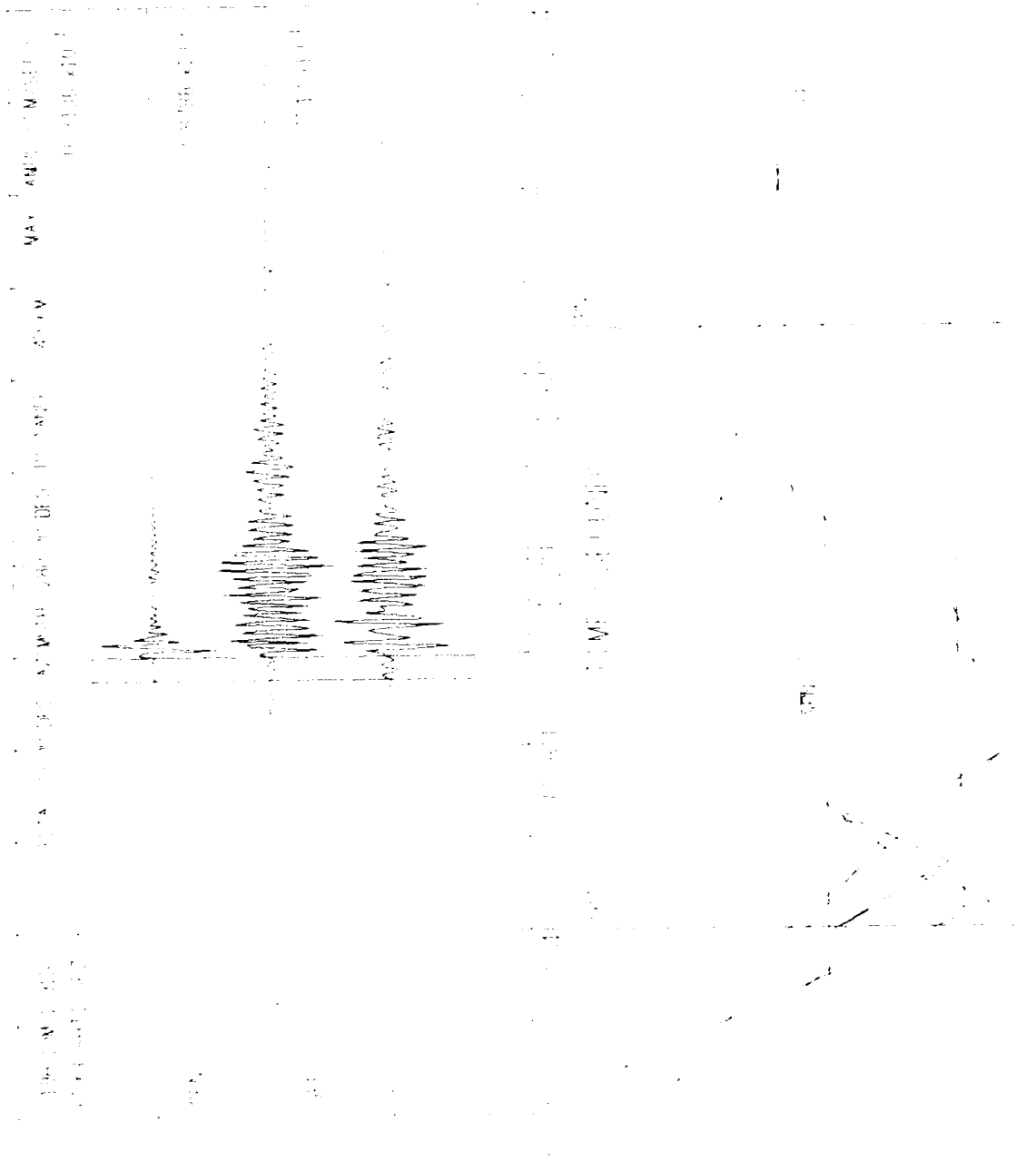


Figure 8. Particle Motion Plots (Cont'd)

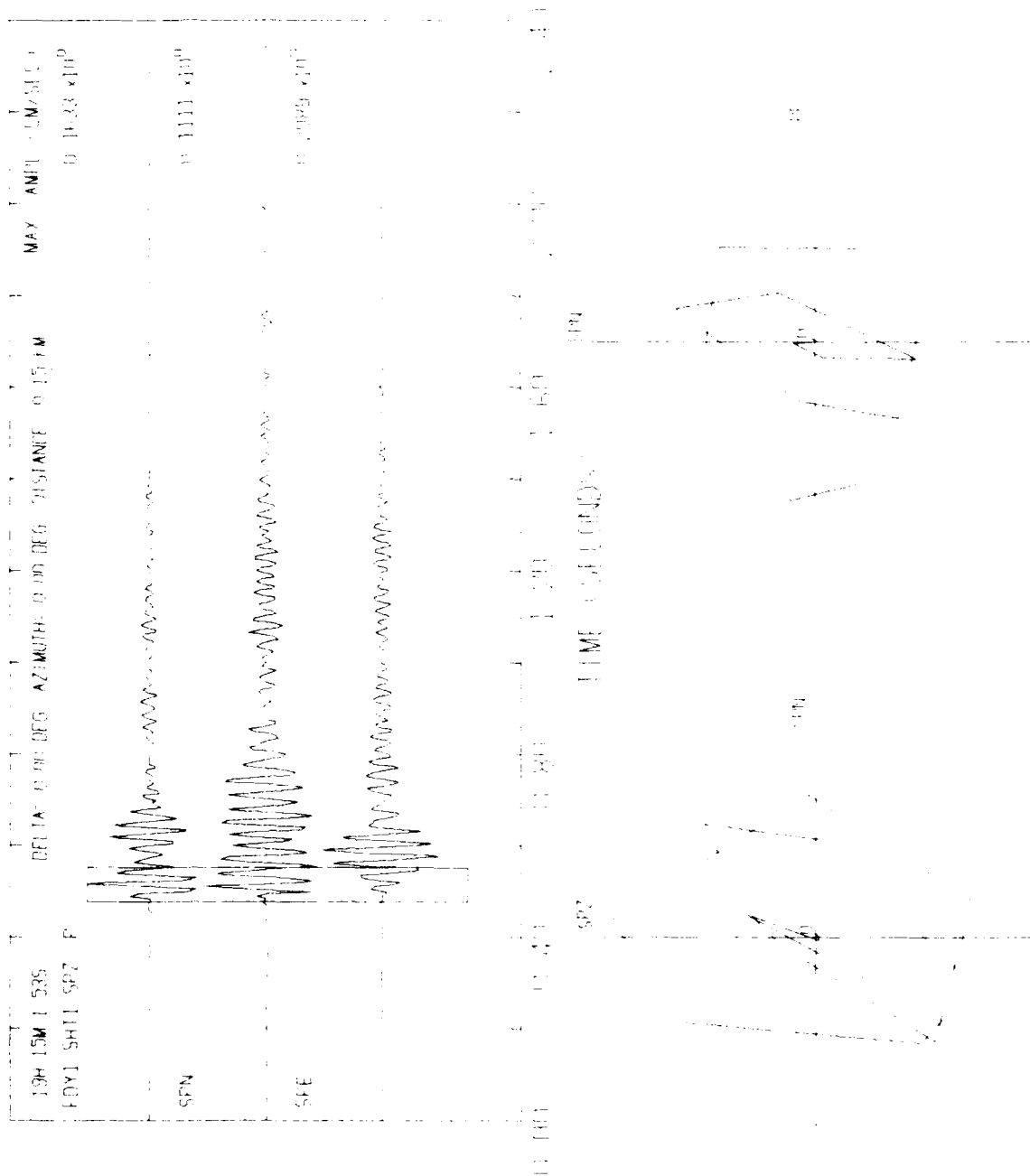


Figure 8. Particle Motion Plots (Cont'd)

Figure 8. Particle Motion Plots (Cont'd)

# IDEAL BLAST WAVE

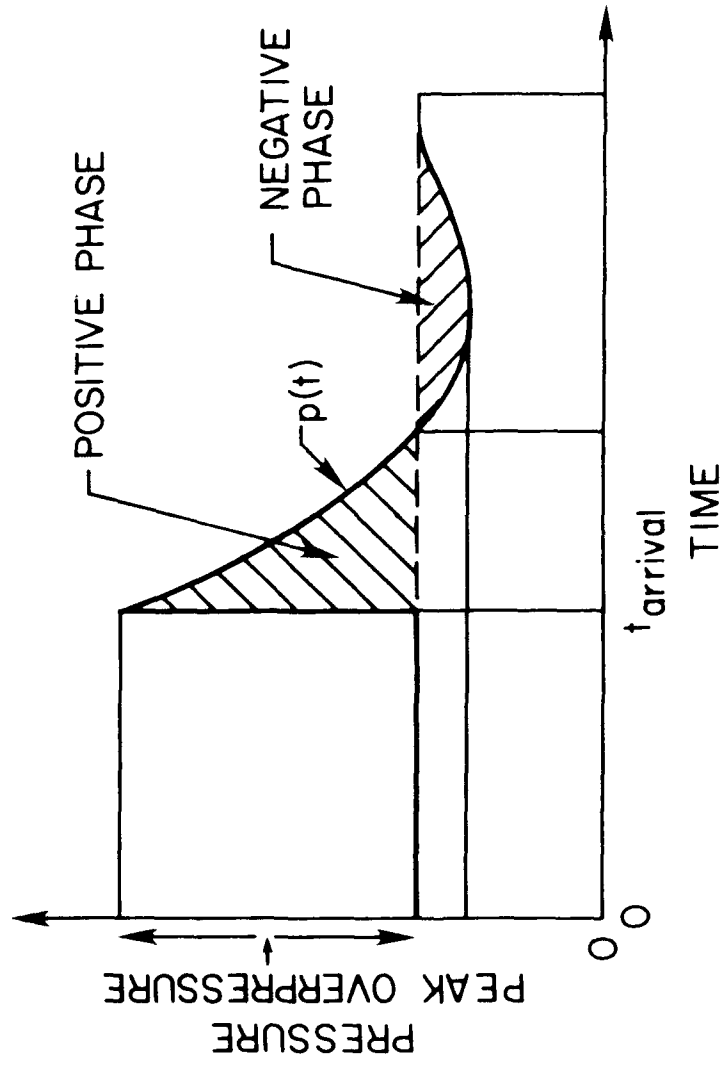


Figure 9. Ideal Blast Wave (Modified from Baker, 1973)<sup>7</sup>

7. Baker, W.E. (1973) *Explosions in Air*, University of Texas Press, Austin and London, pp 10-80.

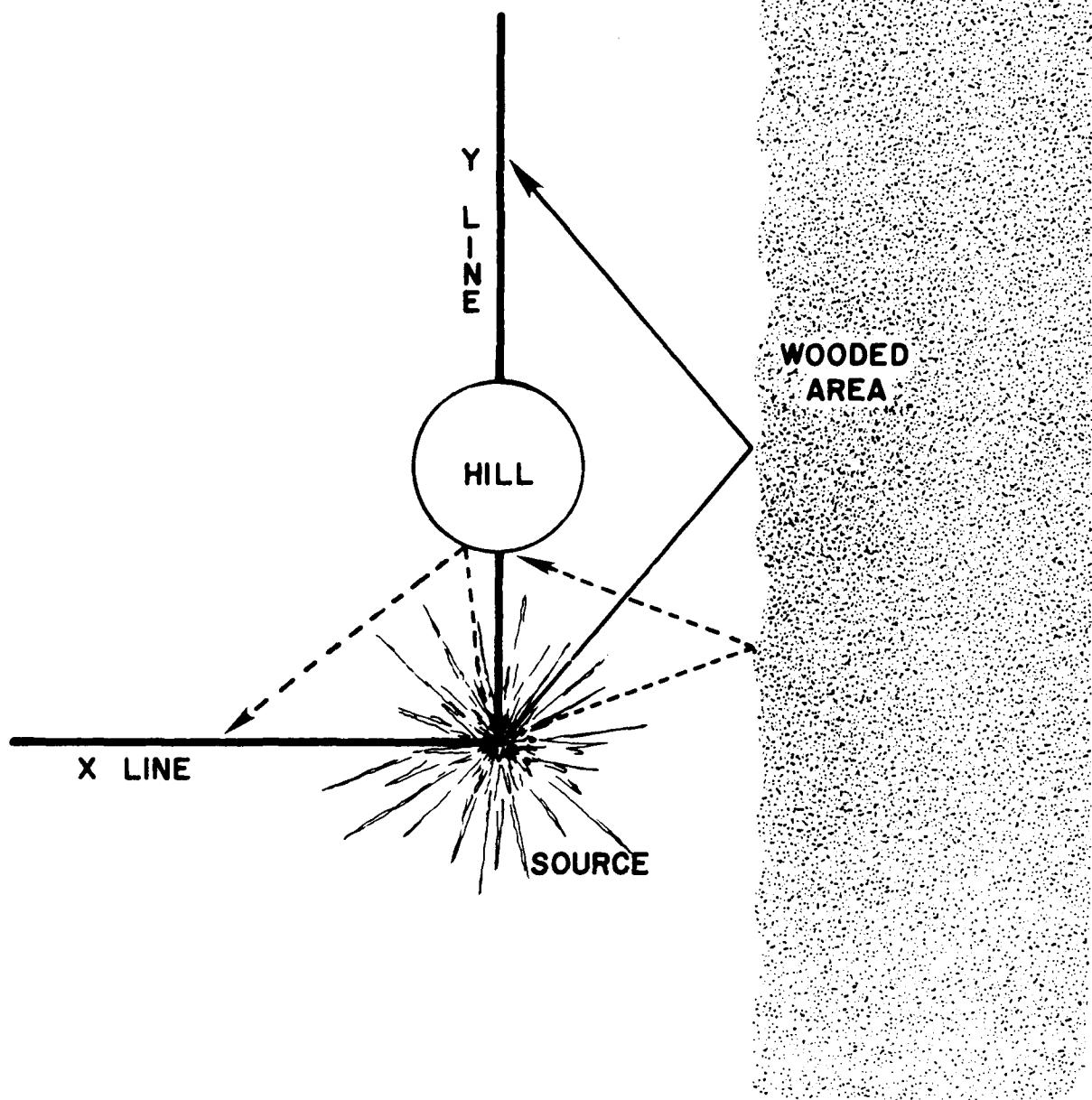


Figure 10. Possible Acoustic Wave Reflective Sources

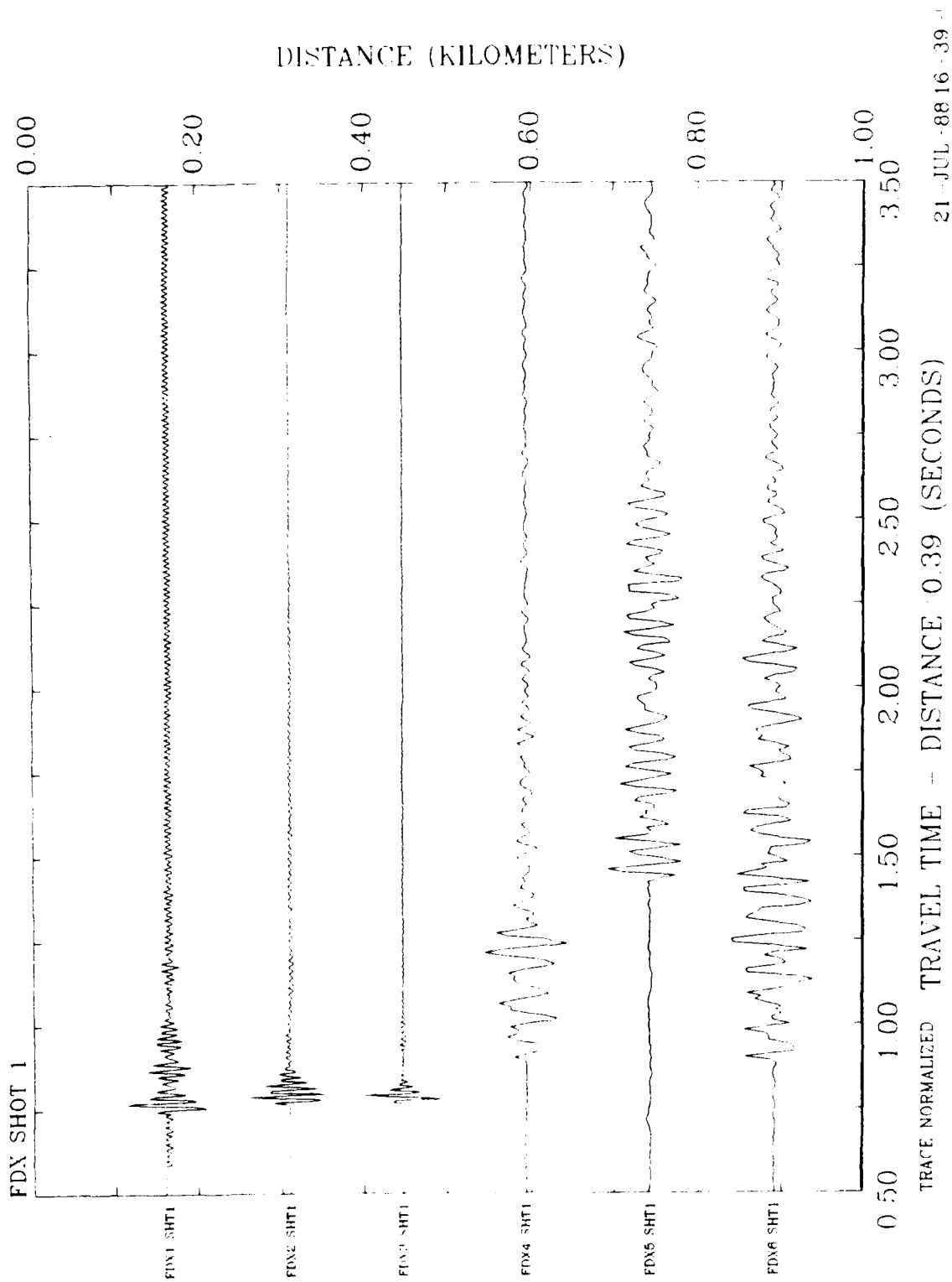


Figure 11. X-Line Record Section

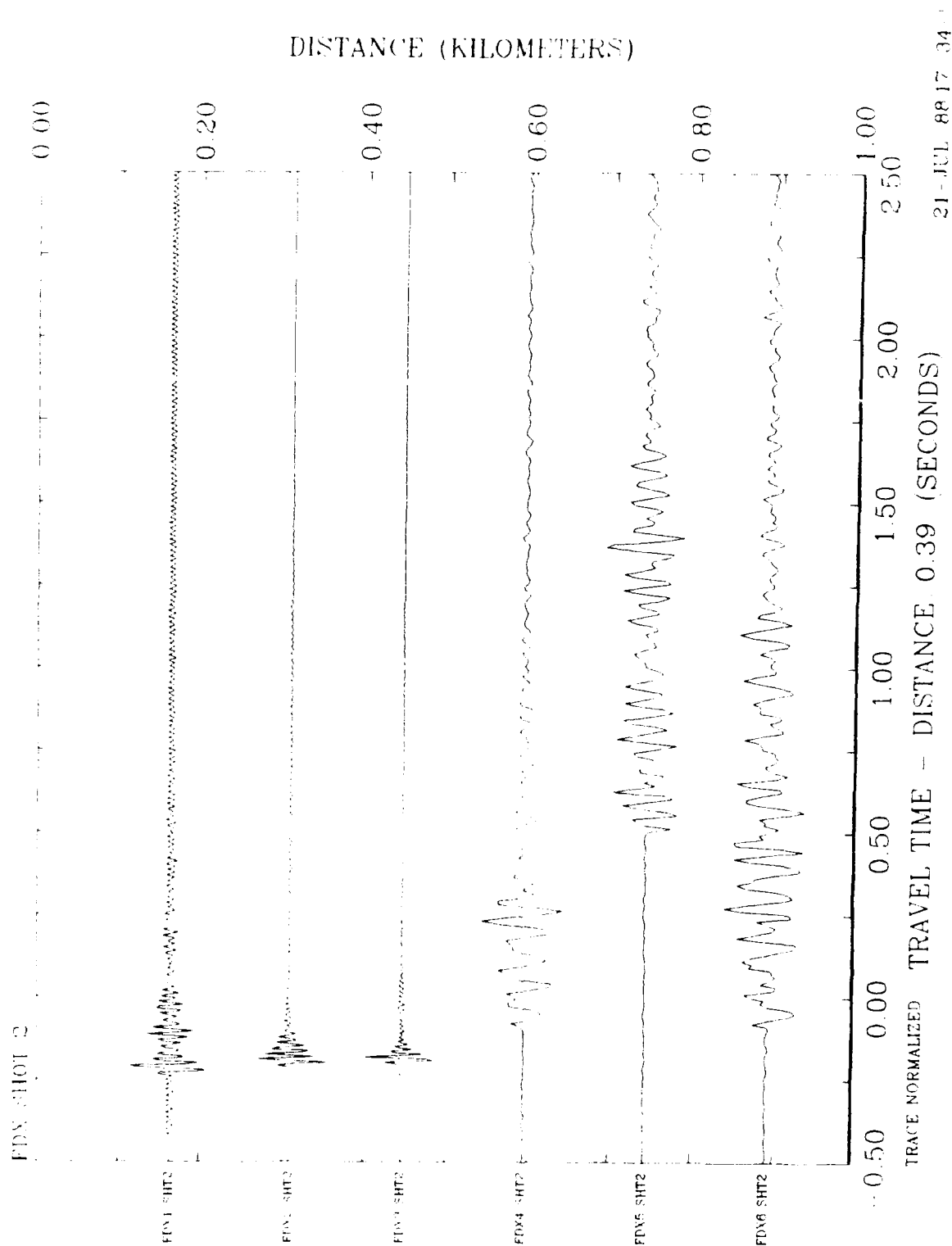


Figure 11. X-Line Record Section (Cont'd)

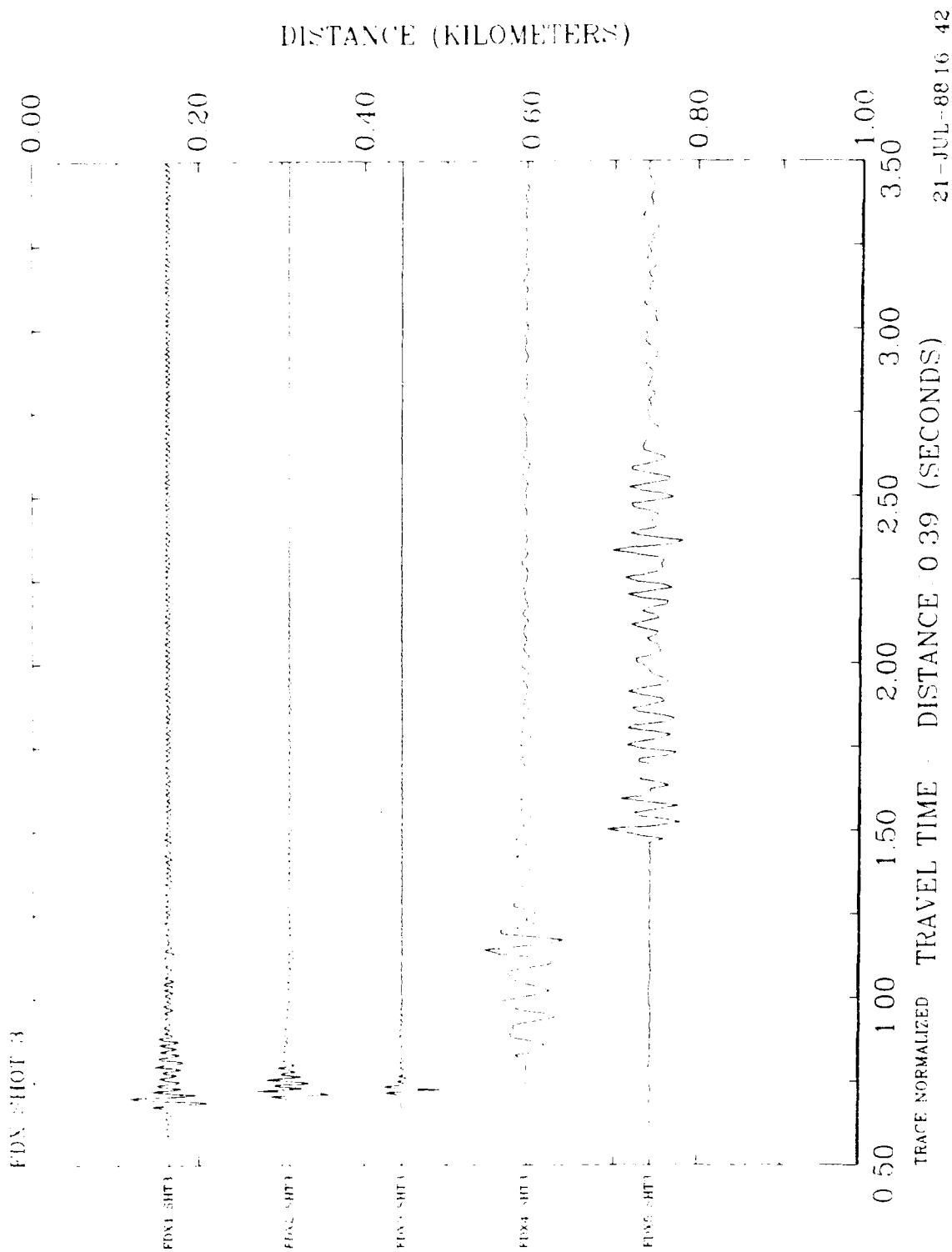


Figure 11. X-Line Record Section (Cont'd)

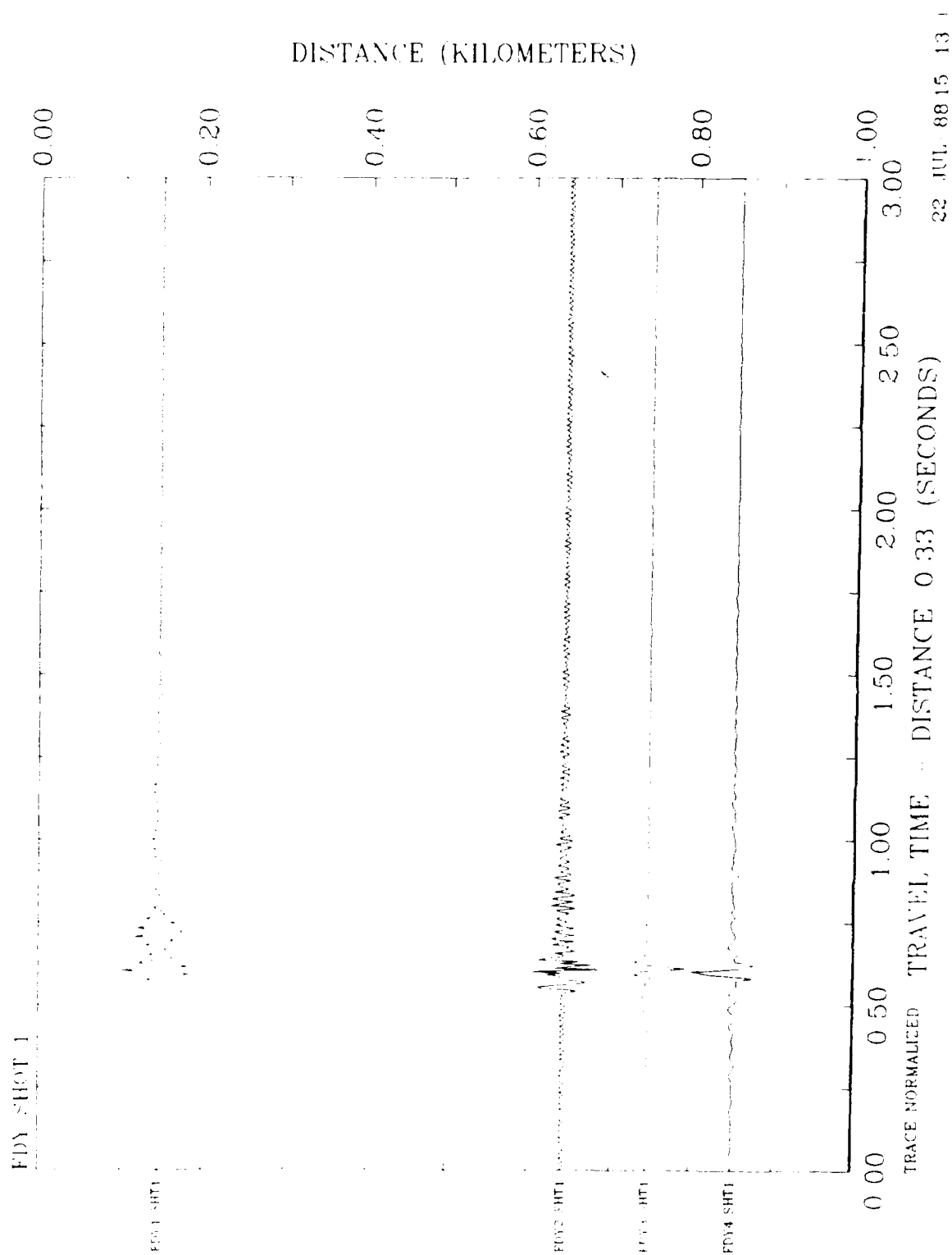


Figure 12. Y-Line Record Section

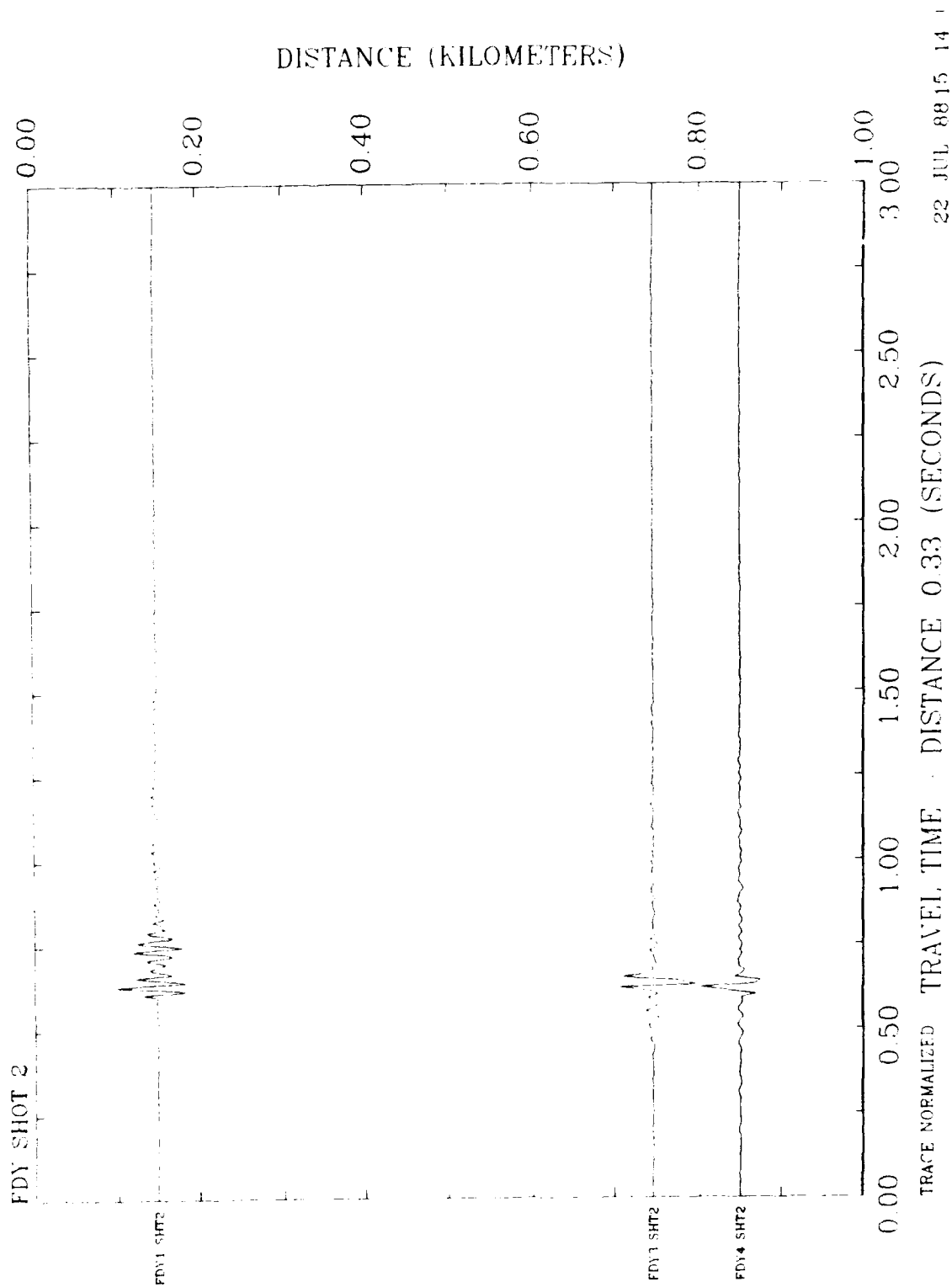


Figure 12. Y-Line Record Section (Cont'd)

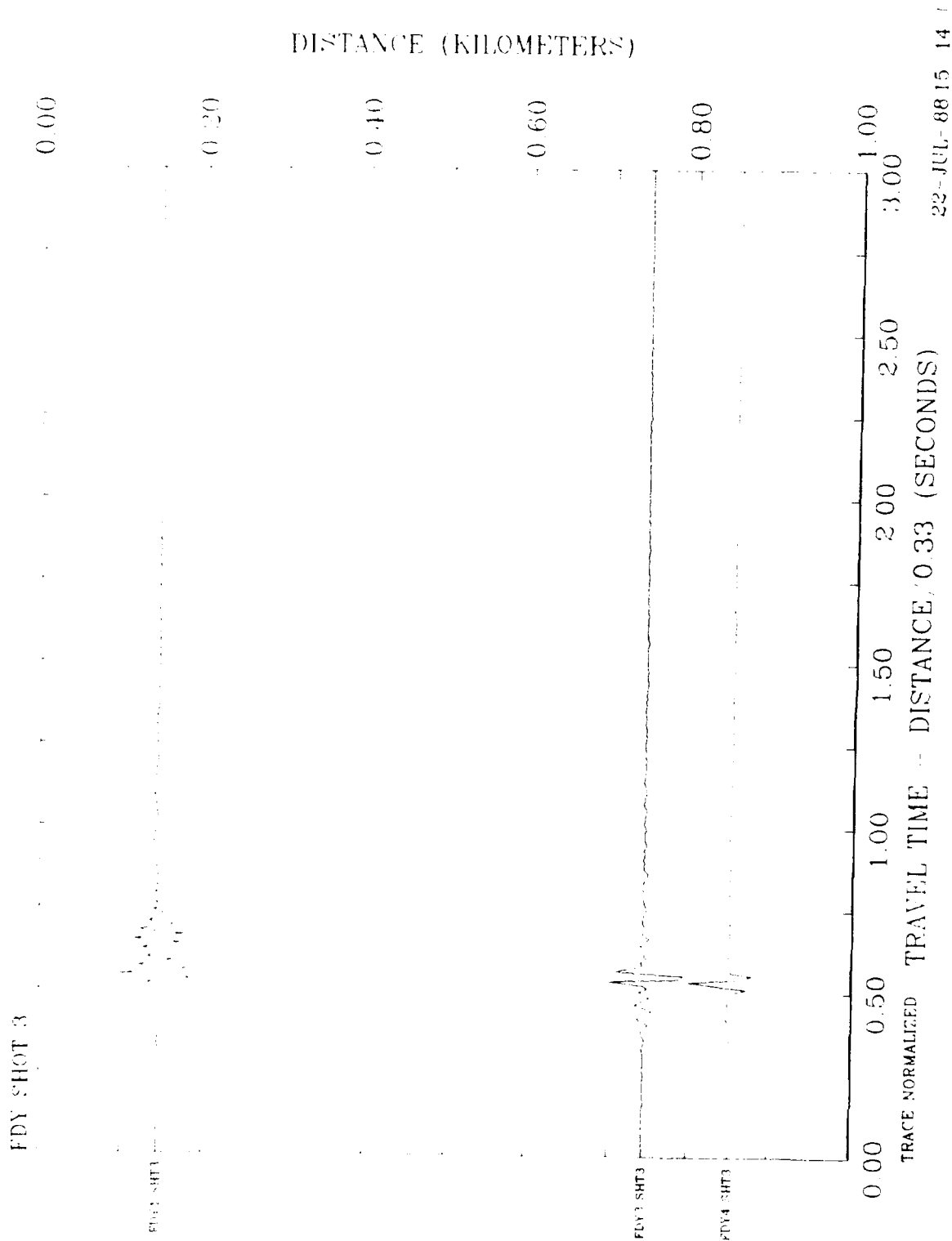
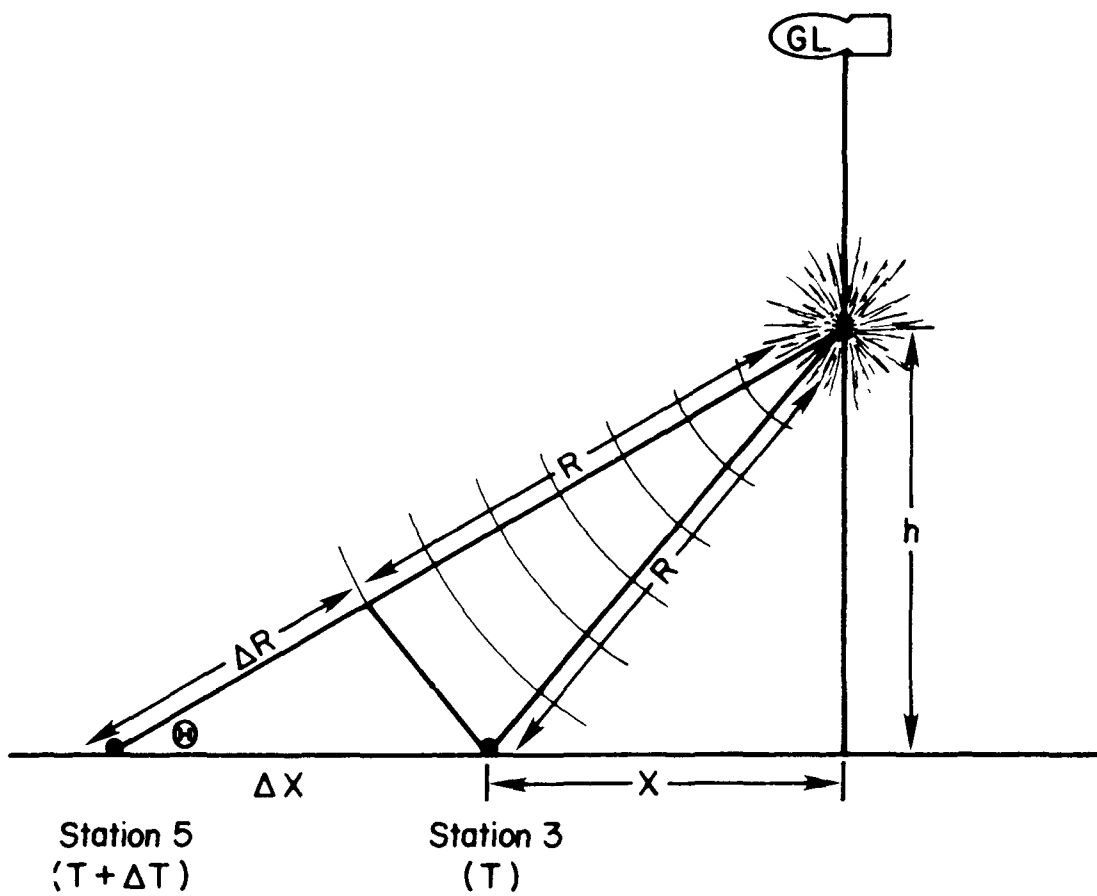


Figure 12. Y-Line Record Section (Cont'd)

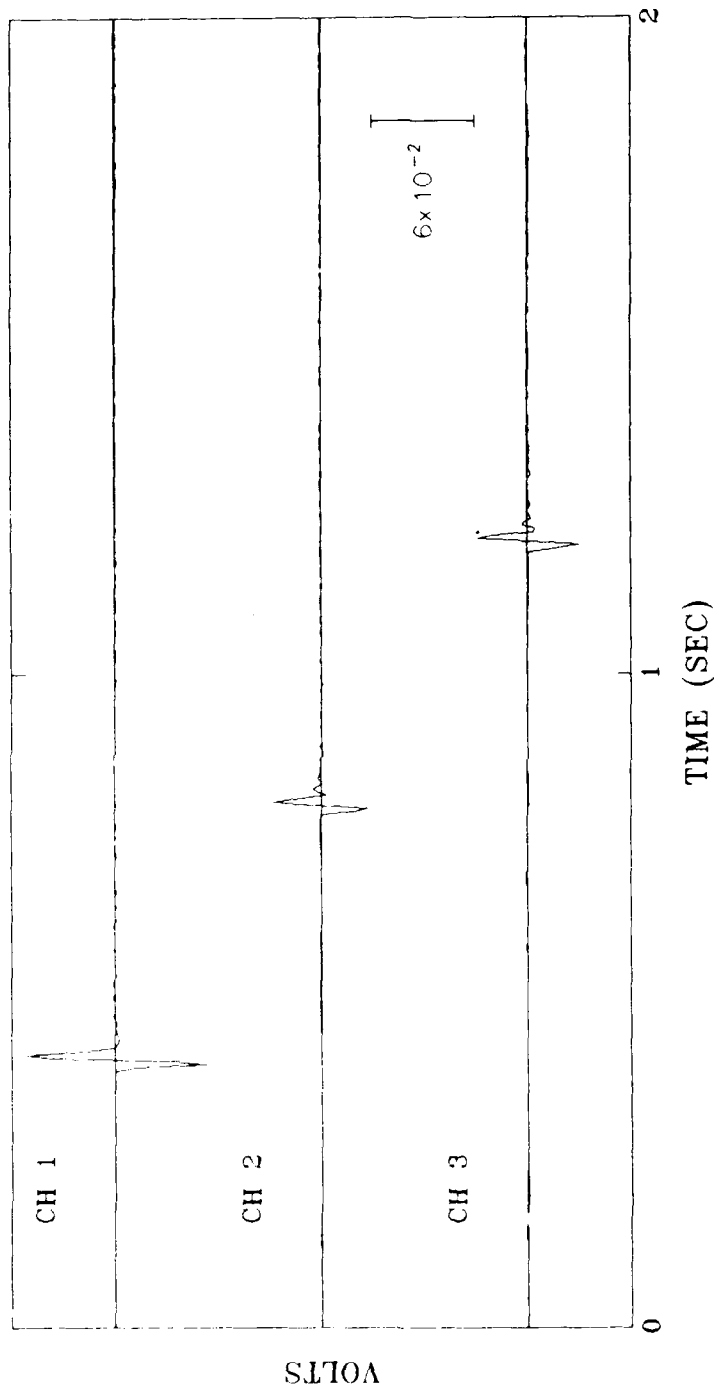


$$V_{\text{air}} = \frac{\Delta R}{\Delta T} \quad \text{where} \quad \Delta R = \frac{h}{\sin \Theta} - R$$

$$\Theta = \tan^{-1} \frac{h}{X + \Delta X}$$

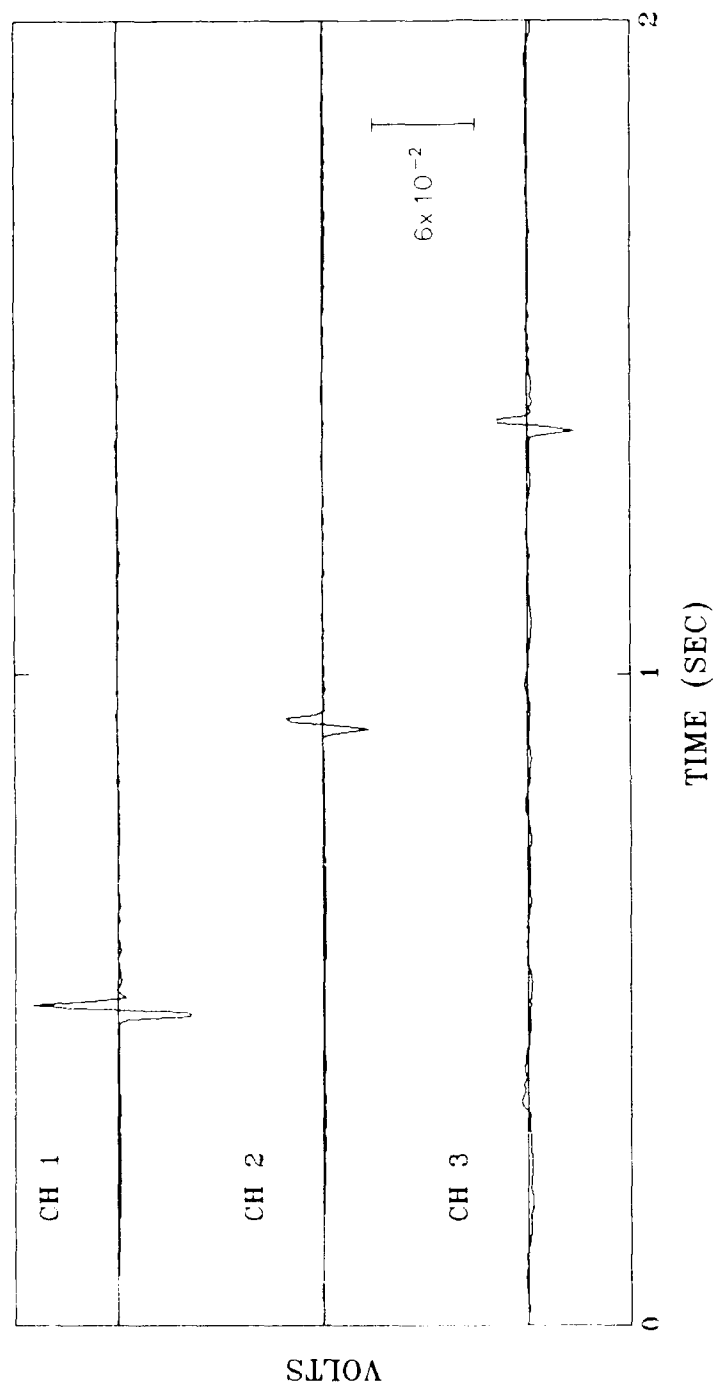
$$R = \sqrt{h^2 + X^2}$$

Figure 13. Air Wave Geometry



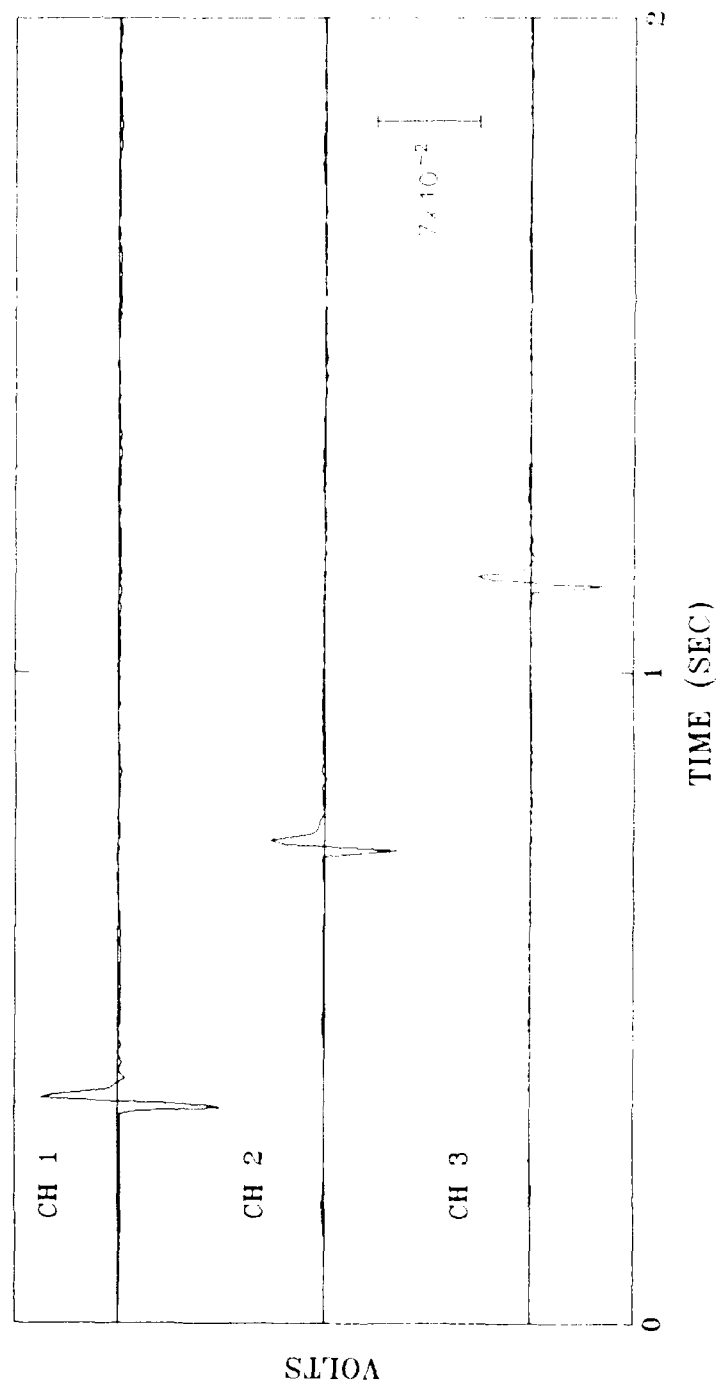
DATA FILE: fdx18s1.DEC

Figure 14. Pressure Sensor Data - X-Line



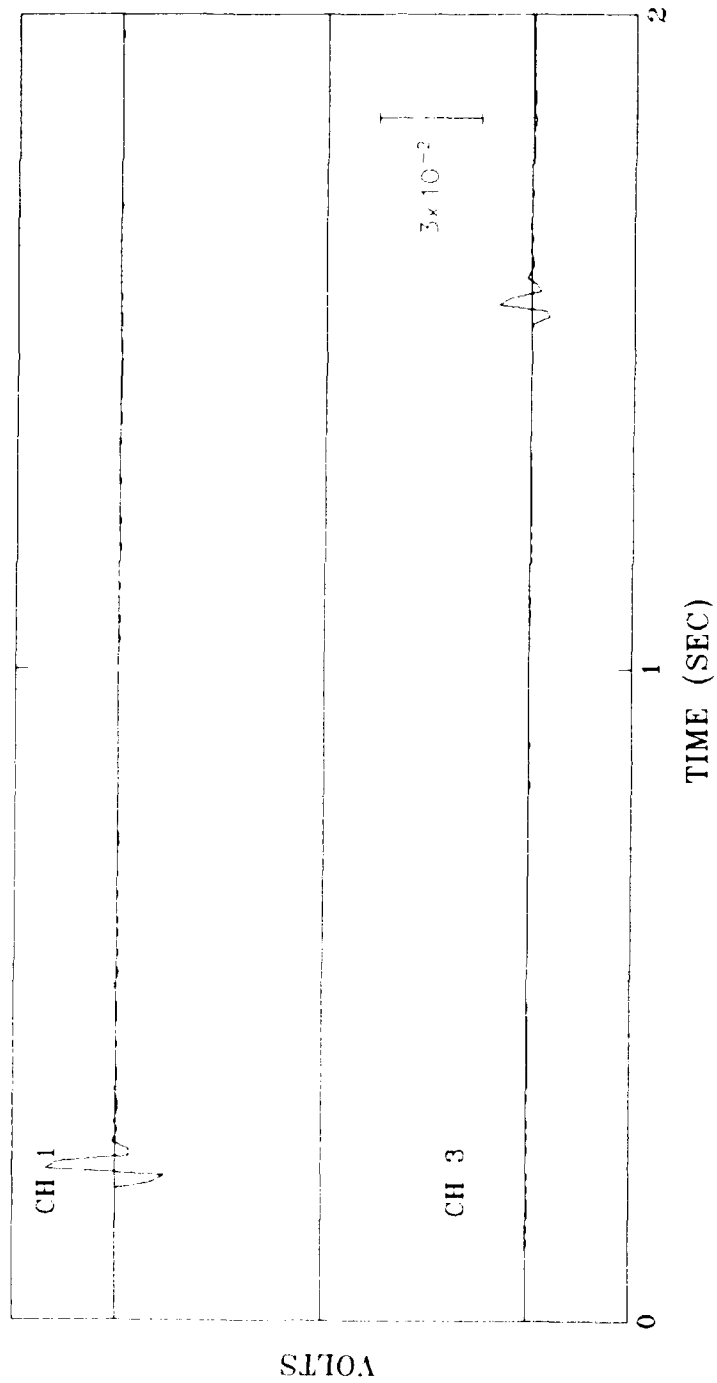
DATA FILE: fdx18s2.DEC

Figure 14. Pressure Sensor Data - X-Line (Cont'd)



DATA FILE: 4x18s3.DEC

Figure 14. Pressure Sensor Data - X-Line (Cont'd)



DATA FILE: fdy26s1.DEC

Figure 15. Pressure Sensor Data -Y-Line

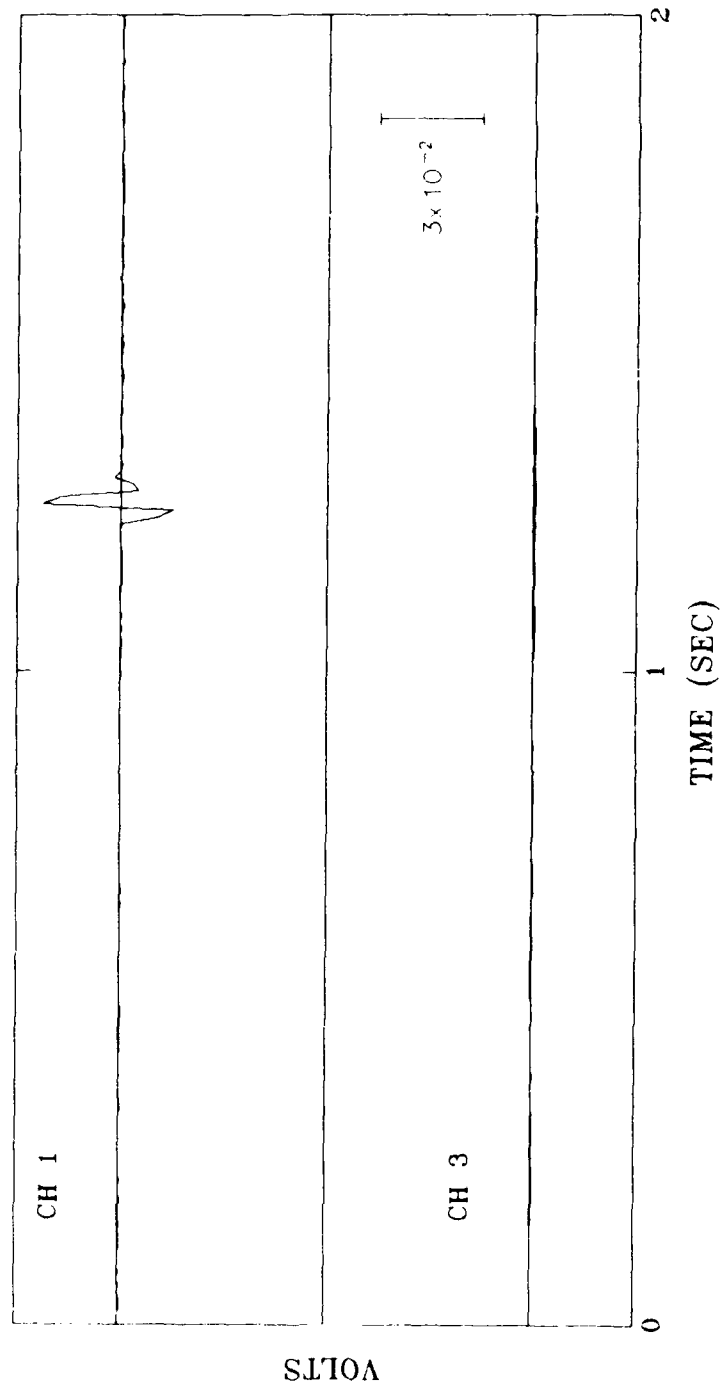
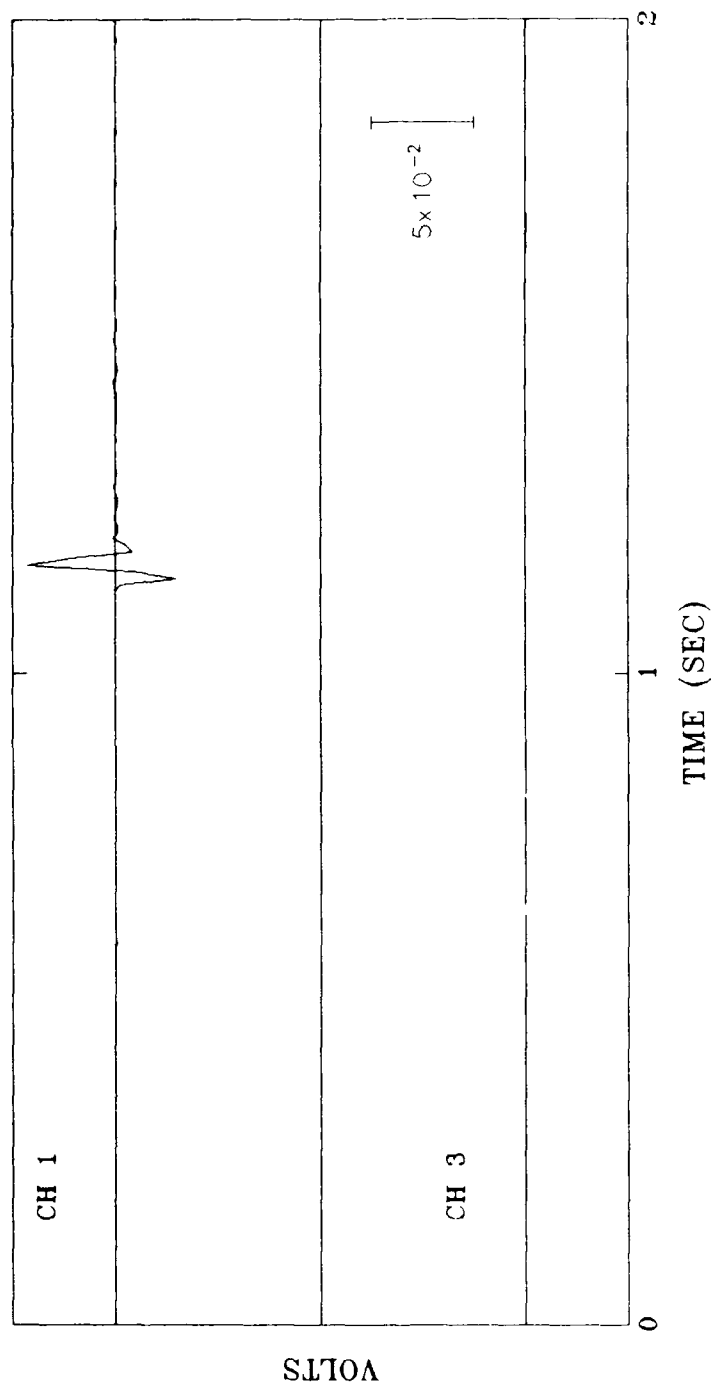


Figure 15. Pressure Sensor Data - Y-Line (Cont'd)



DATA FILE: fdy26s3.DEC

Figure 15. Pressure Sensor Data - Y-Line (Cont'd)

successful recording of all 3 shots at stations FDX4, FDX5, and FDX6. The results of seismo-acoustic calculations (ratios of peak seismic motion to acoustic amplitude) are shown in Table 2. The values

Table 2. Ratio of Peak Vertical Seismic Velocity to Peak Pressure

Station	Distance (m)	Shot 1 (cm/sec/Pa)	Shot 3 (cm/sec/P)
FDX4	593	$1.7 \times 10^{-5}$	$1.9 \times 10^{-5}$
FDX5	742	$1.3 \times 10^{-5}$	$1.4 \times 10^{-5}$
FDX6	891	$1.3 \times 10^{-5}$	
FDY1	147	$3.0 \times 10^{-4}$	$1.8 \times 10^{-4}$
FDY2	643	$4.0 \times 10^{-4}$	

were in the range of  $10^{-4}$  to  $10^{-5}$  cm/sec/Pa. The higher values for the Y-line are probably a reflection of the higher sampling rate instruments at those stations. The values were consistent for shot 1 and shot 3 showing that for these soil conditions and this size source, admittance was independent of shot sizes.

Although the pressure profiles were plagued by equipment failures, some simple observations could be made. Some changes in travel time were probably the result of wind patterns and/or changes in temperature. (The temperature varied from 65 to 70° F during the shots; barometric pressure averaged 29.96 inches of mercury). The ratio of the maximum amplitudes of the third shot (10 lbs) to the maximum amplitudes of the first and second shots (5 lbs) ranged from 1.2 to 1.6. Coincidence of pressure wave and seismic wave arrival times shows that indeed for the X-line and the close in Y-line station, the measured seismic wave was directly induced by the pressure wave hitting the ground at the surface of the station.

However, the complexities of the coda indicate that some of the energy must result from seismic waves that were induced by the blast at other locations. For instance, an examination of a Y-line station behind the hill, FDY2 - shot 1 (Figure 5), shows a seismic precursor arriving at approximately 0.5 sec and a direct acoustically induced seismic wave at 0.65 sec. The precursor could be a seismic wave induced on the blast side of the hill that propagated through the hill at a higher velocity than the pressure wave (which must travel over the hill) and therefore arrived before the direct pressure wave. The hill was approximately 200 to 250 meters wide, so these arrivals are reasonable. Amplitude fall off with distance varied; more data points are needed.

Ratios of peak amplitudes between pairs of stations along the flat array, normalized to 100 meters distance, varied from 0.9 to 0.6. The ratio of peak seismic amplitude from the Y-line for stations FDY1 to FDY2, again normalized to 100 meters, was 0.3. FDY2 was behind the hill; however, because of the evaluation of the shot, the geometry was such that station FDY2 was at a closer straight line distance to the shot (see Figure 3).

## 5. DISCUSSION

From the seismic data, it is clear that the hill sheltered the Y-line stations, and that doubling the amount of explosives increased the peak amplitudes by a factor of 1.1 to 1.3. Considerable transverse motion is apparent on the records. Particle motion plots showed that the transverse motion occurred earlier in the record as the recording distance increased. Reduced time plots show a propagation speed of approximately 0.35 km/sec. For the acoustic data, seismo-acoustic peak amplitude ratios in the range of  $10^{-4}$  to  $10^{-5}$  cm/sec/Pa were observed. Ratios of peak pressure for the larger shot (10 lb TNT) to the smaller shots (5 lb TNT) were in the range of 1.2 to 1.4. The experiment was repeatable: waveforms from shot 1 and shot 2 are nearly identical.

This experiment was performed as a feasibility study for determining the effect of topography, terrain, and vegetation on pressure and pressure-induced seismic signals for low altitude atmospheric explosions. Because of the frequencies involved, follow up tests should employ systems capable of higher sampling rates so that a major percentage of the radiated energy will be recorded. The Turner Drop Zone itself is a very good area to use for a comparison of the effect of snow cover on the signals if the experiment is repeated in the winter. Even with the equipment limitation, it was possible to determine that some of the seismic waves were directly induced by the acoustic wave, and amplitude ratios for changing source strength were obtained as well as some attenuation data. This experiment can easily be repeated in areas of differing vegetation, ground cover, and topography. It is recommended that in follow-up experiments the position of the shot be varied so that the geometry will be changed enough to discriminate the various seismic paths induced by the blasis. GL has continued its program of seismo-acoustic research since the Ft Devens experiment with recordings of B-1 aircraft flyovers<sup>8</sup> and measurements of the ambient seismo-acoustic environment.<sup>9</sup>

- 
8. Crowley, F.A. and Blaney, J.I. (1987) *Surface Disturbances Produced by Low Level, Subsonic B-1 Aircraft*, AFGL-TR-87-0325, ADA192257.
  9. Battis, J.C. and Center, C. (1989) *Temporal Attributes of the Ambient Seismo-Acoustic Environment: La Junta, CO*, AFGL-TR-89-0080, ADA219369.

## References

1. Castle, R.O., Dixon, M.R., Grew, E.S., Griscom, A., and Zietz, I. (1976) *Structural Dislocations in Eastern Massachusetts*, Geological Survey Bulletin 1410, U.S. Government Printing Office, Washington, DC.
2. Van Diver, B.B. (1987) *Roadside Geology of Vermont and New Hampshire*, Mountain Press Publishing Company, Missoula, pp.1-29.
3. United States Army Forces Command, 584th Engineer Company (Cartographic), 30th Engineer Battalion (Topographic) (Army), Fort Belvoir, VA 22060, (Feb, 1986) Fort Devens Special Map, edition 2-DMATC, Series V8145.
4. Medearis, K. (1979) *Dynamic Characteristics of Ground Motions Due to Blasting*, Bull. Seis. Soc. Am., **69**(No. 2):627-639.
5. Nicholls, M.R., Johnson, C.F. , and Duval, W.I. (1971) *Blasting Vibrations and Their Effects on Structures*, Bulletin 656, US Dept. of the Interior, Bureau of Mines, pp. 65-66.
6. Battis, J.C. (1985) *Vibro-Acoustic Forecasts for STS Launches at V23, Vandenberg AFB: Results Summary and the Payload Preparation Room*, AFGL-TR-85-0013, ADA162192.
7. Baker, W.E. (1973) *Explosions in Air*, University of Texas Press, Austin and London, pp 10-80.
8. Crowly, F.A. and Blaney, J.I. (1987) *Surface Disturbances Produced by Low Level, Subsonic B-1 Aircraft*, AFGL-TR-87-0325, ADA192257.
9. Battis, J.C. and Center, C. (1989) *Temporal Attributes of the Ambient Seismo-Acoustic Environment: La Junta, CO*, AFGL-TR-89-0080, ADA219369.

## Appendix A: Equipment Parameters

Table A-1. Clock Correction Data  
Time Slew Relative to Recorder 301 at End of Shot Day

Recorder Number	Sample Rate (s/sec)	Slew*	Time Correction (msec)
284	200	550	-83
283	200	580	-50
269	200	320	-466
301	200	000	0
270	200	(turned off)	
300	200	583	-28
299	200	544	-93
281	100	007	+23
277	100	010	+33
322	100	292	-27
320	100	104	+346
280	100	004	+13
282	100	273	-90
312	100	005	+16

\* Slew is relative to 300 for 100 sps or 600 for 200 sps recorders.

Table A-2. Pressure Sensor Calibration Data  
Scale Factors\*

Sensor Number	Range (psi)	+0.5 psi (V)	0.0 psi (V)	-0.5 psi (V)
1	±0.5	+0.375	+0.009	-0.389
2	±0.5	+0.684	-0.001	-0.656
3	±0.5	+0.499	+0.001	-0.502
4	±0.5	+0.567	-0.022	-0.511
5	±1.5	+0.213	+0.000	-0.214
6	±1.5	+0.258	-0.000	-0.252
7	±1.5	+0.219	-0.000	-0.218
8	±1.5	+0.209	+0.001	-0.212

\* Using (±6.92) 13.84 inches of H<sub>2</sub>O = 0.5 psi

Table A-3. Recorder, Seismometer and Pressure Sensor List

Station Location	Seismic					Pressure		
	Recorder	Sampling Rate	Seismometers			Recorder	Sampling Rate	PT
			Channel 1	2	3			
X1	270	200	8296Z	NS	EW			0.5 PSI #6
X2	283	200	7493Z	NS	EW	284	200	0.125 PSI #7
X3	299	200	7679Z	NS	EW			0.125 PSI #5
X4	312	100	540Rad	T	556Z			0.125 PSI #66
X5	320	100	546N	543E	551Z	300	300	0.125 PSI #
X6	322	100	548N	542E	553Z			0.125 PSI #
Y1	269	200	7680Z	NS	EW			0.5 PSI #
Y2	301	200	9261Z	NS	EW	281	100	0.5 PSI #
Y3	280	100	549N	545E	555Z			0.5 PSI #
Y4	277	100	547N	539E	558Z			

## Appendix B: X- and Y-Line Properties

\*\*\* INDEX OF ARRAY SEISMOGRAMS \*\*\*

					MO	DY	YEAR	HR	MN	SECOND	DISTANCE	DELTA	AZIMUTH
1	FDX1	SHT1	SPZ	P	5	5	1986	19	15	2.000	0.16	0.00	305.00
2	FDX1	SHT1	SPN	P	5	5	1986	19	15	2.000	0.16	0.00	305.00
3	FDX1	SHT1	SPE	P	5	5	1986	19	15	2.000	0.16	0.00	305.00
4	FDX1	SHT2	SPZ	P	5	5	1986	19	39	49.000	0.16	0.00	305.00
5	FDX1	SHT2	SPN	P	5	5	1986	19	39	49.000	0.16	0.00	305.00
6	FDX1	SHT2	SPE	P	5	5	1986	19	39	49.000	0.16	0.00	305.00
7	FDX1	SHT3	SPZ	P	5	5	1986	20	3	39.000	0.16	0.00	305.00
8	FDX1	SHT3	SPN	P	5	5	1986	20	3	39.000	0.16	0.00	305.00
9	FDX1	SHT3	SPE	P	5	5	1986	20	3	39.000	0.16	0.00	305.00
10	FDX2	SHT1	SPZ	P	5	5	1986	19	15	2.000	0.31	40.00	305.00
11	FDX2	SHT1	SPN	P	5	5	1986	19	15	2.000	0.31	40.00	305.00
12	FDX2	SHT1	SPE	P	5	5	1986	19	15	2.000	0.31	40.00	305.00
13	FDX2	SHT2	SPZ	P	5	5	1986	19	39	49.000	0.31	40.00	305.00
14	FDX2	SHT2	SPN	P	5	5	1986	19	39	49.000	0.31	40.00	305.00
15	FDX2	SHT2	SPE	P	5	5	1986	19	39	49.000	0.31	40.00	305.00
16	FDX2	SHT3	SPZ	P	5		1986	20	3	39.000	0.31	40.00	305.00
17	FDX2	SHT3	SPN	P	5	5	1986	20	3	39.000	0.31	40.00	305.00
18	FDX2	SHT3	SPE	P	5	5	1986	20	3	39.000	0.31	40.00	305.00
19	FDX3	SHT1	SPZ	P	5	5	1986	19	15	2.000	0.44	20.00	280.00
20	FDX3	SHT1	SPN	P	5	5	1986	19	15	2.000	0.44	20.00	280.00
21	FDX3	SHT1	SPE	P	5	5	1986	19	15	2.000	0.44	20.00	280.00
22	FDX3	SHT2	SPZ	P	5	5	1986	19	39	49.000	0.44	20.00	280.00
23	FDX3	SHT2	SPN	P	5	5	1986	19	39	49.000	0.44	20.00	280.00
24	FDX3	SHT2	SPE	P	5	5	1986	19	39	49.000	0.44	20.00	280.00
25	FDX3	SHT3	SPZ	P	5	5	1986	20	3	39.000	0.44	20.00	280.00
26	FDX3	SHT3	SPN	P	5	5	1986	20	3	39.000	0.44	20.00	280.00
27	FDX3	SHT3	SPE	P	5	5	1986	20	3	39.000	0.44	20.00	280.00
28	FDX4	SHT1	RADL	P	5	5	1986	19	15	2.000	0.59	80.00	295.00
29	FDX4	SHT1	TRNS	P	5	5	1986	19	15	2.000	0.59	80.00	295.00
30	FDX4	SHT1	SPZ	P	5	5	1986	19	15	2.000	0.59	80.00	295.00
31	FDX4	SHT2	RADL	P	5	5	1986	19	39	49.000	0.59	80.00	295.00
32	FDX4	SHT2	TRNS	P	5	5	1986	19	39	49.000	0.59	80.00	295.00
33	FDX4	SHT2	SPZ	P	5	5	1986	19	39	49.000	0.59	80.00	295.00
34	FDX4	SHT3	RADL	P	5	5	1986	20	3	39.000	0.59	80.00	295.00
35	FDX4	SHT3	TRNS	P	5	5	1986	20	3	39.000	0.59	80.00	295.00
36	FDX4	SHT3	SPZ	P	5	5	1986	20	3	39.000	0.59	80.00	295.00
37	FDX5	SHT1	SPN	P	5	5	1986	19	15	2.000	0.74	30.00	300.00
38	FDX5	SHT1	SPE	P	5	5	1986	19	15	2.000	0.74	30.00	300.00
39	FDX5	SHT1	SPZ	P	5	5	1986	19	15	2.000	0.74	30.00	300.00
40	FDX5	SHT2	SPN	P	5	5	1986	19	39	49.000	0.74	30.00	300.00
41	FDX5	SHT2	SPE	P	5	5	1986	19	39	49.000	0.74	30.00	300.00
42	FDX5	SHT2	SPZ	P	5	5	1986	19	39	49.000	0.74	30.00	300.00
43	FDX5	SHT3	SPN	P	5	5	1986	20	3	39.000	0.74	30.00	300.00
44	FDX5	SHT3	SPE	P	5	5	1986	20	3	39.000	0.74	30.00	300.00
45	FDX5	SHT3	SPZ	P	5	5	1986	20	3	39.000	0.74	30.00	300.00
46	FDX6	SHT1	SPN	P	5	5	1986	19	15	2.000	0.89	0.00	305.00
47	FDX6	SHT1	SIE	P	5	5	1986	19	15	2.000	0.89	0.00	305.00
48	FDX6	SHT1	SPZ	P	5	5	1986	19	15	2.000	0.89	0.00	305.00
49	FDX6	SHT2	SPN	P	5	5	1986	19	39	49.000	0.89	0.00	305.00
50	FDX6	SHT2	SPE	P	5	5	1986	19	39	49.000	0.89	0.00	305.00
51	FDX6	SHT2	SPZ	P	5	5	1986	19	39	49.000	0.89	0.00	305.00

Table B.1. Seismometer Constants (X-Line Properties)

SEISMOGRAM	STARTING TIME	CORRECTION (SECONDS)	SEISMOMETER ORIENTATION (DEGREES)	SEISMOMETER SENSITIVITY (VOLTS M SEC)	PENDULUM PERIOD (SECONDS)	DAMPING RATIO	SERIAL NUMBER	CALIBRATION DATE
FDX1 SH11 SPZ	5 MAY 1986 125 19 15	0.0000 NONE	15.00	200.0000	0.500	0.406	8306	0 JAN 0
FDX1 SH11 SPN	5 MAY 1986 125 19 15	0.0000 NONE	15.00	200.0000	0.500	0.406	8306	0 JAN 0
FDX1 SH11 SPF	5 MAY 1986 125 19 15	0.0000 NONE	75.00	200.0000	0.500	0.406	8306	0 JAN 0
FDX1 SH12 SPZ	5 MAY 1986 125 19 39 49 000	0.0000 NONE	15.00	200.0000	0.500	0.406	8306	0 JAN 0
FDX1 SH12 SPN	5 MAY 1986 125 19 39 49 000	0.0000 NONE	15.00	200.0000	0.500	0.406	8306	0 JAN 0
FDX1 SH12 SPF	5 MAY 1986 125 19 39 49 000	0.0000 NONE	75.00	200.0000	0.500	0.406	8306	0 JAN 0
FDX1 SH17 SPZ	5 MAY 1986 125 20 3 39 000	0.0000 NONE	15.00	200.0000	0.500	0.406	8306	0 JAN 0
FDX1 SH17 SPN	5 MAY 1986 125 20 3 39 000	0.0000 NONE	15.00	200.0000	0.500	0.406	8306	0 JAN 0
FDX1 SH17 SPF	5 MAY 1986 125 20 3 39 000	0.0000 NONE	75.00	200.0000	0.500	0.406	8306	0 JAN 0
FDX2 SH11 SPZ	5 MAY 1986 125 19 15 2 000	0.0500 SLEW	15.00	200.0000	0.500	0.406	8306	0 JAN 0
FDX2 SH11 SPN	5 MAY 1986 125 19 15 2 000	0.0500 SLEW	15.00	200.0000	0.500	0.406	8306	0 JAN 0
FDX2 SH11 SPF	5 MAY 1986 125 19 15 2 000	0.0500 SLEW	75.00	200.0000	0.500	0.406	8306	0 JAN 0
FDX2 SH12 SPZ	5 MAY 1986 125 19 15 2 000	0.0500 SLEW	15.00	200.0000	0.500	0.406	8306	0 JAN 0
FDX2 SH12 SPN	5 MAY 1986 125 19 15 2 000	0.0500 SLEW	15.00	200.0000	0.500	0.406	8306	0 JAN 0
FDX2 SH12 SPF	5 MAY 1986 125 19 15 2 000	0.0500 SLEW	75.00	200.0000	0.500	0.406	8306	0 JAN 0
FDX3 SH11 SPZ	5 MAY 1986 125 19 15 2 000	0.0930 SLEW	15.00	222.3760	0.418	0.409	7679	0 JAN 0
FDX3 SH11 SPN	5 MAY 1986 125 19 15 2 000	0.0930 SLEW	15.00	222.3760	0.418	0.409	7679	0 JAN 0
FDX3 SH11 SPF	5 MAY 1986 125 19 15 2 000	0.0930 SLEW	75.00	222.3760	0.418	0.409	7679	0 JAN 0
FDX3 SH12 SPZ	5 MAY 1986 125 19 15 2 000	0.0930 SLEW	15.00	222.3760	0.418	0.409	7679	0 JAN 0
FDX3 SH12 SPN	5 MAY 1986 125 19 15 2 000	0.0930 SLEW	15.00	222.3760	0.418	0.409	7679	0 JAN 0
FDX3 SH12 SPF	5 MAY 1986 125 19 15 2 000	0.0930 SLEW	75.00	222.3760	0.418	0.409	7679	0 JAN 0
FDX4 SH11 SPZ	5 MAY 1986 125 19 15 2 000	0.0160 SLEW	15.00	1133.5156	1.020	0.299	104540	0 JAN 0
FDX4 SH11 SPN	5 MAY 1986 125 19 15 2 000	0.0160 SLEW	15.00	1133.5156	1.020	0.299	104540	0 JAN 0
FDX4 SH11 SPF	5 MAY 1986 125 19 15 2 000	0.0160 SLEW	75.00	1133.5156	1.020	0.299	104540	0 JAN 0
FDX4 SH12 SPZ	5 MAY 1986 125 19 15 2 000	0.0160 SLEW	15.00	1133.5156	1.020	0.299	104540	0 JAN 0
FDX4 SH12 SPN	5 MAY 1986 125 19 15 2 000	0.0160 SLEW	15.00	1133.5156	1.020	0.299	104540	0 JAN 0
FDX4 SH12 SPF	5 MAY 1986 125 19 15 2 000	0.0160 SLEW	75.00	1133.5156	1.020	0.299	104540	0 JAN 0
FDX4 SH17 SPZ	5 MAY 1986 125 20 3 39 000	0.0160 SLEW	15.00	1133.5156	1.020	0.299	104540	0 JAN 0
FDX4 SH17 SPN	5 MAY 1986 125 20 3 39 000	0.0160 SLEW	15.00	1133.5156	1.020	0.299	104540	0 JAN 0
FDX4 SH17 SPF	5 MAY 1986 125 20 3 39 000	0.0160 SLEW	75.00	1133.5156	1.020	0.299	104540	0 JAN 0
FDX5 SH11 SPZ	5 MAY 1986 125 19 15 2 000	0.0160 SLEW	15.00	1156.5354	1.042	0.321	104546	0 JAN 0
FDX5 SH11 SPN	5 MAY 1986 125 19 15 2 000	0.0160 SLEW	15.00	1156.5354	1.042	0.321	104546	0 JAN 0
FDX5 SH11 SPF	5 MAY 1986 125 19 15 2 000	0.0160 SLEW	75.00	1156.5354	1.042	0.321	104546	0 JAN 0
FDX5 SH12 SPZ	5 MAY 1986 125 19 15 2 000	0.0160 SLEW	15.00	1156.5354	1.042	0.321	104546	0 JAN 0
FDX5 SH12 SPN	5 MAY 1986 125 19 15 2 000	0.0160 SLEW	15.00	1156.5354	1.042	0.321	104546	0 JAN 0
FDX5 SH12 SPF	5 MAY 1986 125 19 15 2 000	0.0160 SLEW	75.00	1156.5354	1.042	0.321	104546	0 JAN 0
FDX6 SH11 SPZ	5 MAY 1986 125 19 15 2 000	0.0270 SLEW	15.00	1152.5781	1.031	0.321	104548	0 JAN 0
FDX6 SH11 SPN	5 MAY 1986 125 19 15 2 000	0.0270 SLEW	15.00	1152.5781	1.031	0.321	104548	0 JAN 0
FDX6 SH11 SPF	5 MAY 1986 125 19 15 2 000	0.0270 SLEW	75.00	1152.5781	1.031	0.321	104548	0 JAN 0
FDX6 SH12 SPZ	5 MAY 1986 125 19 15 2 000	0.0270 SLEW	15.00	1152.5781	1.031	0.321	104548	0 JAN 0
FDX6 SH12 SPN	5 MAY 1986 125 19 15 2 000	0.0270 SLEW	15.00	1152.5781	1.031	0.321	104548	0 JAN 0
FDX6 SH12 SPF	5 MAY 1986 125 19 15 2 000	0.0270 SLEW	75.00	1152.5781	1.031	0.321	104548	0 JAN 0

SEISMOMETER ORIENTATION IS MEASURED AS DEGREES CLOCKWISE FROM GEOGRAPHIC NORTH

Table B1. Seismometer Constants (X-Line Properties) (Cont'd)

SEISMOGRAM	STARTING TIME	TIME CORRECTION (SECONDS)	SEISMOMETER ORIENTATION (DEGREES)	SEISMOMETER SENSITIVITY (VOLTS M SEC) (SECONDS)	PENDULUM PERIOD (SECONDS)	DAMPING RATIO	SERIAL NUMBER	CALIBRATION DATE
FDX6 SHI2 SPN	5 MAY 1986 125 19 39 49.000	-0.0270 SLEW	15.00	1152.5781	1.031	0.321	104548	0 JAN 0
FDX6 SHI2 SPE	5 MAY 1986 125 19 39 49.000	-0.0270 SLEW	75.00	1100.4688	1.020	0.321	104542	0 JAN 0
FDX6 SHI2 SPZ	5 MAY 1986 125 19 39 49.000	0.0270 SLEW		1183.4646	1.064	0.329	104553	0 JAN 0

SEISMOMETER ORIENTATION IS MEASURED AS DEGREES CLOCKWISE FROM GEOGRAPHIC NORTH

Table B-2. DCS-302 Recorder Constants (X-Line Properties)

SEISMOGRAM	CUT OFF FREQUENCY (HERTZ)	RECORDER GAINS (MILLIVOLTS COUNT)		SERIAL NUMBER
		GAIN 1	GAIN 2	
FDX1 SHT1 SPZ	30.00	2.44141	0.48828	0.09766
FDX1 SHT1 SPN	30.00	2.44141	0.48828	0.09766
FDX1 SHT1 SPE	30.00	2.44141	0.48828	0.09766
FDX1 SHT2 SPZ	30.00	2.44141	0.48828	0.09766
FDX1 SHT2 SPN	30.00	2.44141	0.48828	0.09766
FDX1 SHT2 SPE	30.00	2.44141	0.48828	0.09766
FDX1 SHT3 SPZ	30.00	2.44141	0.48828	0.09766
FDX1 SHT3 SPN	30.00	2.44141	0.48828	0.09766
FDX1 SHT3 SPE	30.00	2.44141	0.48828	0.09766
FDX2 SHT1 SPZ	30.00	2.44141	0.48828	0.09766
FDX2 SHT1 SPN	30.00	2.44141	0.48828	0.09766
FDX2 SHT1 SPE	30.00	2.44141	0.48828	0.09766
FDX2 SHT2 SPZ	30.00	2.44141	0.48828	0.09766
FDX2 SHT2 SPN	30.00	2.44141	0.48828	0.09766
FDX2 SHT2 SPE	30.00	2.44141	0.48828	0.09766
FDX2 SHT3 SPZ	30.00	2.44141	0.48828	0.09766
FDX2 SHT3 SPN	30.00	2.44141	0.48828	0.09766
FDX2 SHT3 SPE	30.00	2.44141	0.48828	0.09766
FDX3 SHT1 SPZ	30.00	2.44141	0.48828	0.09766
FDX3 SHT1 SPN	30.00	2.44141	0.48828	0.09766
FDX3 SHT1 SPE	30.00	2.44141	0.48828	0.09766
FDX3 SHT2 SPZ	30.00	2.44141	0.48828	0.09766
FDX3 SHT2 SPN	30.00	2.44141	0.48828	0.09766
FDX3 SHT2 SPE	30.00	2.44141	0.48828	0.09766
FDX3 SHT3 SPZ	30.00	2.44141	0.48828	0.09766
FDX3 SHT3 SPN	30.00	2.44141	0.48828	0.09766
FDX3 SHT3 SPE	30.00	2.44141	0.48828	0.09766
FDX4 SHT1 RADL	30.00	0.24396	0.04864	0.00974
FDX4 SHT1 TRNS	30.00	0.24396	0.04864	0.00974
FDX4 SHT1 SPZ	30.00	0.24374	0.04893	0.00982
FDX4 SHT2 RADL	30.00	0.24396	0.04864	0.00974
FDX4 SHT2 TRNS	30.00	0.24396	0.04864	0.00974
FDX4 SHT2 SPZ	30.00	0.24374	0.04893	0.00982
FDX4 SHT3 RADL	30.00	0.24396	0.04864	0.00974
FDX4 SHT3 TRNS	30.00	0.24396	0.04864	0.00974
FDX4 SHT3 SPZ	30.00	0.24374	0.04893	0.00982
FDX5 SHT1 SPN	30.00	0.24381	0.04926	0.00980
FDX5 SHT1 SPE	30.00	0.24344	0.04917	0.00990
FDX5 SHT2 SPN	30.00	0.24381	0.04918	0.00983
FDX5 SHT2 SPE	30.00	0.24344	0.04926	0.00980
FDX5 SHT3 SPN	30.00	0.24381	0.04918	0.00983
FDX5 SHT3 SPE	30.00	0.24344	0.04926	0.00980
FDX5 SHT3 SPZ	30.00	0.24381	0.04926	0.00980
FDX5 SHT3 SPN	30.00	0.24344	0.04917	0.00990
FDX5 SHT3 SPZ	30.00	0.24381	0.04918	0.00983
FDX6 SHT1 SPN	30.00	0.25326	0.04907	0.00970
FDX6 SHT1 SPE	30.00	0.25511	0.04952	0.00980
FDX6 SHT1 SPZ	30.00	0.25564	0.04973	0.00981

Table B-2. DCS-302 Recorder Constants (X-Line Properties)(Cont'd)

SEISMOGRAM	CUT OFF FREQUENCY ( HERTZ )	RECORDER GAINS ( MILLIVOLTS COUNT )			SERIAL NUMBER
		GAIN 1	GAIN 2	GAIN 3	
FDX6 SHT2 SPN	30.00	0.25328	0.04907	0.00970	0.00245
FDX6 SHT2 SPE	30.00	0.25511	0.04952	0.00980	0.00248
FDX6 SHT2 SPZ	30.00	0.25562	0.04973	0.00981	0.00242

# INDEX OF ARRAY SEISMOGRAMS

					MO	DY	YEAR	HR	MN	SECOND	DISTANCE	DELTA	AZIMUTH
1	FDY1	SHT1	SPZ	P	5	5	1986	19	15	2.000	0.15	0.00	0.00
2	FDY1	SHT1	SPN	P	5	5	1986	19	15	2.000	0.15	0.00	0.00
3	FDY1	SHT1	SPE	P	5	5	1986	19	15	2.000	0.15	0.00	0.00
4	FDY1	SHT2	SPZ	P	5	5	1986	19	39	49.000	0.15	0.00	0.00
5	FDY1	SHT2	SPN	P	5	5	1986	19	39	49.000	0.15	0.00	0.00
6	FDY1	SHT2	SPE	P	5	5	1986	19	39	49.000	0.15	0.00	0.00
7	FDY1	SHT3	SPZ	P	5	5	1986	20	3	39.000	0.15	0.00	0.00
8	FDY1	SHT3	SPN	P	5	5	1986	20	3	39.000	0.15	0.00	0.00
9	FDY1	SHT3	SPE	P	5	5	1986	20	3	39.000	0.15	0.00	0.00
10	FDY2	SHT1	SPZ	P	5	5	1986	19	15	2.000	0.64	0.00	0.00
11	FDY2	SHT1	SPN	P	5	5	1986	19	15	2.000	0.64	0.00	0.00
12	FDY2	SHT1	SPE	P	5	5	1986	19	15	2.000	0.64	0.00	0.00
13	FDY3	SHT1	SPN	P	5	5	1986	19	15	2.000	0.74	0.00	0.00
14	FDY3	SHT1	SPE	P	5	5	1986	19	15	2.000	0.74	0.00	0.00
15	FDY3	SHT1	SPZ	P	5	5	1986	19	15	2.000	0.74	0.00	0.00
16	FDY3	SHT2	SPN	P	5	5	1986	19	39	49.000	0.74	0.00	0.00
17	FDY3	SHT2	SPE	P	5	5	1986	19	39	49.000	0.74	0.00	0.00
18	FDY3	SHT2	SPZ	P	5	5	1986	19	39	49.000	0.74	0.00	0.00
19	FDY3	SHT3	SPN	P	5	5	1986	20	3	39.000	0.74	0.00	0.00
20	FDY3	SHT3	SPE	P	5	5	1986	20	3	39.000	0.74	0.00	0.00
21	FDY3	SHT3	SPZ	P	5	5	1986	20	3	39.000	0.74	0.00	0.00
22	FDY4	SHT1	SPN	P	5	5	1986	19	15	2.000	0.85	0.00	15.00
23	FDY4	SHT1	SPE	P	5	5	1986	19	15	2.000	0.85	0.00	15.00
24	FDY4	SHT1	SPZ	P	5	5	1986	19	15	2.000	0.85	0.00	15.00
25	FDY4	SHT2	SPN	P	5	5	1986	19	39	49.000	0.85	0.00	15.00
26	FDY4	SHT2	SPE	P	5	5	1986	19	39	49.000	0.85	0.00	15.00
27	FDY4	SHT2	SPZ	P	5	5	1986	19	39	49.000	0.85	0.00	15.00
28	FDY4	SHT3	SPN	P	5	5	1986	20	3	39.000	0.85	0.00	0.00
29	FDY4	SHT3	SPE	P	5	5	1986	20	3	39.000	0.85	0.00	0.00
30	FDY4	SHT3	SPZ	P	5	5	1986	20	3	39.000	0.85	0.00	0.00

Table B-3. Seismometer Constants (Y-Line Properties)

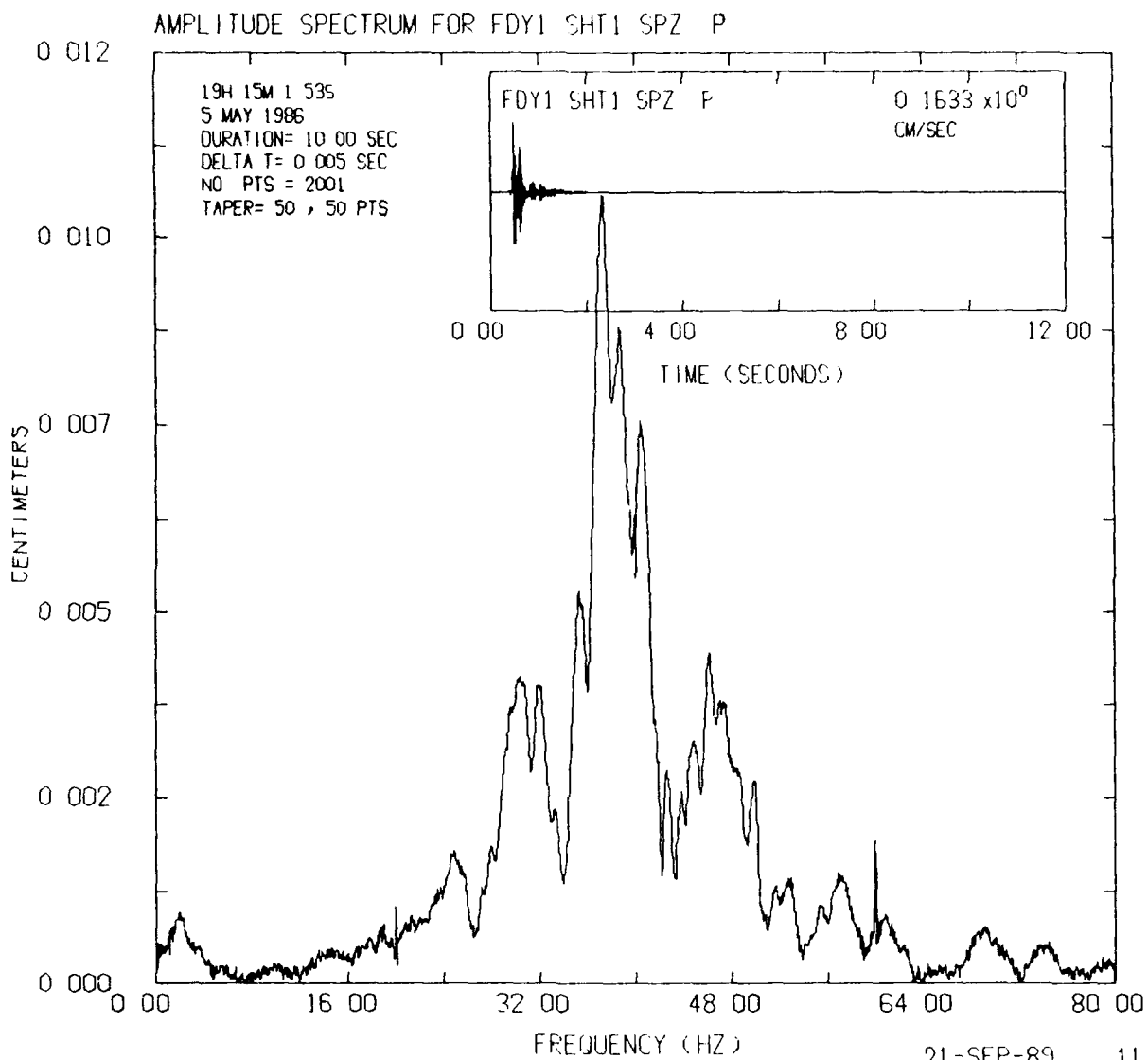
SEISMOGRAM	STARTING TIME	TIME CORRECTION (SECONDS)	SEISMOMETER ORIENTATION (DEGREES)	SEISMOMETER SENSITIVITY (VOLTS M SEC)	PENDULUM PERIOD (SECONDS)	DAMPING RATIO	SERIAL NUMBER	CALIBRATION DATE
FDY1 SHT1 SP2	5 MAY 1986 125 19 15	2 000	0 4660 SLEW	200.0000	0 500	0.400	7680	0 JAN 0
FDY1 SHT1 SPN	5 MAY 1986 125 19 15	2 000	0 4660 SLEW	200.0000	0 500	0.400	7680	0 JAN 0
FDY1 SHT1 SPE	5 MAY 1986 125 19 15	2 000	0 4660 SLEW	200.0000	0 500	0.400	7680	0 JAN 0
FDY1 SHT2 SP2	5 MAY 1986 125 19 39	49 000	0 4660 SLEW	200.0000	0 500	0.400	7680	0 JAN 0
FDY1 SHT2 SPN	5 MAY 1986 125 19 39	49 000	0 4660 SLEW	200.0000	0 500	0.400	7680	0 JAN 0
FDY1 SHT2 SPE	5 MAY 1986 125 19 39	49 000	0 4660 SLEW	200.0000	0 500	0.400	7680	0 JAN 0
FDY1 SHT3 SP2	5 MAY 1986 125 20 3 39	000	0 4660 SLEW	200.0000	0 500	0.400	7680	0 JAN 0
FDY1 SHT3 SPN	5 MAY 1986 125 20 3 39	000	0 4660 SLEW	200.0000	0 500	0.400	7680	0 JAN 0
FDY1 SHT3 SPE	5 MAY 1986 125 20 3 39	000	0 4660 SLEW	200.0000	0 500	0.400	7680	0 JAN 0
FDY2 SHT1 SP2	5 MAY 1986 125 19 15	2 000	0 0000 SLEW	200.0000	0 500	0.400	9261	0 JAN 0
FDY2 SHT1 SPN	5 MAY 1986 125 19 15	2 000	0 0000 SLEW	200.0000	0 500	0.400	9261	0 JAN 0
FDY2 SHT1 SPE	5 MAY 1986 125 19 15	2 000	0 0000 SLEW	200.0000	0 500	0.400	9261	0 JAN 0
FDY3 SHT1 SP2	5 MAY 1986 125 19 15	2 000	0 0130 SLEW	1152.5391	1.042	0.337	104549	0 JAN 0
FDY3 SHT1 SPN	5 MAY 1986 125 19 15	2 000	0 0130 SLEW	1152.5391	1.042	0.337	104549	0 JAN 0
FDY3 SHT1 SPE	5 MAY 1986 125 19 15	2 000	0 0130 SLEW	1152.5391	1.042	0.337	104549	0 JAN 0
FDY3 SHT2 SP2	5 MAY 1986 125 19 39	49 000	0 0130 SLEW	1152.5391	1.053	0.325	104555	0 JAN 0
FDY3 SHT2 SPN	5 MAY 1986 125 19 39	49 000	0 0130 SLEW	1152.5391	1.053	0.325	104555	0 JAN 0
FDY3 SHT2 SPE	5 MAY 1986 125 19 39	49 000	0 0130 SLEW	1152.5391	1.053	0.325	104555	0 JAN 0
FDY3 SHT3 SP2	5 MAY 1986 125 20 3 39	000	0 0130 SLEW	1152.5391	1.042	0.337	104549	0 JAN 0
FDY3 SHT3 SPN	5 MAY 1986 125 20 3 39	000	0 0130 SLEW	1152.5391	1.042	0.337	104549	0 JAN 0
FDY3 SHT3 SPE	5 MAY 1986 125 20 3 39	000	0 0130 SLEW	1152.5391	1.042	0.337	104549	0 JAN 0
FDY4 SHT1 SP2	5 MAY 1986 125 19 15	2 000	0 0330 SLEW	1103.1250	1.042	0.306	104547	0 JAN 0
FDY4 SHT1 SPN	5 MAY 1986 125 19 15	2 000	0 0330 SLEW	1103.1250	1.042	0.306	104547	0 JAN 0
FDY4 SHT1 SPE	5 MAY 1986 125 19 15	2 000	0 0330 SLEW	1103.1250	1.042	0.306	104547	0 JAN 0
FDY4 SHT2 SP2	5 MAY 1986 125 19 39	49 000	0 0330 SLEW	1218.7402	1.020	0.346	104539	0 JAN 0
FDY4 SHT2 SPN	5 MAY 1986 125 19 39	49 000	0 0330 SLEW	1218.7402	1.020	0.346	104539	0 JAN 0
FDY4 SHT2 SPE	5 MAY 1986 125 19 39	49 000	0 0330 SLEW	1218.7402	1.020	0.346	104539	0 JAN 0
FDY4 SHT3 SP2	5 MAY 1986 125 20 3 39	000	0 0330 SLEW	1103.1250	1.042	0.306	104547	0 JAN 0
FDY4 SHT3 SPN	5 MAY 1986 125 20 3 39	000	0 0330 SLEW	1103.1250	1.042	0.306	104547	0 JAN 0
FDY4 SHT3 SPE	5 MAY 1986 125 20 3 39	000	0 0330 SLEW	1103.1250	1.042	0.306	104547	0 JAN 0
FDY4 SHT4 SP2	5 MAY 1986 125 20 3 39	000	0 0330 SLEW	1218.7402	1.042	0.346	104558	0 JAN 0

SEISMOMETER ORIENTATION IS MEASURED AS DEGREES CLOCKWISE FROM GEOGRAPHIC NORTH

Table B-4. DCS-302 Recorder Constants (Y-Line Properties)

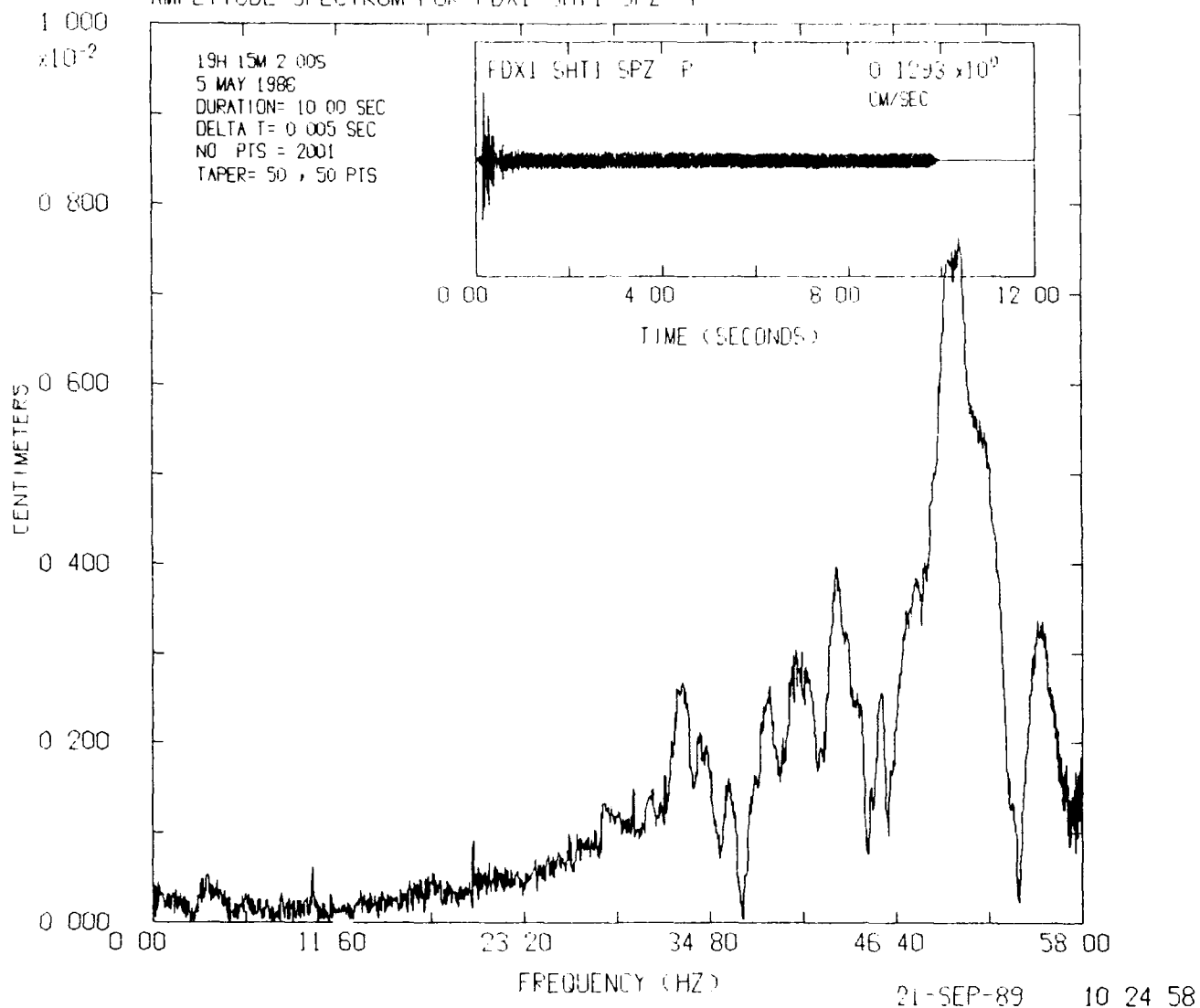
SEISMOGRAM	CUT OFF FREQUENCY (HERTZ)	RECORDER GAINS (MILLIVOLTS COUNT)			SERIAL NUMBER
		GAIN 1	GAIN 2	GAIN 3	
FDY1 SH11 SP2	30 00	2 44141	0 48828	0 09766	269
FDY1 SH11 SPN	30 00	2 44141	0 48828	0 09766	269
FDY1 SH11 SPE	30 00	2 44141	0 48828	0 09766	269
FDY1 SH12 SP2	30 00	2 44141	0 48828	0 09766	269
FDY1 SH12 SPN	30 00	2 44141	0 48828	0 09766	269
FDY1 SH12 SPE	30 00	2 44141	0 48828	0 09766	269
FDY1 SH13 SP2	30 00	2 44141	0 48828	0 09766	269
FDY1 SH13 SPN	30 00	2 44141	0 48828	0 09766	269
FDY1 SH13 SPE	30 00	2 44141	0 48828	0 09766	269
FDY2 SH11 SP2	30 00	2 44141	0 48828	0 09766	301
FDY2 SH11 SPN	30 00	2 44141	0 48828	0 09766	301
FDY2 SH11 SPE	30 00	2 44141	0 48828	0 09766	301
FDY3 SH11 SP2	30 00	0 24561	0 04947	0 00978	280
FDY3 SH11 SPN	30 00	0 24531	0 04949	0 00980	280
FDY3 SH11 SPE	30 00	0 24538	0 04964	0 00977	280
FDY3 SH12 SP2	30 00	0 24561	0 04947	0 00978	280
FDY3 SH12 SPN	30 00	0 24531	0 04949	0 00977	280
FDY3 SH12 SPE	30 00	0 24538	0 04964	0 00977	280
FDY3 SH13 SP2	30 00	0 24531	0 04949	0 00978	280
FDY3 SH13 SPN	30 00	0 24531	0 04949	0 00978	280
FDY3 SH13 SPE	30 00	0 24531	0 04949	0 00978	280
FDY3 SH13 SP2	30 00	0 24531	0 04949	0 00978	280
FDY3 SH13 SPN	30 00	0 24531	0 04949	0 00978	280
FDY3 SH13 SPE	30 00	0 24531	0 04949	0 00978	280
FDY4 SH11 SP2	30 00	0 23894	0 05039	0 00974	277
FDY4 SH11 SPN	30 00	0 23851	0 04903	0 00964	277
FDY4 SH11 SPE	30 00	0 23872	0 04906	0 00971	277
FDY4 SH12 SP2	30 00	0 23894	0 05039	0 00974	277
FDY4 SH12 SPN	30 00	0 23851	0 04903	0 00964	277
FDY4 SH12 SPE	30 00	0 23872	0 04906	0 00971	277
FDY4 SH13 SP2	30 00	0 23894	0 05039	0 00974	277
FDY4 SH13 SPN	30 00	0 23851	0 04903	0 00964	277
FDY4 SH13 SPE	30 00	0 23872	0 04906	0 00971	277

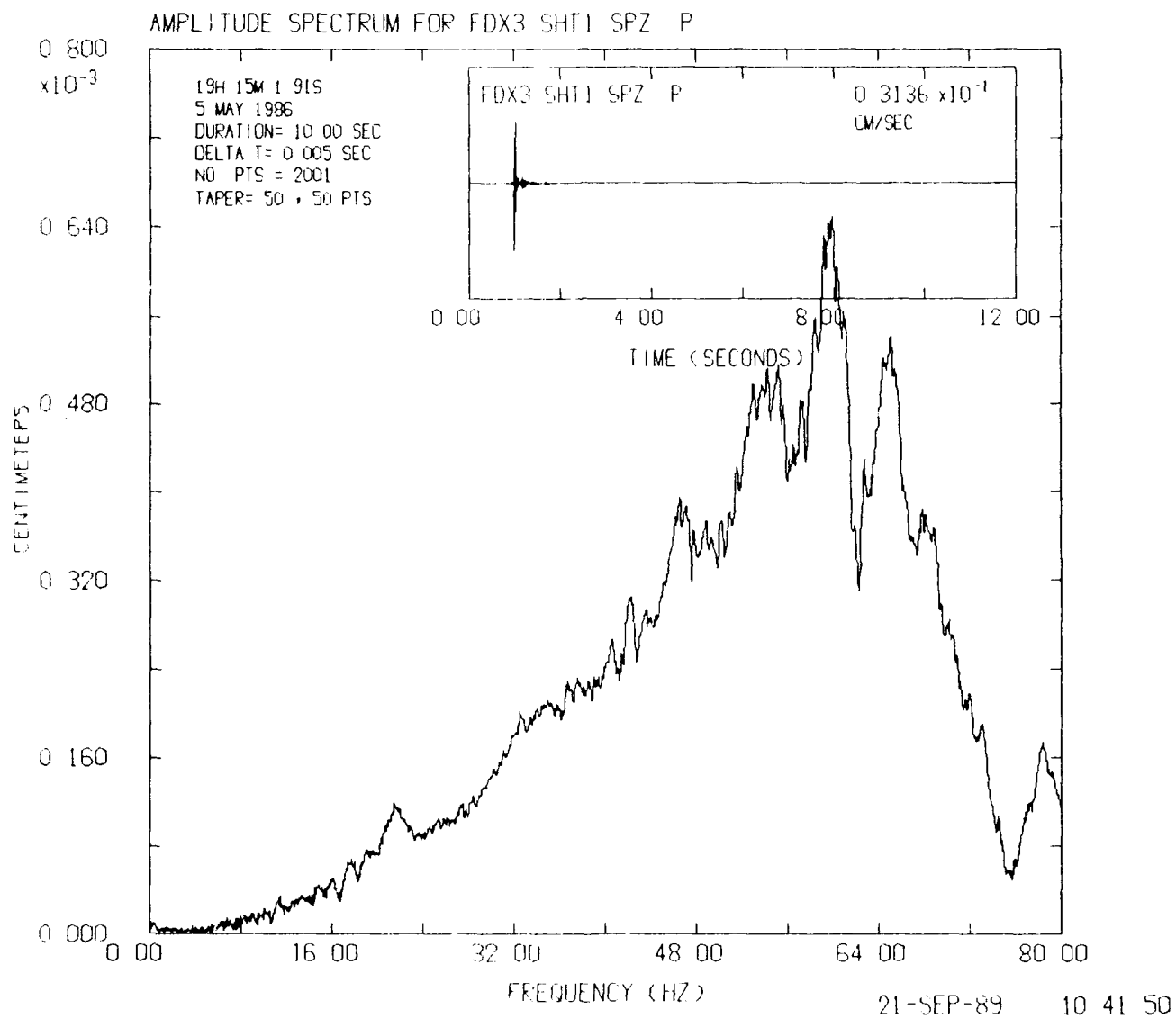
## **Appendix C: Amplitude Spectra for Selected Seismograms**



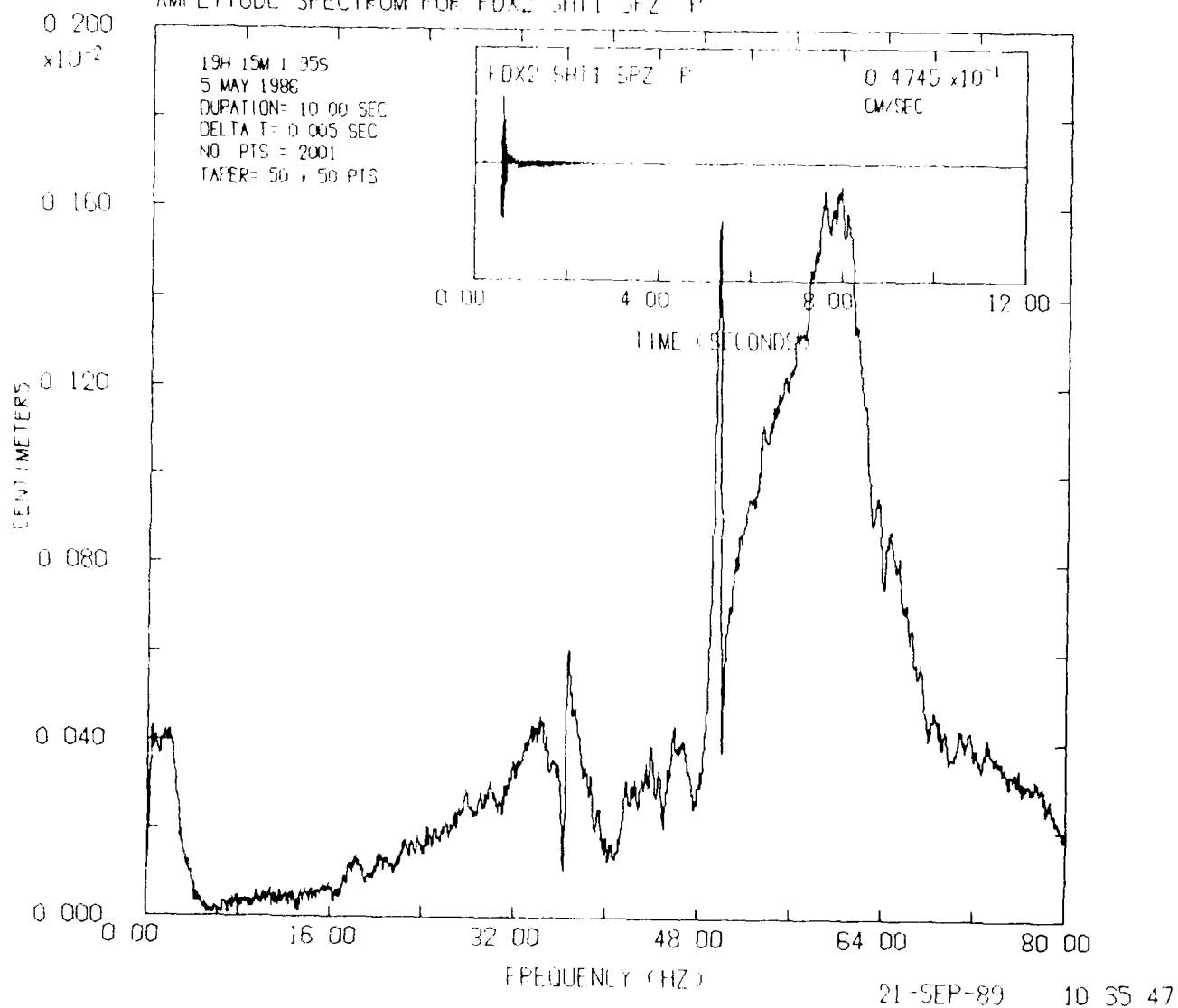
21-SEP-89 11 00 08

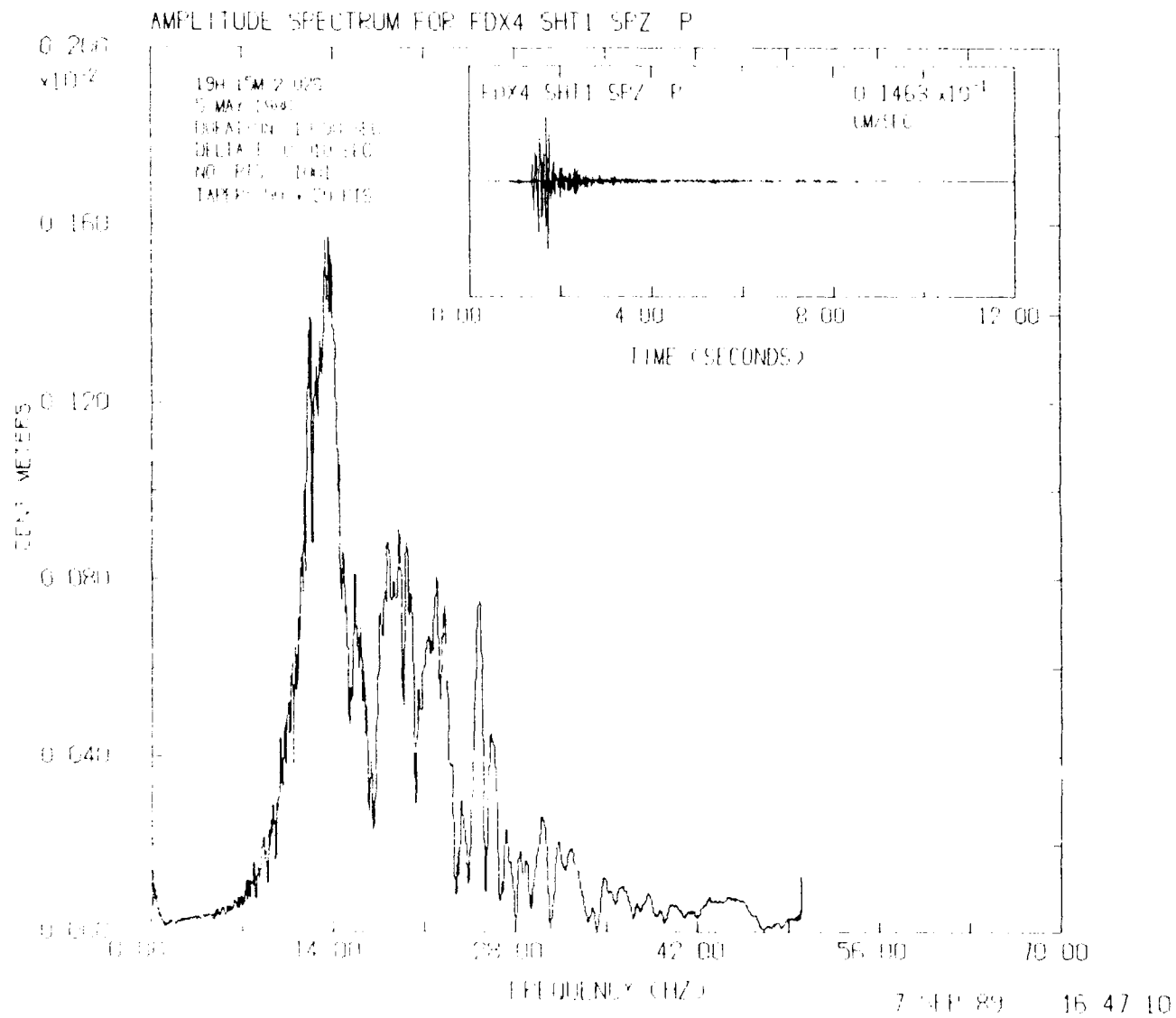
# AMPLITUDE SPECTRUM FOR FDX1 SHT1 SPZ P

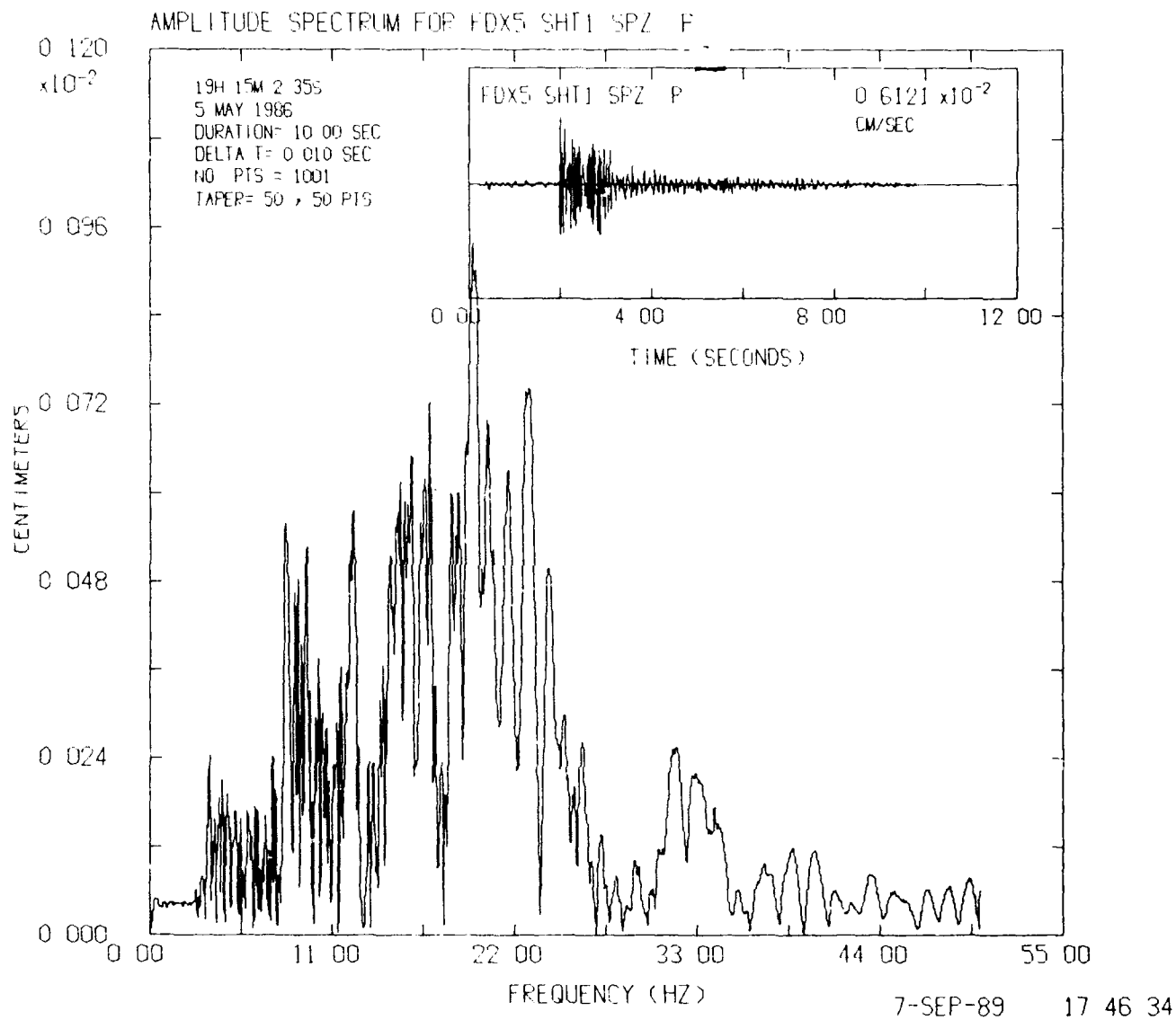




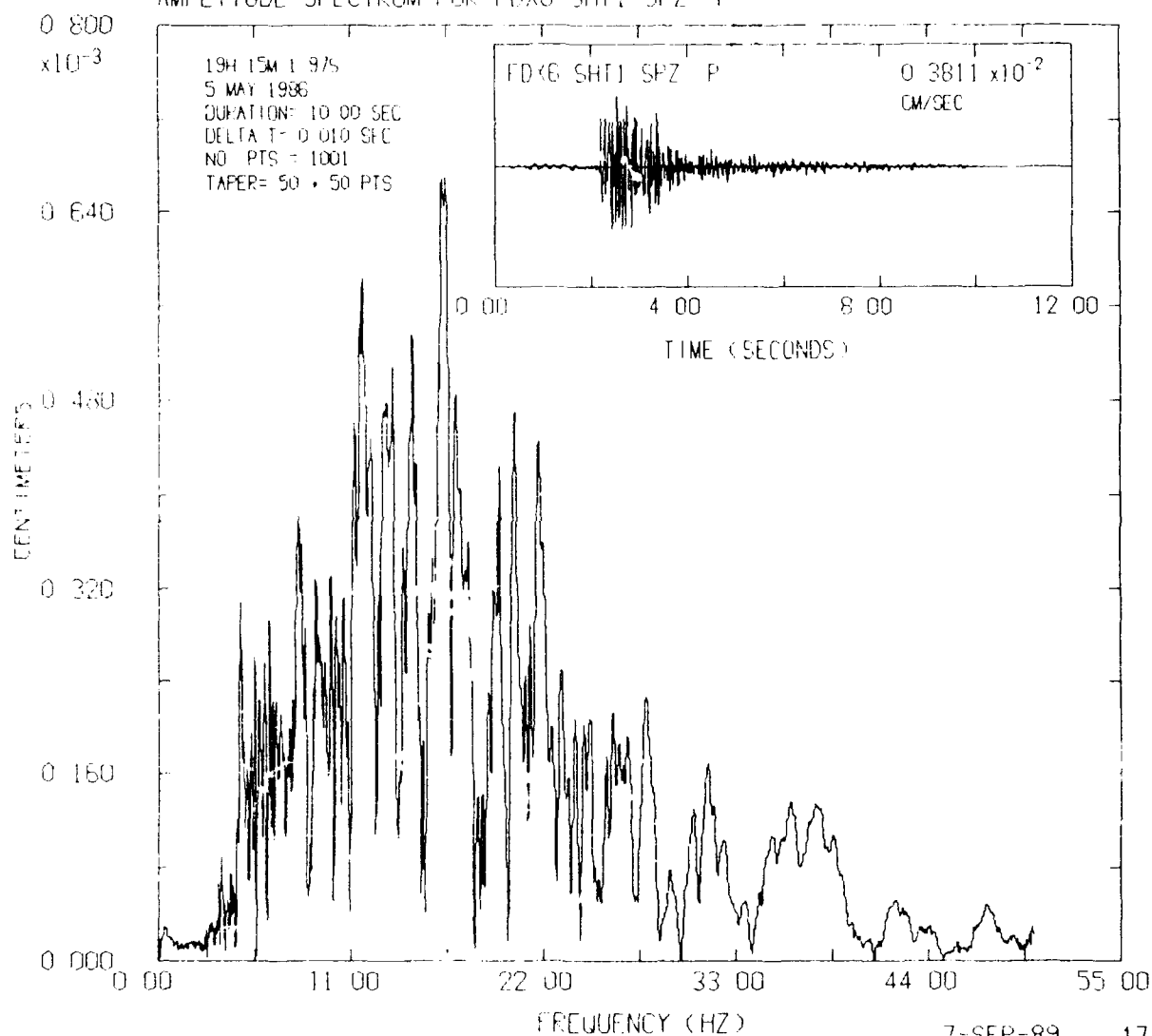
# AMPLITUDE SPECTRUM FOR FDX2 SH11 SPZ P



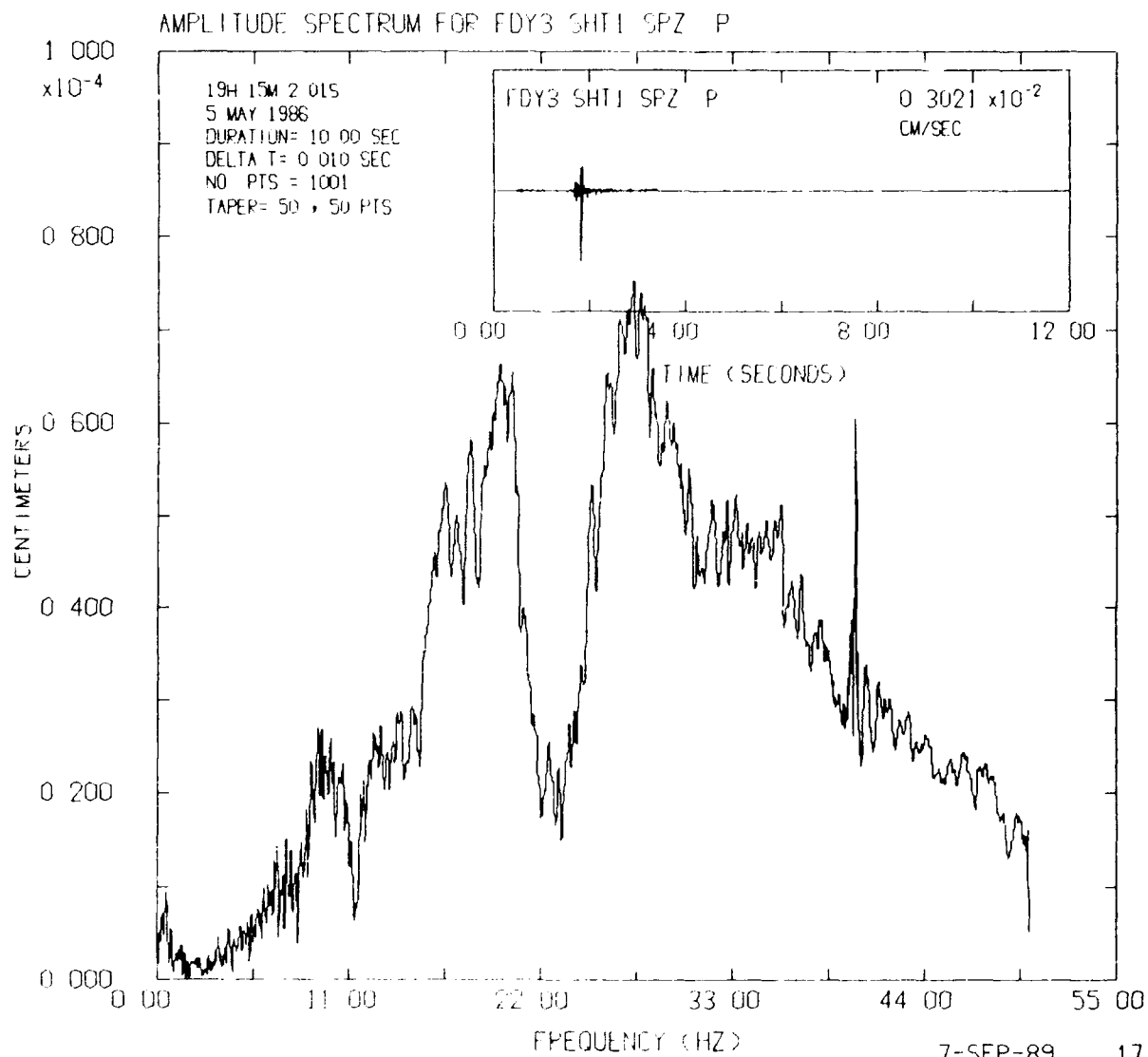




# AMPLITUDE SPECTRUM FOR FDX6 SHT1 SPZ P



7-SEP-89 17 52 17



7-SEP-89 17 23 39

